Zeitschrift: IABSE reports = Rapports AIPC = IVBH Berichte
Band: 37 (1982)

Rubrik: Theme 4: Structural steel elements

THEME 4

Structural Steel Elements

Eléments de construction en acier

Bauteile aus Stahl

Leere Seite
Blank page
Page vide

Ermüdungsversuche an geschweissten Biegeträgern

Fatigue Testing of Welded Beams

Essais à la fatigue de poutres soudées

PETER BERGER
Dr. -Ing.
VEB Metalleichtbaukombinat
Leipzig, DDR

ZUSAMMENFASSUNG
Zur Festlegung von Tragfähigkeitswerten für ermüdungsbeanspruchte geschweisste Bauteile wurden Ermüdungsversuche an Trägern durchgeführt. Die Ergebnisse der Versuche führten zu neuen zulässigen Spannungen und zur Anwendung des $\Delta\sigma$-Konzepts in der Neufassung der Stahlbauvorschriften der DDR.

SUMMARY
To determine values of load carrying capacity for fatigue loaded, welded structures, fatigue tests on beams were carried out. The test results led to new allowable stresses and to the use of the stress range concept in the new edition of the specifications for steel structures in the GDR.

RESUME
Des essais à la fatigue de poutres ont été réalisés afin de déterminer la capacité portante d'éléments de construction soudés sollicités à la fatigue. Les résultats de ces essais ont conduit à de nouvelles valeurs des contraintes admissibles et à l'utilisation du concept $\Delta\sigma$ dans la nouvelle édition des normes de construction métallique en RDA.

1. EINLEITUNG

Zur wirklichkeitsnäheren Erfassung der Belastung und Tragfähigkeit ermüdungsbeanspruchter Tragwerke wird in der Neufassung der Stahlbauvorschriften der DDR ein Betriebsfestigkeitsnachweis gefordert[1]. Den für diesen Nachweis vorgesehenen zulässigen Spannungen liegen Spannungswerte zugrunde, die für Einstufenbeanspruchung und $N = 2 \cdot 10^6$ Spannungszyklen gelten. Diese Grundwerte der zulässigen Spannungen waren auf der Grundlage der Ergebnisse von Ermüdungsversuchen neu festzulegen.

Aus den Veröffentlichungen über Ermüdungsversuche an großen geschweißten Bauteilen [2], [3] war bekannt, daß deren Ergebnisse von denjenigen, die an kleinen Proben mit entsprechenden Schweißdetails ermittelt wurden, abweichen:

- Die an Bauteilen ermittelten Tragfähigkeitswerte liegen teilweise beträchtlich, besonders im Bereich negativer Spannungsverhältnisse $R = \min\sigma/\max\sigma$, unter den Ergebnissen von Kleinprobenversuchen.
- Die maßgebende, die Tragfähigkeit ermüdungsbeanspruchter geschweißter Bauteile charakterisierende Größe ist neben dem Kerbfall die Differenz der Maximal- und Minimalspannung $\Delta\sigma = \max\sigma - \min\sigma$, nicht die Maximalspannung $\max\sigma$ und das Spannungsverhältnis R.

Zur Festlegung von Tragfähigkeitswerten für die Vorschriften und zur weiteren Klärung dieser Zusammenhänge wurde im Forschungsinstitut des VEB Metalleichtbaukombinat Leipzig ein umfangreiches Programm von Ermüdungsversuchen an Bauteilen in Angriff genommen. Zunächst wurden Versuche an geschweißten Biegeträgern mit Schweißdetails, für die bereits Versuchsergebnisse an Kleinproben vorliegen, durchgeführt. Über den ersten Teil dieser Versuche wird nachfolgend berichtet. Er umfaßt 85 Träger mit 7 verschiedenen Schweißdetails, an denen insgesamt 164 Versuche durchgeführt wurden.

2. VERSUCHE

Die Versuchsträger (Bild 1) wurden unter normalen Praxisbedingungen auf einer Trägerfertigungsstraße hergestellt. Als Werkstoff wurde St 52-3 verwendet, um im Schwellbereich noch möglichst große Spannungsamplituden aufbringen zu können.

Die zu untersuchenden Schweißdetails wurden im Prüflabor angebracht. Als Schweißverfahren kam die CO_2-Schweißung zur Anwendung. Die Träger wurden auf ihren Endstirnplatten in Prüfrahmen gelagert und in den Drittelspunkten mit Prüfzylindern belastet. Alle Versuche erfolgten mit Einstufenbelastung bei einer Prüffrequenz von $f = 172\ \text{min}^{-1}$. Um den Mittelspannungseinfluß möglichst gut beurteilen zu können, wurde für jede Probenform jeweils eine Versuchsreihe bei $R = -1$ und $R = +0{,}5$ vorgesehen. Jede Versuchsreihe besteht aus mindestens 8 wertbaren Versuchen. Damit kann der Wöhlerlinienexponent und näherungsweise auch die Streuung bestimmt werden.

Folgende Schweißdetails wurden untersucht (Bild 1):

1. Seitlich an die Gurte geschweißte ausgerundete Knotenbleche
2. Seitlich an die Gurte geschweißte rechteckige Knotenbleche
3. Zusätzlich aufgeschweißte Gurtplatten
- 3.1. Gurtplattenenden mit verstärkten, ungleichschenkligen Stirnkehlnähten, Nahtübergänge bearbeitet, Nähte und Gurtplattenenden auf eine Neigung 1 : 2 abgearbeitet
- 3.2. Gurtplattenenden mit verstärkten, ungleichschenkligen Stirnkehlnähten, Nahtübergänge unbearbeitet
- 3.3. Gurtplattenenden mit nicht verstärkten, gleichschenkligen Stirnkehlnähten, Nahtübergänge unbearbeitet (nur R = -1)
4. Quer auf die Gurte geschweißte Knotenbleche, Kehlnähte ringsum geschweißt, Nahtübergänge unbearbeitet
5. Längs auf die Gurte geschweißte Knaggen (20 mm dick) zur Kranschienenbefestigung, Kehlnähte an 3 Seiten der Knaggen, Nahtübergänge unbearbeitet.

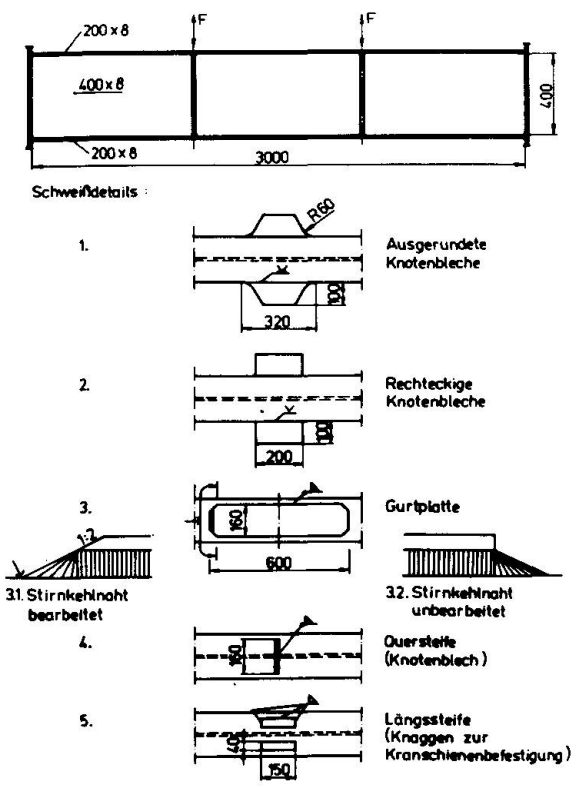

Bild 1 Versuchsträger Schweißdetails

Die Versuche wurden im Zeitfestigkeits- ($N > 10^5$) und Dauerfestigkeitsbereich durchgeführt. Versuche, die bei einer Lastspielzahl von $N = 2$ bis $4 \cdot 10^6$ nicht zum Bruch führten, wurden abgebrochen. Bei der Versuchsauswertung wurden die Zeitfestigkeitsgeraden der Wöhlerlinien bis zu den Grenzlastspielzahlen jeweils des Kerbfalles, in den das untersuchte Schweißdetail nach der Neufassung der Stahlbauvorschriften der DDR einzustufen ist, geführt. Diese Grenzlastspielzahlen N_G liegen zwischen $N = 2 \cdot 10^6$ und 10^7 und wurden aus einer großen Zahl von Versuchen bestimmt, die an Kleinproben durchgeführt wurden.

Als Bruchkriterium wurde der Rißfortschritt entweder bis zum Steg (seitlich angeschweißte Knotenbleche) oder bis zur Gurtaußenkante angenommen.

Träger, die bei der oben angegebenen Versuchsgrenzlastspielzahl keinen Bruch aufwiesen, wurden in einem 2. Versuch mit einer größeren Spannungsamplitude beaufschlagt. Die Ergebnisse dieser "hochgesetzten Durchläufer" ordnen sich (sofern nicht ein nicht

erkannter Anriß vorhanden war) in das Streuband der Versuchsergebnisse ein [4], blieben aber bei der statistischen Auswertung und in den Bildern 2 bis 7 unberücksichtigt.

Bei einigen Versuchsreihen wurden die zu prüfenden Schweißdetails an Ober- und Untergurt der Träger angebracht. Damit erhielten bei Schwellbeanspruchung (R = +0,5) im ersten Versuchsabschnitt die Details am Obergurt eine Druckschwellbeanspruchung. Nach erfolgtem Bruch im Zuggurt wurden die Träger um 180° um ihre Längsachse gedreht und mit der gleichen Belastung wie im ersten Versuchsabschnitt die Versuche fortgesetzt. Die druckschwell-vorbelasteten Details wurden damit im zweiten Versuchsabschnitt zugschwellbeansprucht. Die Ergebnisse dieser Versuche ordnen sich in das Streuband der Versuchsergebnisse der nicht vorbelasteten Träger ein [4], wurden aber ebenfalls bei der statistischen Auswertung und in den Bildern 2 bis 7 nicht berücksichtigt.

3. VERSUCHSERGEBNISSE

Die Auswertung der Versuchsergebnisse erfolgte nach dem von HOBBACHER vorgeschlagenen Verfahren der ausgemittelten Regression [5]. In den Bildern 2 bis 7 ist neben der so berechneten Regressionsgeraden (Wöhlerlinie für eine Überlebenswahrscheinlichkeit von $P_{ü}$ = 50 %) die untere Streubandbegrenzung $\overline{N} - 2\,s_N$ (Wöhlerlinie $P_{ü}$ = 97,7 % für die ausgewerteten Versuchspunkte) als strichlierte Gerade angegeben. Es ist zu erkennen, daß die aktuelle Streuung einer Versuchsreihe wegen der geringen Zahl von Versuchspunkten zufälligen Charakter hat und von Versuchsreihe zu Versuchsreihe stark schwankt. Deshalb wurden der Gesamtauswertung, die auf den Vergleich mit den Versuchsergebnissen von Kleinproben und den in den Bemessungsvorschriften angegebenen Tragfähigkeitswerten hinausläuft, nicht die berechneten Reststreuungen der Versuchsreihen zugrunde gelegt. In die Wöhlerliniendiagramme der Bilder 2 bis 7 wurden dafür als Streubandbegrenzungen Wöhlerlinien eingetragen, die eine Lastspielzahlstreuung T_N = 1 : 4 ergeben. Diese Streuung beruht auf der Auswertung der Ergebnisse von mehr als 9000 Einzelversuchen an Kleinproben und stellt das Verhältnis der Bruchlastspielzahlen eines Spannungshorizonts für Überlebenswahrscheinlichkeiten von $P_{ü}$ = 90 und 10 % dar. Sie kann mit genügender Genauigkeit für alle Kerbfälle und Wöhlerlinienexponenten als annähernd konstant angenommen werden. Diese Verfahrensweise wurde für die einheitliche Beurteilung der vorliegenden Ergebnisse, die in Abhängigkeit vom Kerbfall unterschiedliche Wöhlerlinienexponenten aufweisen, dem Verfahren von OLIVIER [6], das von einem einheitlichen Wöhlerlinienexponenten für Schweißverbindungen ausgeht, vorgezogen.

Die Versuchsergebnisse zeigen in Übereinstimmung mit [2], [3] keinen Mittelspannungseinfluß. Sie sind in den Bildern 2 bis 7 in doppeltlogarithmischer Darstellung aufgetragen. Die Wöhlerlinien ($P_{ü}$ = 50 %) folgen der Gleichung

$$\lg N = \lg C - \varphi \cdot \lg \Delta\sigma \,.$$

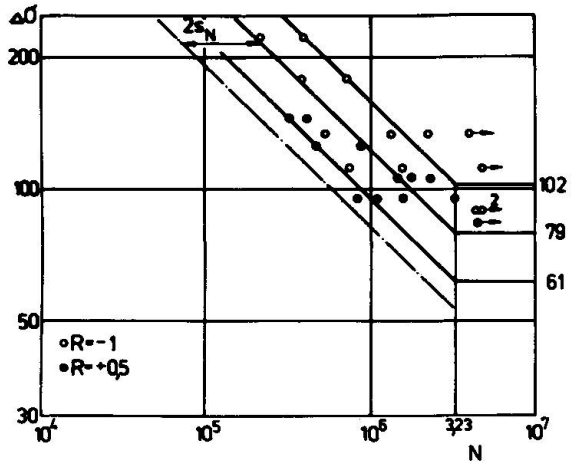

Bild 2 Ausgerundete Knotenbleche

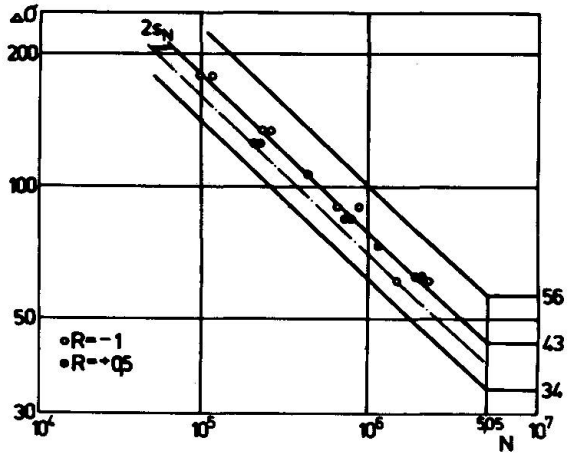

Bild 3 Rechteckige Knotenbleche

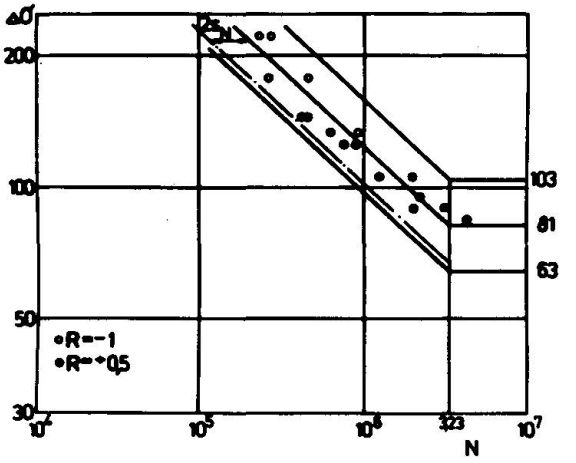

Bild 4 Gurtplatte, Stirnkehlnaht bearbeitet

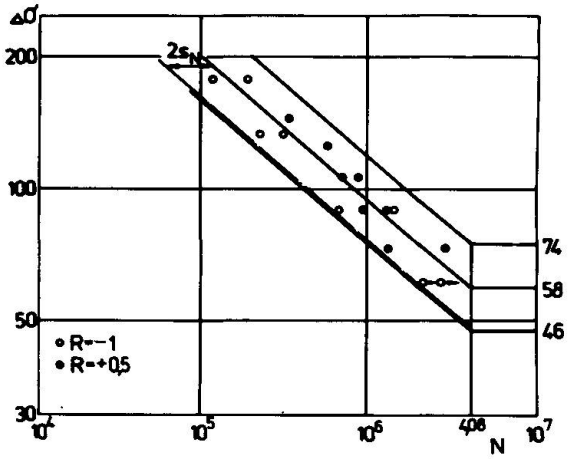

Bild 5 Gurtplatte, Stirnkehlnaht unbearbeitet

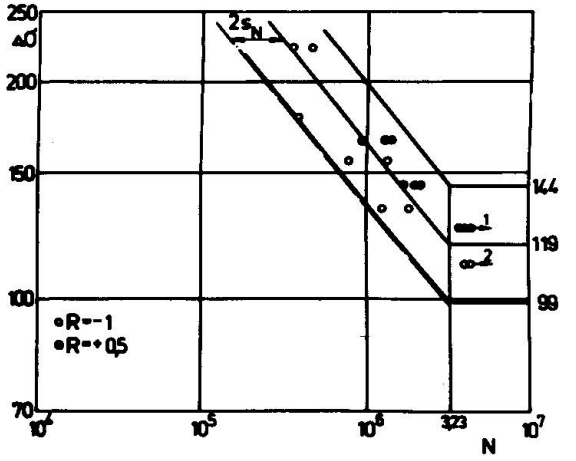

Bild 6 Quersteife(Knotenblech) Kehlnaht unbearbeitet

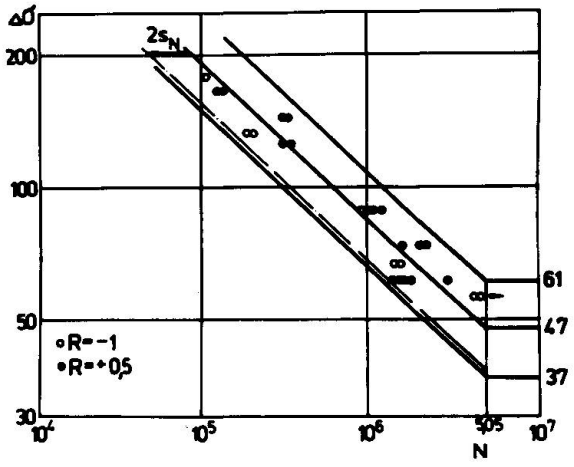

Bild 7 Längssteife(Knagge) Kehlnaht unbearbeitet

Tabelle 1 enthält eine Zusammenstellung der Ergebnisse mit den Parametern der statistischen Auswertung.

Versuchs-reihe	Anzahl der Versuche	lg C	φ	lg s_N	$\Delta\sigma_{D,50\%}$ bei $N_D=2.10^6$ N/mm^2
1	25	11,596	2,681	0,2384	95
2	16	11,236	2,770	0,0682	61
3.1	16	11,898	2,826	0,1191	96
3.2	16	11,928	3,010	0,1411	74
3.3	8	10,701	2,422	0,0470	66
4	18	14,131	3,669	0,1551	136
5	25	11,371	2,789	0,1310	66

In Tabelle 2 sind zum Vergleich die von FISHER [2], [3] erzielten Versuchsergebnisse von Trägern mit folgenden vergleichbaren Schweißdetails angegeben:

a) Überlappt auf die Gurte geschweißte rechteckige Knotenbleche, l = 200 mm

b) Zusätzlich aufgeschweißte Gurtplatten mit unbearbeiteten Endstirnkehlnähten

c) Quer auf die Gurte geschweißte Knotenbleche

d) Stegaussteifungen, mit dem Gurt durch Querkehlnaht verbunden

Die erneute Auswertung dieser Versuche erfolgte nach den gleichen Gesichtspunkten wie die der Leipziger Versuche.

Tabelle 2 Versuchsergebnisse nach [2] und [3]

Versuchs-reihe	Anzahl der Versuche	lg C	φ	lg s_N	$\Delta\sigma_{D,50\%}$ bei $N_D=2.10^6$ N/mm^2
a	27	12,408	3,269	0,1186	74
b	103	11,475	2,897	0,0956	61
c	19	14,429	3,851	0,0917	129
d	88	14,005	3,724	0,1042	117

Unter Berücksichtigung der unterschiedlichen Herstellungs- und Prüfbedingungen der Versuchsträger sowie Schweißdetails ist die Übereinstimmung der Ergebnisse gut. Auch die Streuungen innerhalb der Versuchsreihen haben etwa die gleiche Größe.

4. FESTLEGUNG VON TRAGFÄHIGKEITSWERTEN FÜR DIE DIMENSIONIERUNG

Die Ergebnisse der Bauteilversuche waren die wichtigste Grundlage für die Festlegung der Grundwerte der zulässigen Spannungen für den Ermüdungsfestigkeitsnachweis in den neuen Stahlbauvorschriften [7] der DDR. Es wurden auch Ergebnisse von Versuchen an Kleinproben berücksichtigt, jedoch erfolgte eine entsprechende Abwertung der Spannungswerte. Tabelle 3 zeigt eine Gegenüberstellung von Kleinprobenergebnissen mit Ergebnissen von Bauteilversuchen am Beispiel der Probenform "Seitlich angeschweißte rechteckige Knotenbleche". Für die Bauteilversuche wurden die Spannungswerte verwendet, die sich für die untere Streubandbegrenzung unter Verwendung der Lastspielzahlstreuung $T_N = 1 : 4$ ergeben.

Tabelle 3 Versuchsergebnisse für $N_D = 2 \cdot 10^6$
Probenform: Seitlich angeschweißte rechteckige Knotenbleche

Spannungsverhältnis R	Trägerversuche σ_D N/mm²	Versuche an Kleinproben Anzahl der Versuchsreihen	$\sigma_{D,90\%}$ N/mm²
-1	23,5	14	45,1
+0,5	98	13	129

Aus der Gegenüberstellung wird deutlich, daß infolge des Mittelspannungseinflusses bei Kleinproben die Abweichungen im Bereich negativer Spannungsverhältnisse R besonders groß sind.

Entsprechend den Ergebnissen der Bauteilversuche wurde dem Ermüdungsfestigkeitsnachweis der neuen Vorschrift das $\Delta\sigma$ -Konzept zugrunde gelegt.

Tabelle 4 zeigt die Einstufung der untersuchten Schweißdetails in die Kerbfälle der Vorschrift. Zum Vergleich sind die entsprechenden amerikanischen Versuchsergebnisse und ihre Einstufung in die Kerbfälle nach [8] angegeben. Die Tabelle enthält die Versuchsergebnisse bei $N_D = 2 \cdot 10^6$, und zwar sowohl die Spannungsdifferenzen $\overline{\Delta\sigma} - 2\,s$ (Mittelwert minus 2 Standardabweichungen, berechnet für die jeweilige Versuchsreihe) als auch die Werte min $\Delta\sigma$, die sich bei Zugrundelegung einer konstanten Lastspielzahlstreuung $T_N = 1 : 4$ ergeben.

Zur Überprüfung der Einstufung in die Kerbfälle der Vorschrift werden die Bauteilversuche mit weiteren Details fortgesetzt. In diesem Zusammenhang sind auch Versuche an spannungsarm geglühten Bauteilen vorgesehen, um zu genaueren Kenntnissen über den Einfluß der Eigenspannungen auf die Tragfähigkeit von Bauteilen bei Ermüdungsbeanspruchung zu gelangen.

Tabelle 4 Einstufung der untersuchten Schweißdetails in die Kerbfälle der Vorschriften

Versuchsreihe	Versuchsergebnisse $\overline{\Delta\sigma} - 2\,s_{\Delta\sigma}$ N/mm²	min $\Delta\sigma$	TGL 13 500 Kerbfall	zul $\Delta\sigma_D$ N/mm²	AISC Kerbfall	zul $\Delta\sigma_D$ N/mm²
1	63	73	4	84	D	70
2 5 a [3]	54 53 62	47 51 60	6	58	E	56
3.1	79	75	4	84	-	-
3.2	60	59	5	70	-	-
3.3 b [2]	60 52	49 48	6	58	E	56
4 c [3] d [3]	112 116 103	113 108 97	4 x)	84 x)	C	90

x) bei kerbfreiem Nahtübergang Kerbfall 3, zul $\Delta\sigma_D$ = 106 N/mm²

LITERATUR

1 GRASSE, W.; BERGER, P.: Der Ermüdungsfestigkeitsnachweis in den neuen Stahlbauvorschriften der DDR. IVBH Kolloquium Ermüdung von Stahl- und Betonkonstruktionen. Lausanne 1982

2 FRANK, K. H.; FISHER, J. W.: The fatigue strength of welded coverplated beams. Fritz Engineering Laboratory Report No. 334.1. Lehigh University, Bethlehem, Pa., 1969

3 FISHER, J. W.; ALBRECHT, P. A.; YEN, B. T.; KLINGERMAN, D.J.; MC NAMEE, B. M.: Fatigue strength of steel beams with welded stiffeners and attachments. NCHRP Report No. 147 Transportation Research Board, Washington, D. C., 1974

4 BERGER, P.: Ermüdungsversuche an geschweißten Trägern. Schweißtechnik, Berlin 31(1981)2, S. 78 - 82

5 HOBBACHER, A.: Zur Auswertung von Schwingfestigkeitsversuchen an Schweißverbindungen. Schweißen u. Schneiden, Düsseldorf 29(1977)4, S. 143 - 146

6 OLIVIER, R.; RITTER, W.: Wöhlerlinienkatalog für Schweißverbindungen aus Baustählen, Teil 1 bis 3. DVS-Berichte 56/I bis /III. Deutscher Verlag für Schweißtechnik Düsseldorf, 1979, 1980 und 1981

7 TGL 13 500 (Entwurf 10.81), Stahlbau, Stahltragwerke, Berechnung und bauliche Durchbildung, Leipzig, Oktober 1981

8 AISC Specification, Specification for the Design, Fabrication and Erection of Structural Steel for Buildings. American Institute of Steel Construction, New York, 1978

Fatigue Strength of Welded Butt Joints of Multiple Plate Flanges of Beams

Résistance à la fatigue d'assemblages en bout, des ailes de poutres constituées de tôles multiples

Ermüdungsfestigkeit der Stumpfnahtschweissverbindungen von Mehrblech-Trägergurten

K.P. BOLSHAKOV
cand. of techn. science
All-Union Res. Inst. of Transp. Constr.
Moscow, USSR

I.M. SHAFERMAN
Engineer
All-Union Res. Inst. of Transp. Constr.
Moscow, USSR

SUMMARY

The main cause of premature fracture of multiple-plate beam flanges is considered to be the concentration of stress at the point of intersection of the joint and the gap between the plates. A value of the effective concentration coefficient of B = 1.68 has been obtained for experimental specimens whereas, until now, B = 1 has been used. This new value of B should be considered as a lower bound for real structures because of possible assembly and welding defects.

RESUME

La rupture prématurée des ailes de poutres constituées de tôles multiples a pour principale cause la concentration de contraintes au point d'intersection de l'assemblage soudé et du vide entre les tôles. Une valeur du coefficient de concentration effectif B égale à 1.68 a été obtenue lors d'essais, alors que jusqu'à maintenant la valeur B = 1 a été utilisée. Cette nouvelle valeur de B doit être considérée comme une limite inférieure pour les structures réelles, en raison des imperfections possibles d'assemblage et de soudure.

ZUSAMMENFASSUNG

Die Hauptursache der vorzeitigen Ermüdungsbrüche der üblicherweise verwendeten geschweissten Stösse bei Mehrblech-Trägergurten ist die Spannungskonzentration im Kreuzungsbereich der Stossfuge mit dem Spielraum zwischen den Blechen. Aus Versuchen wurde ein Wert des Koeffizienten der effektiven Spannungskonzentration von B = 1.68 ermittelt, während bisher B = 1 angenommen worden war. Wegen der eventuellen Montage- und Schweissfehler ist der im Versuch ermittelte B-Wert als unterer Grenzwert für wirkliche Konstruktionen zu betrachten.

Conditions of superstructures erection determine the type of welded butt joints of multiple plate flanges of beams not typical for plant fabrication. Two weldment technologies are known: single-V (butt) joint with prefusion of gap between buut ends of welding edges [1-3] and separate joints by means of insersion pieces in pack plates [4].

At our Institute attention has been paied for the first time to reliability of such joints during fatigue test of I-beams with double plate flanges. Beam flanges were welded with single - V (butt) joint according to the technology [1-3]. Tests were supposed to be conducted under variable load of 2 million cycles, however fatigue fracture of joints was found to initiate before specified time. In all cases fatigue crack occurred at the point of joint intersection with gap between plates (fig. 1).

The problem of fatigue strength of mentioned joints has not been sufficiently studied at the literature. In their investigations [2] the authors have made an attempt to define the cause of fracture. Irregularity of anglular contraction when performing single butt joint has been assumed to be the cause of fracture. As a result symmetrical grooves such as double V (butt) joint done by means of overhead welding have been recommended.

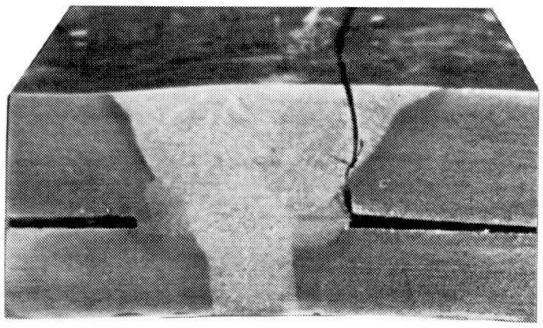

fig.1. Fatigue fracture of double plate beam flange joint

To estimate technologies applied we have conducted four series tests of double plate specimens on fatigue strength limit at variable tension (fig.2,a); series 1 - specimens of base metal; series 2 - specimens with single - V (butt) joints done according to the technology applied for one plate flanges; series 3 - specimens with single - V (butt joint) done according to the technology [1-3]; series 4 - specimens with insertion in one of plates and three separate single - V (butt) joints done according to the technology [4]. In all specimens the gap between plates was welded along end block contours to provide coincidence of deformation of pack plates. After welding single - V (butt) joints were trimmed flush with base metal surface.

Series 1-3 were tested at two values of cycles asymmetry: ρ =0,125 and ρ = 0,40; while series 4 - at ρ = 0,40. Crack being detected at one of the plates, tests were stopped. Obtained results were processed by the method of mathematical statistics. The fatigue strength curves were plotted in logarithmic coordinates (fig.2,b,c).

Tests have demonstrated that regardless of the technology applied all specimens fracture (in beams as well - fig. 1) occurred at the point of joint intersection with gap between plates. Fatigue strength limit in series 2 and 4 (fig. 2,d) appeared to be the lowest and approximately the same at ρ = 0,40; fatigue strength limit in series 3 is slightly higher comparing with series 2 and 4, but lower in comparison with base metal (series 1). Tests conducted at ρ = 0,125 support the conclusions relative to series 2 and 3 (fig. 2,c). The value of fatigue strength limit given in

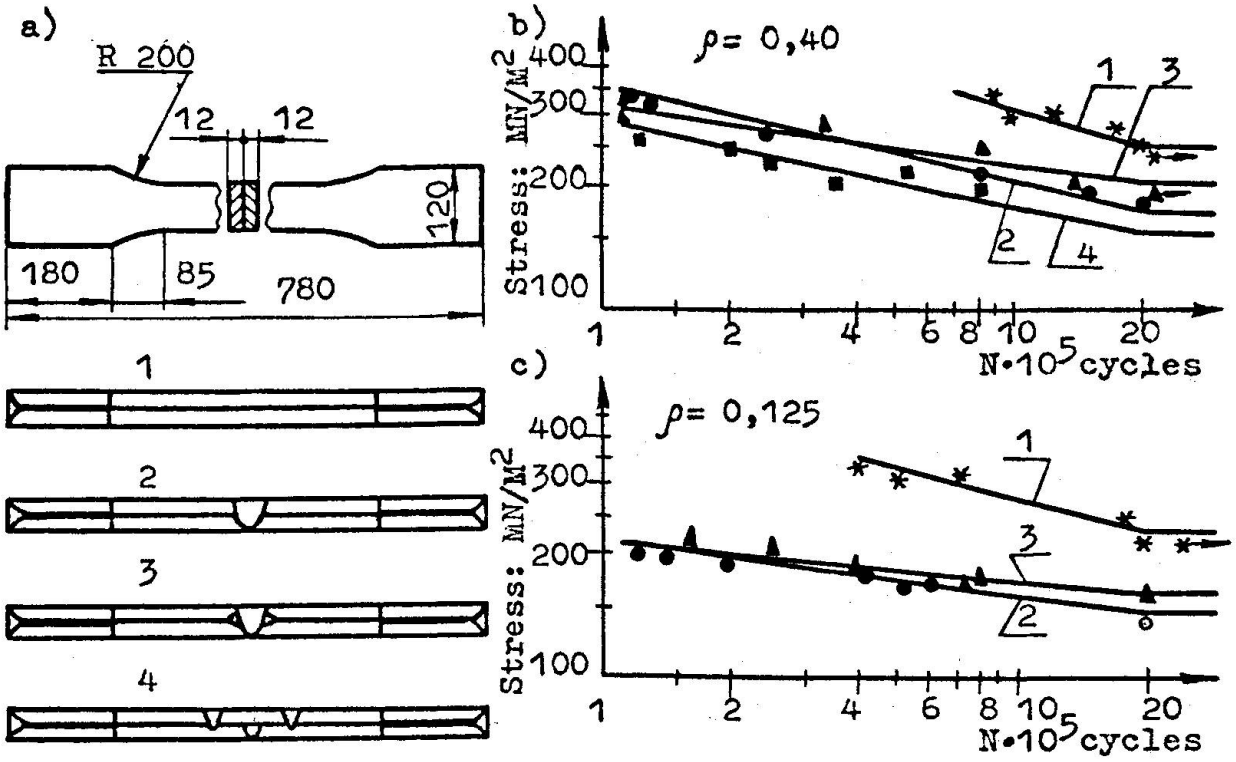

fig. 2. The curves of specimens fatigue strength (O – data from ref [2])

reference [2] for double V butt joint is shown here too. Fatigue strength limit of such joint obtained from "weak regime" tests (ρ= 0,18) appeared to be similar to fatigue strength limit at ρ= 0,125 in series 2. Therefore recommendations [2] haven't provided significant advantages.

Efficient coefficient of concentration was defined by means of maximum ultimate stress diagram by Smith [5] as ratio of base metal fatigue strength limit to joint fatigue strength limit at ρ= -1. For series 2 - B = 1,83, for series 3 - B = 1,68, the values being representative of quite high stress concentration in welded butt joints of multiple plate flanges, though up to the present it was considered to be absent and B = 1.

To find out the conditions of stress concentration occurrence the contours of points of joint intersection with gap between plates were investigated by means of microscope. It has been determined that in most cases the contours are close to rectangular (fig.3a). However in a number of cases distortions (defects) were observed such as spherical expansion with radius r at $\Delta < r << \delta_1, \delta_2$ (fig. 3b); sharp cross expansion of a specific size - $2a \gg 2b$, $b \cong \Delta < 2a << \delta_1, \delta_2$ and section form similar to elliptical (fig. 3c); branching from intersection point, section shape being close to elliptical with similar sizes ratio (fig. 3d). The mentioned defects have been induced by slag inclusions along the line of joint - gap intersection.

The methods of mathematical theory of elasticity have been used to estimate stress concentration in the above stated cases [6]. It was taken into account that thickness of pack plates and width of welded butt joint were much more than gap and defects sizes. This factor allowed the problem to be considered regardless of number and thickness of plates in a pack and mulual influence of gaps, and defects situated symmetrically relative to butt joint axis to be neglected.

After geometrical approximation of points of joint intersection with gap (fig.3) it has been decided that mathematical problem of elasticity theory on extention of plane with various apertures is equivalent to the problem of elongation of welded butt joints of multiple plate packs.

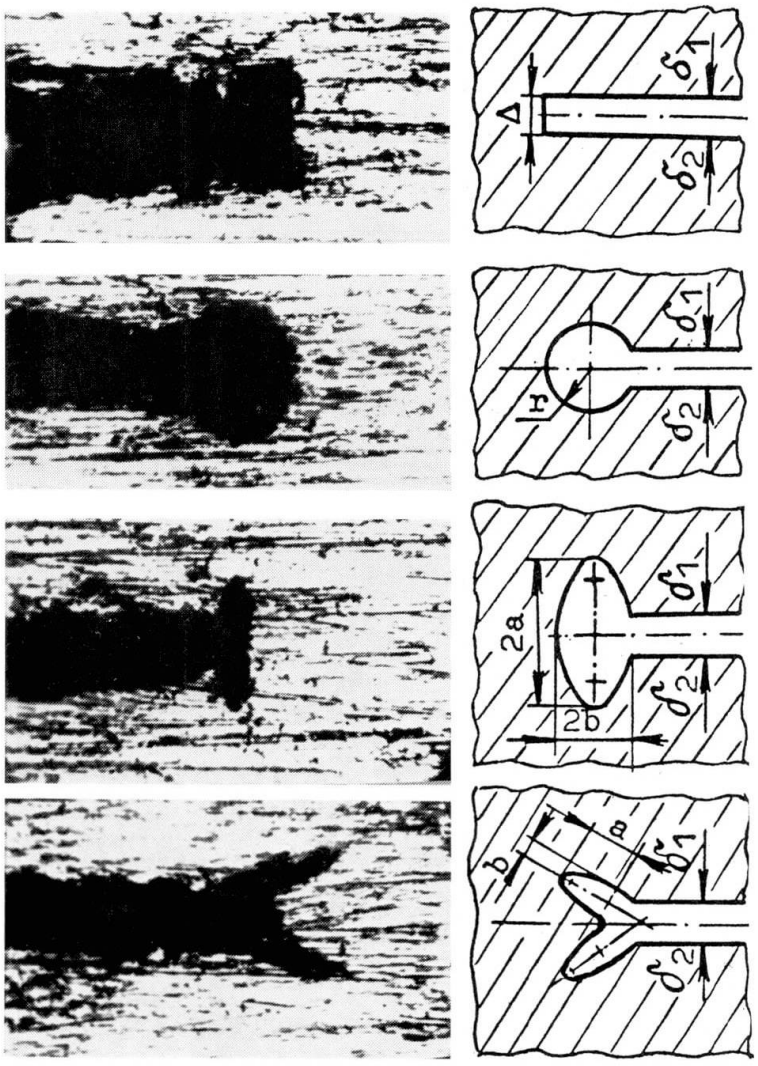

fig. 3. Zones of joint intersection with the gap

Rectangular aperture of $a/\Delta = 2+2,5$ (sides ratio, fig 4a) was considered for fig.3a. In such aperture mutual influence of cross sides might be neglected within 3–4% [7]. It was found out that the value of theoretical coefficient of concentration K_t depends on radius r of aperture angle rounding off and is approximately identical for all long apertires, when ratio r/Δ is the same. In chart 1 it is obvions that value $K_t = 2,15$ even for the case when $r/\Delta = 0,5$. Such concentration coefficient will be evidently minimum for real connections. The results of analytical solution are qualitatively confirmed by investigations conducded by photoelasticity method (chart 2). In practice there appears to be more cases when $r/\Delta < 0,5$. Charts 1 and 2 show that with r/Δ decrease the coefficient of concentration sharply increases.

The case of fig. 3 is interpolated as extention of plane with round aperture (fig. 4b) when $K_t = 3$ [6].

When plane with elliptical aperture extends the coefficient of concentration K_t depends on angle α, characterizing inclination

of ellipse large axis to extention direction [6] Maximum meaning of K_t will be at the ends of large axis when $\alpha = \pi/2$ and corresponds to defects shown in fig. 3b. Such defects existing, coefficient of concentration [8] might be very high (fig. 4c). In all considered cases, where defects resulted from slag inclusions(fig.3,b,c,d), the gap should not affect concentration level as it is situated in the zone of least stresses.

Displacement of jointing pack plates is likely to take place when assembling butt joints and in the process of welding (fig. 5). In this case eccentricity of load occurs this being the cause of additional bending stress resulting in increase of total stress level. Thus displacement of 15% and 32% increases stress level by 1,34 and 1,84 [9] . Similar increase of total stress level occurs where there is residual angle deformations of connected plates [2] . Accordingly stress concentrators influence becomes larger.

Under construction conditions the occurrence of various assembling and welding defects is practically inevitable; that's why laboratory obtained value of efficient concentration coefficient B = 1,68 should be considered as lower meaning for real structures.

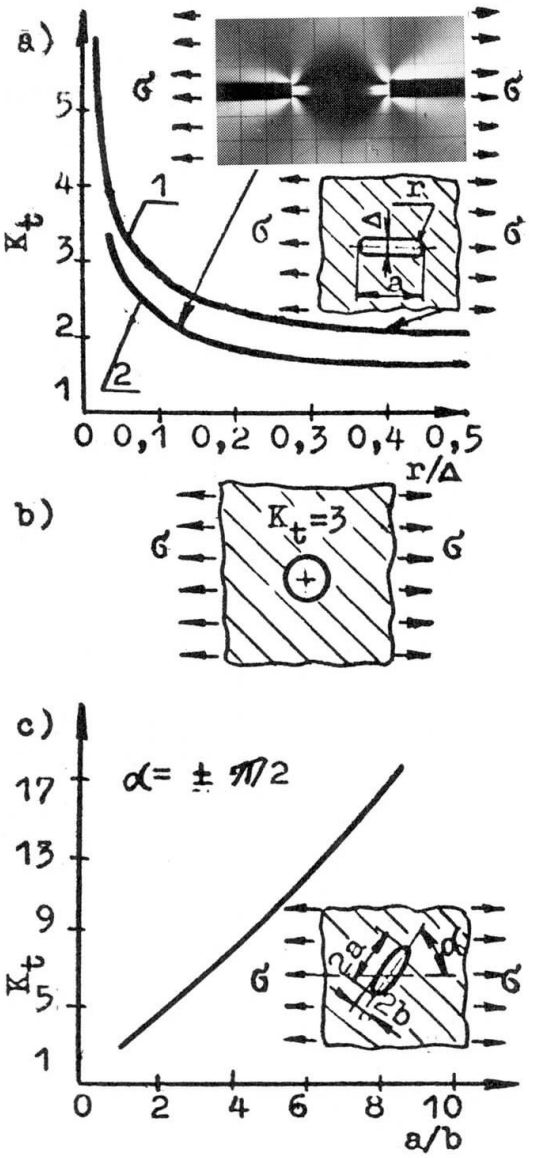

fig. 4. Theoretical concentration coefficients

Higher fatigue strenght of series 3 (fig. 2) may be explained as follows. Joint circumjacent zone includes five sections of thermic influence zone (fig. 6). The sections hardness decreases as it is moved away from joint axis at HRB = 86 (in the first section) up to HRB = 68 (in the fifth section) These zones plasticity varies inversely with hardness. In series 2 concentrator is located in the zone of high hardness,but less elasticity (fig. 6a). In series 3 – in the zone of less hardness,but higher elasticity (fig. 6b). These factors determine the difference in connections behaviour under fatigue loading.

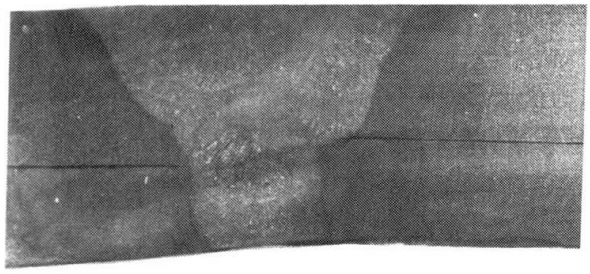

fig. 5. Fatigue fracture with displacement of plates in joint

In series 4 complete fusion (poor fusion is inadmissible in brid-

ge building results in fusion of butt joints metal with lower pack plate. Stress concentrators in connections of this series just as in series 2 are located in the zone of high hardness. As a result developed fatigue strength curves for this series appeared to be close one (fig. 2b) to another.
To determine the fracture mechanism of welded butt joint of multiple plate pack tests have been carried out on static tension of specimens possessing higher efficient coefficient of concentration B and specimens with artificial defects - apertures of 1,5 mm diameter simulating defect shown in fig. 3b. In both cases fracture initiated from the point of joint intersection with the gap (fig.7).

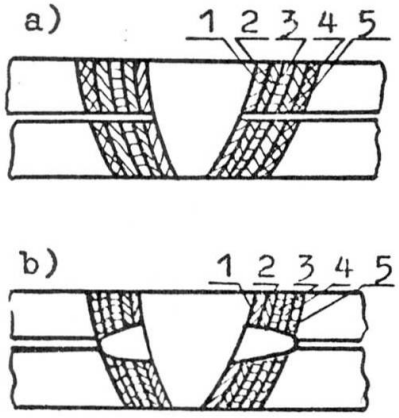

fig. 6. Concentrators location in joint circumjacent zone

Thus, in our opinion, high concentration of stress in the point of joint intersection with the gap between plates should be considered to be the main cause of fatigue fracture of welded butt joints of multiple plate beam flanges (packs). Such factors as hardness increase in joint circumjacent zone residual strains including angular, stresses and assembling and welding defects intensify the effect of the main cause.

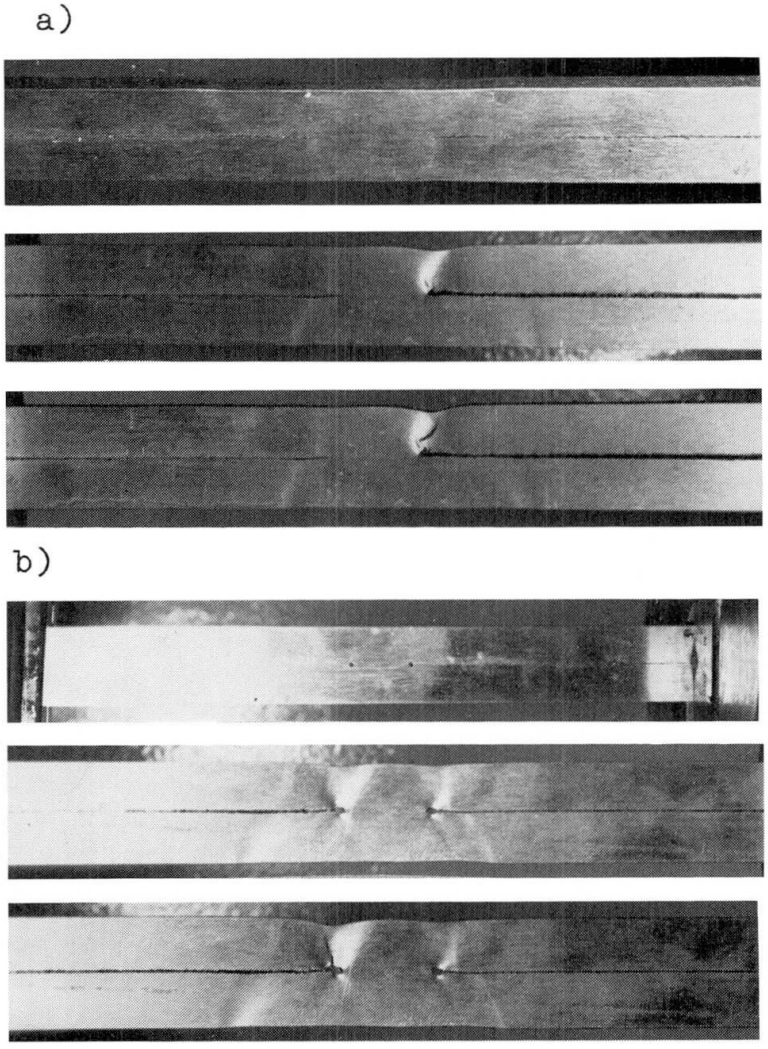

fig. 7. Static tension fracture

References

1. Koder E. Montageschweissung in Stahlbrückenbau. Technische Mitteilungen Krupp. 1972, 30, N2, S. 69-74.
2. Tshemmernegg F., Reutter K. Probleme des Herstellens und Prufens von geschweissten Stumpfstossen dicker Lamellenpakete. Bauingenieur, 1974, N 10, S. 397-399.
3. Podemski J. Styki i połączenia elementów spawanych w konstrukcjach mostowych. Przegląd Drogowy, 1977, N 3, S. 65-68.
4. Masaharu Katoh. On the Field Welding of Bridges in Recent Years. Journal of Japan Welding Society, 1975, 44, N 12, p. 4-10.

Predicting the Fatigue Life of Unpainted Steel Structures

Prédiction de la durée de vie de fatigue des structures métalliques non peintes

Vorhersage der Lebensdauer von Stahlkonstruktionen ohne Anstrich

PEDRO ALBRECHT
Assoc. Professor
University of Maryland
College Park, MD, USA

SUMMARY
Unpainted steel structures that are exposed to atmospheric environments loose initiation life due to rust pitting and propagation life due to corrosion fatigue. The former loss is determined from an analysis of 1,195 fatigue tests of six types of details that were weathered up to four years, the latter from corrosion fatigue crack growth rates. Proposed equations predict the total loss in life of stress range for Category A through Category E details. The losses are largest for Category A and diminish with increasing severity of the detail. The findings are applied to simple-span bridges.

RESUME
Les structures métalliques non peintes qui sont exposées aux conditions atmosphériques voient leur durée de vie à la fatigue sous corrosion diminuée, ceci aussi bien pour la durée d'initiation que pour la durée de propagation. On a déterminé cette perte à partir de l'analyse de 1195 essais de fatigue pour six types de détails qui furent exposés durant plus de quatre ans, dont la dernière consacrée à l'observation de l'accroissement des fissures de fatigue sous corrosion. Des équations sont proposées pour prédire la perte totale de durée de vie ou de différence de contrainte pour les catégories A à E de détails. Les pertes sont plus grandes pour la catégorie A et elles diminuent avec l'accroissement de la sévérité du détail. Les résultats sont appliqués au cas de ponts à portée simple.

ZUSAMMENFASSUNG
Bei Stahlkonstruktionen ohne Anstrich reduzieren sich die Phasen des Rissbeginns durch den Lochfrass und die Phase der Rissfortpflanzung durch Ermüdungskorrosion. Der Verlust in der Phase des Rissbeginns wurde durch 1195 Ermüdungsversuche an sechs verschiedenen Details, die bis zu vier Jahren im Freien gelagert wurden, bestimmt. Der Verlust an Lebensdauer infolge Korrosionsermüdung wird mit der Beobachtung des Risswachstums hergeleitet. Die vorgeschlagenen Gleichungen sagen den totalen Verlust an Lebensdauer oder an ertragbarer Spannungsamplitude für Details der Kategorie A bis E voraus. Die Verluste sind am grössten für die Details der Kategorie A und nehmen mit zunehmend ungünstigen Details ab.

Structures fabricated from atmospheric corrosion resisting steels, so-called weathering steels, [8,15] are expected to develop a dense patina which would greatly reduce the long-term corrosion of the underlying steel base. Necessary conditions for such behavior are bold exposure, intermittent wetting and drying, and absence of heavy concentrations of corrosive pollutants, especially roadway deicing salts. Under those ideal conditions of exposure, weathering steel structures are not normally painted. Bare steel is subjected to rust pitting and to corrosion fatigue under cyclic loading, phenomena known to decrease the crack initiation and propagation lives, respectively. This paper shows how to account in design for the loss in fatigue life. The background information is presented in great detail in Ref. 4.

Three sets of data are available for steels that were weathered naturally for up to four years prior to fatigue testing. Attempts to artifically accelerate the weathering process were not successful [1]. Kunihiro, et.al., [9] tested plain specimens and butt-welded ground flush specimens fabricated from either SMA weathering steel [8] or SM rolled steel with no enhanced atmospheric corrosion resistance [11]. Figure 1 shows a typical set of data. The 0-year nonweathered control specimens exhibited a fatigue strength slightly greater than the mean for Category A. Four years of weathering significantly reduced that strength, with 18.3 percent (15 out of 82) of the data points falling below the AASHTO allowable Category A line [14]. Albrecht, et.al., [2,4,7] tested specimens with transverse stiffeners and 102-mm attachments fabricated from A588 steel [15].. The third set of data comes from Nihei, et.al., [10] who tested notched plate specimens and butt-welded specimens with the weld reinforcement not removed. Both were fabricated from SM steels [11]..

Table 1 summarizes the results of the 1,195 fatigue tests cited previously. The data from all series were compared at 500,000 cycles, in the manner illustrated in Fig. 2. The fatigue notch factor [3] , defined as the ratio of mean stress ranges for Category A (solid circle) and the detail under consideration (open circle),

$$K_f = \frac{f_{rA}}{f_{r2}} = \frac{350\ MPa}{f_{r2}} \tag{1}$$

established the severity of the detail before weathering. The relative loss in stress range, Δf_r, between the weathered and nonweathered specimens was:

$$\Delta f_r = 1 - \frac{f_{r1}}{f_{r2}} \tag{2}$$

where f_{r1}/f_{r2} is the ratio of the smaller to larger stress range at 500,000 cycles. See the two open circles on the solid mean lines in Figs. 1 and 2. Since the fatigue life, N, is about a third-power expontential function of f_r, $m \cong 3$, the corresponding relative loss in fatigue life is:

$$\Delta N = 1 - \left(\frac{f_{r1}}{f_{r2}}\right)^3 \tag{3}$$

This procedure compares data about midway in the range of cycles to failure usually measured in testing programs. It estimates mean changes in life in a way that makes them relatively insensitive to slope variations of the two S-N lines being compared.

The calculated losses in stress range and fatigue life due to weathering are listed in Table 1. Each data point in Fig. 3 shows the mean loss in life for one type of specimen and length of weathering, as a function of the fatigue notch factor of the corresponding nonweathered control specimens. Vertical

lines were drawn at the fatigue notch factors for the mean regression line of the Category A through Category E data [3] to permit a comparison of the results with the AASHTO fatigue specifications [14].

The following equation, drawn solidly in Fig. 3, envelops the points for relative loss in life due to weathering.

$$\Delta N_w = 1 - 0.38\ K_f \tag{4}$$

It is backed by data in the region $0.69 \leq K_f \leq 2.04$ and assumed to be valid up to $K_f \leq 2.63$. Above that value, the loss in life would vanish, $\Delta N_w = 0$. The only data point that falls above Eq. 4 in Fig. 3 was excluded because of the uncertainty in using the stress amplitude, $f_a = 0.5\ f_r$, to calculate K_f for Nihei's nonwelded notched plate specimens. Note also that weathering steels (A588 and SMA) and regular steels (SM) exhibit comparable losses in life.

The total fatigue life consists of a crack initiation phase plus a crack propagation phase. Weathering reduced only the crack initiation phase, because all but 48 specimens were fatigue tested after the weathering periods shown in Table 1. In reality, unpainted steel structures are exposed to the environment during both phases of fatigue cracking. The latter effect, termed corrosion fatigue, can be estimated from measurements of crack growth rate for A588 steel in distilled water and 3-percent sodium chloride solution [5]. The aqueous data fell along the upper bound of the factor-of-two scatter band for the air data. Hence, the aqueous environments increased the crack growth rate by a factor of $\sqrt{2} = 1.4$. For the purpose of this estimation, it is assumed that the crack growth rate and the crack propagation life are proportional, and that weathering consumes the crack initiation life. Under these assumptions, the area above the weathering line, Eq. 4 in Fig. 3, represents the crack propagation life, $0.4/1.4 = 29$ percent of which is lost to corrosion fatigue.

$$\Delta N_{cf} = 0.29(1-\Delta N_w) = 0.11\ K_f \tag{5}$$

Adding Eq. 4 and Eq. 5 gives the total relative loss in life due to weathering and corrosion fatigue, ΔN_t, shown with a dashed line in Fig. 3.

$$\Delta N_t = \Delta N_w + \Delta N_{cf} = 1 - 0.27\ K_f \tag{6}$$

When $K_f \geq 2.63$, the effect of weathering vanishes, and the total loss in life remains at 29 percent, equal to the loss due to corrosion fatigue alone.

Subtracting Eq. 6 from unity yields the relative net life after weathering and corrosion fatigue

$$N_{net} = 1 - \Delta N_t = 0.27\ K_f \tag{7}$$

with the corresponding relative net stress range given by

$$f_{r,net} = (0.27\ K_f)^{1/3} \tag{8}$$

The net relative life (stress range) varies from 27 percent (65 percent) for Category A to 71 percent (89 percent) for Category D and below.

The fatigue notch factors and, hence, all previous equations were derived for the mean regression lines. To obtain allowable stress ranges for fatigue design of unpainted steel structures, it seems reasonable to multiply the AASHTO allowable stress ranges [14], which are based on clear air data, by the net relative stress range given by Eq. 8. For redundant load-path structures:

$$F_{sr,t} = \left(\frac{10^{b-2s}}{N_d} 0.27\ K_f\right)^{1/3} \qquad (9)$$

where N_d = design fatigue life, b = intercept of mean S-N Line, and s = standard deviation on log of life. The same reductions should also be applied to the fatigue limit until better threshold data are developed.

Figure 4 compares the AASHTO allowable stress ranges for redundant load-path structures at 500,000 cycles [14] with those proposed herein for: (1) weathering; and (2) weathering and corrosion fatigue. The reductions are largest for Category A and diminish with increasing severity of the detail, that is K_f.

As an example, to assess the potential impact on existing highway bridge designs, the stress ranges were calculated at various details of simple-span bridges with multiple rolled beams [12,13] and compared in Fig. 5 with the values allowed by AASHTO and with those proposed herein. For the type of bridge examined, fatigue would control the design of unpainted Category A rolled beams and Category C diaphragm gussets. Transverse stiffeners in welded plate girders are another example of bridge details that would be affected.

In summary, weathering steels offer potentially large savings in maintenance costs and are basically a sound concept. Unpainted weathering steel should not be specified for structures exposed to a salt-bearing environment, as the Michigan experience shows [6] . In suitable applications, new designs should counter the anticipated losses in fatigue life with moderate reductions in allowable stress ranges, at low additional cost, and without sacrificing the economic advantages gained from reduced maintenance.

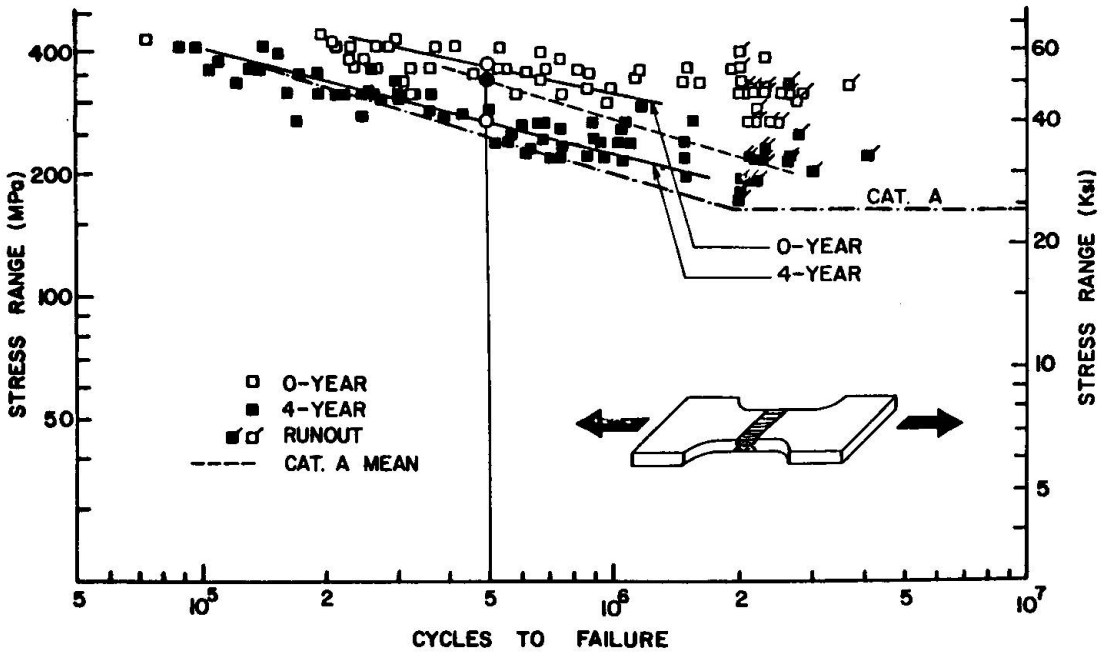

Fig. 1 Fatigue Strength of 4-Year Weathered Butt-Welded Ground Flush Specimens Fabricated from SMA steel [9].

Table 1 Summary of All Fatigue Test Data (Bold Exposure, Salt-free Environment)

Ref.	Type of Detail	No. of Specim. Tested	Weather. Time, in Years	Str. Range at 500,000 Cycles f_r(MPa)	Loss in Stress Range Δf_r(Pct)	Loss in Fatigue Life ΔN(Pct)	Fatigue Notch Factor K_f
			ASTM A588 and JIS SMA Steels				
9	Base metal	73	0	373	--	--	0.94
		56	2	287	23	54	1.22
		83	4	294	21	51	1.19
9	Butt weld	64	0	380	--	--	0.92
	ground	70	2	285	25	58	1.23
	flush	82	4	278	27	61	1.26
2	Transv.	12	0	221	--	--	1.59
	stiffener	16	3	189	15	38	1.85
4,7	Transv.	29	0	172	--	--	2.04
	stiffener	20	2 cont.	160	7	19	2.18
		16	2 alt.	175	2[a]	5[a]	2.00
		20	4 cont.	159	8	21	2.19
		16	4 alt.	163	5	15	2.15
4,7	102 - mm	24	0	179	--	--	1.95
	attachm.	15	2 cont.	177	--	6	1.98
		8	2 alt.	-	--	8[a]	--
		20	2 alt.	173	4	10	2.03
		8	4 alt.	-	--	9	--
			JIS SM Steels				
9	Base metal	62	0	359	--	--	0.98
		69	2	274	24	56	1.28
		85	4	265	26	60	1.32
9	Butt weld	50	0	362	--	--	0.97
	ground	71	2	272	25	58	1.29
	flush	88	4	264	27	61	1.33
10	Notched	11	0	506	--	--	0.69
	Plate	11	3	332	34	72	1.05
10	Notched	17	0	257[b]	--	--	1.36[b]
	plate	9	3	196[b]	24	55	1.79[b]
10	Butt weld	18	0	302	--	--	1.16
	as welded	10	3	252	17	42	1.39
10	Butt weld	41	0	396[c]	--	--	0.88[c]
	as welded	11	3	279[c]	30	65	1.25[c]

[a]Increase in life. [b]R = - 1; based on amplitude. [c]R = - 1; based on range.

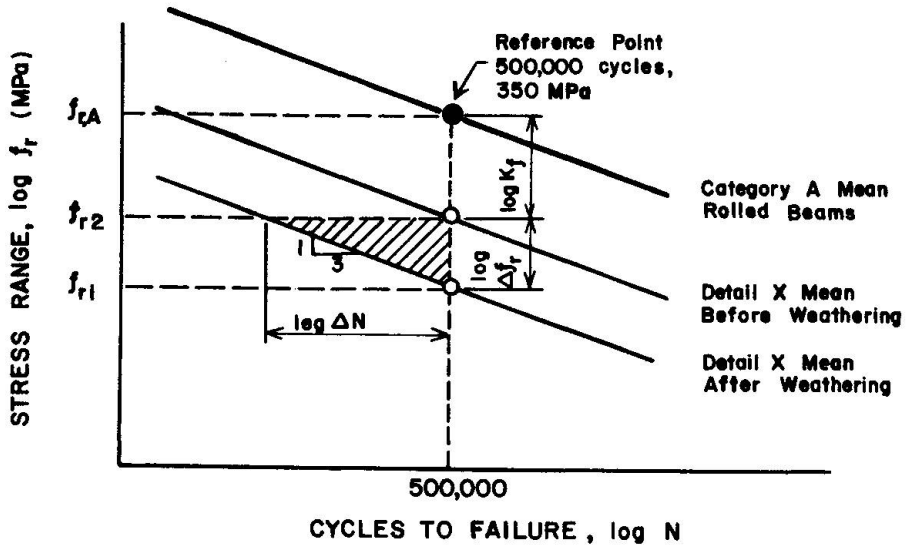

Fig. 2 Definition of Fatigue Notch Factor, Loss in Stress Range, and Loss in Fatigue Life.

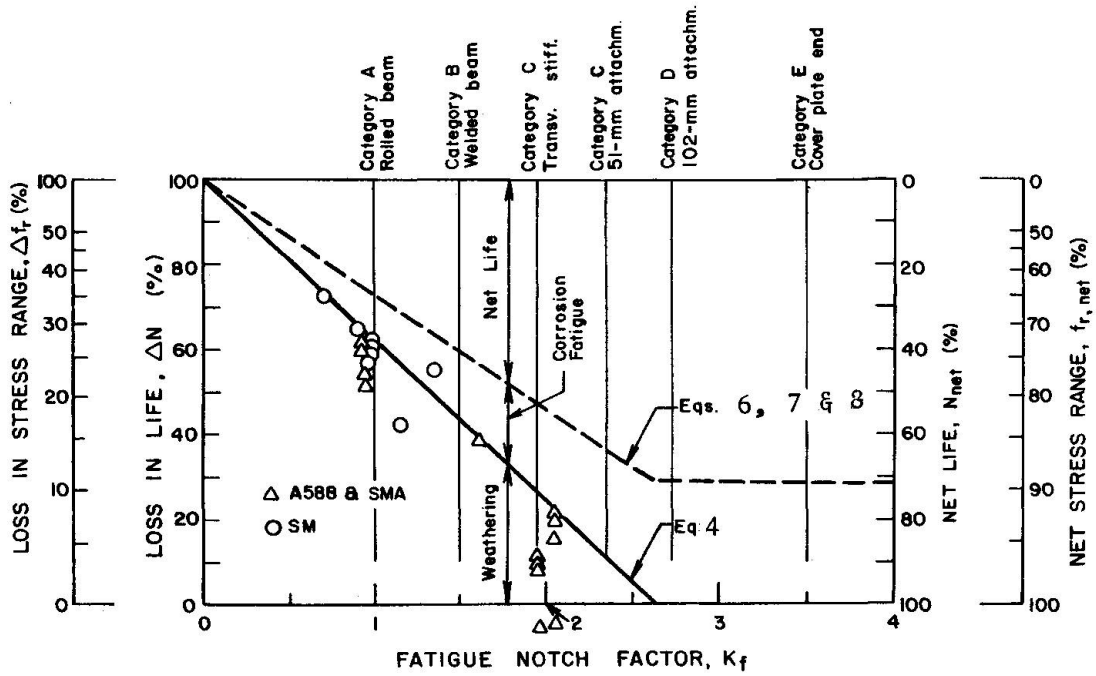

Fig. 3 Net Life and Net Stress Strange after Losses due to Weathering and Corrosion Fatigue.

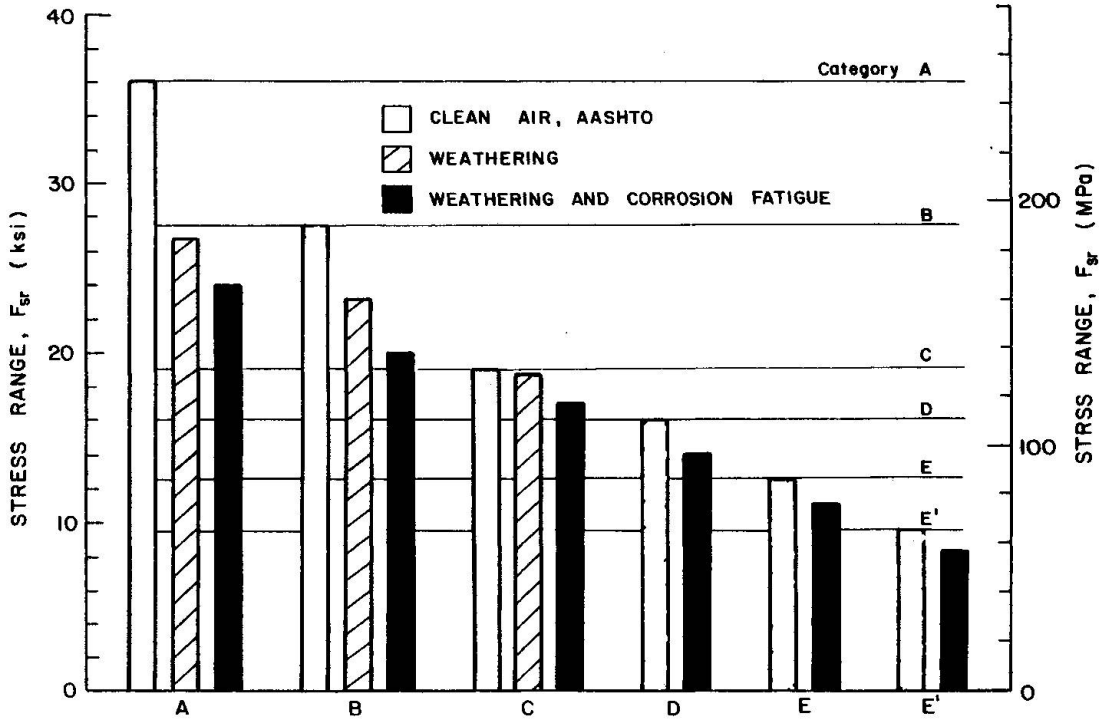

Fig. 4 Comparison of Allowable Stress Ranges for Redundant Load-Path Structures at 500,000 Cycles: (1) Current AASHTO, in Clean Air; (2) after Weathering; and (3) after Weathering and Corrosion Fatigue.

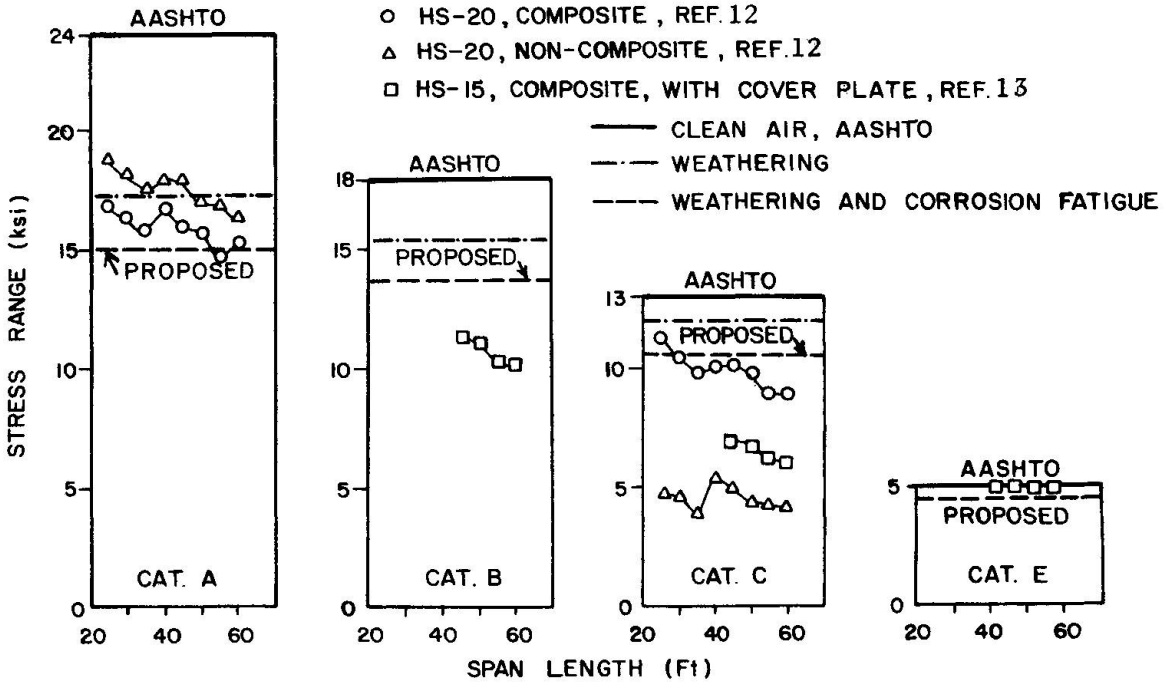

Fig. 5 Comparison of Calculated Stress Ranges in Simple-Span Bridges and Allowable Stress Ranges for: (1) Clean Air, Current AASHTO; (2) after Weathering; and (3) after Weathering and Corrosion Fatigue.

REFERENCES

1 Albrecht, P., "SEM Characterization of Naturally and Artifically Weathered A588 Steel," Scanning Electron Microscopy, Vol. 1, IIT Research Institute, Chicago, Illinois, March 1977.

2 Albrecht, P., and Friedland, I.M., "Fatigue Tests of 3-Year Weathered A588 Steel Weldment," Journal of the Structural Division, American Society of Civil Engineers, Vol. 106, No. ST5, May 1980.

3 Albrecht, P., and Simon, S., "Fatigue Notch Factors for Structural Details," Journal of the Structural Division, American Society of Civil Engineers, July 1981.

4 Albrecht, P., "Fatigue Behavior of 4-Year Weathered A588 Steel Specimens with Stiffeners and Attachments," Report FHWA/MD-81/02, Department of Civil Engineering, University of Maryland, College Park, Maryland, July 1981.

5 Barsom, J.M., and Novak, S.R., "Subcritical Crack Growth and Fracture of Bridge Steels," NCHRP Report 181, Transportation Research Board-National Research Council, Washington, D.C., 1977.

6 Culp, J.D., and Tinklenberg, G.L., "Interim Report on Effects of Corrosion on Bridges of Unpainted A588 Steel and Painted Steel Types," Report No. R-1142, Michigan Department of Transportation, Lansing, Michigan, June 1980.

7 Friedland, I.M., Albrecht, P., and Irwin, G.R., "Fatigue Behavior of 2-Year Weathered A588 Stiffeners and Attachments," Journal of the Structural Division, American Society of Civil Engineers, January 1982.

8 "Hot-Rolled Atmospheric Corrosion Resisting Steels for Welded Structure," Japanese Industrial Standard G 3114, Japanese Standards Association, Tokyo, Japan, 1977.

9 Kunihiro, T., Inove, K., and Fukuda, T., "Atmospheric Exposure Study of Weathering Steel," Research Lab. Report Br. 71-08, Ministry of Construction, Tokyo, Japan, 1972. (in Japanese)

10 Nihei, M., Yohda, M., and Sasaki, E., "Fatigue Properties for Butt Welded Joint of SM 50 A High Tensile Strength Steel Plate," Transactions of National Research Institute for Metals, Japan, Vol. 20, No. 4, 1978.

11 "Rolled Steels for Welded Structure," Japanese Industrial Standard G 3106, Japanese Standards Association, Tokyo, Japan, 1977.

12 "Short Span Steel Bridges," Report ADUSS 88-4551-02, United States Steel, Pittsburgh, Pennsylvania, November 1975.

13 Simon, S. and Albrecht, P., "Adding Fatigue Life to Cover Plate Ends," Journal of the Structural Division, American Society of Civil Engineers, Vol. 107, No. ST5, May 1981.

14 "Specifications for Highway Bridges," American Association of State Highway and Transportation Officials, Washington, D.C., 1977.

15 "Standard Specification for High Strength Low-Alloy Structural Steel with 50,000 spi Minimum Yield Point to 4 Inches Thick," ASTM Designation A588-80-a Annual Book of Standards, Part 4.

Fatigue Crack Growth in the Corner Weld of Box-Section Bridge Truss Chords

Propagation de fissures dues à la fatigue dans les soudures d'angle des membrures en caisson d'un pont à poutres en treillis

Analyse des Wachstums von Ermüdungsrissen an Ecknahtschweissungen von Trägergurten

CHITOSHI MIKI
Associate Professor
Inst. of Technology
Tokyo, Japan

FUMIO NISHINO
Professor
University of Tokyo
Tokyo, Japan

YASUAKI HIRABAYASHI
Engineer
Metr. Expressway Public Corp.
Tokyo, Japan

SUMMARY
Fracture mechanics concepts of fatigue crack growth are applied to investigate the effects of weld defects and residual stresses on the fatigue life of the corner welds in box-section members of a bridge truss.

RESUME
Les concepts de la mécanique de la rupture concernant la propagation de fissures dues à la fatigue, sont appliqués pour contrôler les effets des défauts de soudure et des contraintes résiduelles sur la durée de vie des soudures d'angle dans les membrures en caisson d'un pont à poutres en treillis.

ZUSAMMENFASSUNG
Konzepte der Bruchmechanik werden auf das Wachstum von Ermüdungsrissen angewandt. Dies erfolgt zur Untersuchung der Auswirkungen von Schweissnahtstellen und Restspannungen auf die Dauerfestigkeit von Ecknahtschweissungen an Kastenträgern.

1. INTRODUCTION

Recently in Japan, partially penetrated single-bevel-groove welding is usually employed for fabrication of box section truss member. For railway bridges in Japan [1], this joint is classified into Category A regardless of steels, which is the highest design fatigue allowable stress group in joint classification. (O - Tension : 150 MPa). The same value of allowable stress had been considered to be employed in Honshu-Shikoku Bridges which use up to 800 MPa class high tensile strength steel [2].

In the large-scale-model fatigue tests carried out by Honshu-Shikoku Bridge Authority in 1975 [3] and 1978, fatigue cracks occurred at corner weld of truss chord member after by far smaller number of repetitive loadings such as could hardly expected from the fatigue test results in the past. It was considered that these cracks were caused by such defects as bad penetration and blowholes at the root of corner weld, and extremely high tensile residual stress existed in the cracked zone.

The main objective of this paper is to clarify the properties of initiation and growth of fatigue cracks from the various weld defects at the root of corner welds. It is also examined that the influence of residual stress on fatigue crack growth rate. Furthermore, based on the results of these, fatigue crack growth life are predicted using fracture mechanics concept.

2. FATIGUE STRENGTH OF PARTIALLY PENETRATED LONGITUDINAL WELDS

2.1 Influence of Weld Residual Stress

Influence of residual stress was examined by comparing the fatigue strengths between joint specimens and small test pieces. Fig. 1 shows the configurations and dimensions of these specimens. Small test pieces were cut off from the weld zone of joint including weld root. Steel for testing was 800 MPa class high tensile strength steel. Both of joint specimen and small test piece were welded manually. The measured residual tensile stress in the direction of welded line was about 400 MPa in weld zone of joint specimen, while residual stress of small test piece was

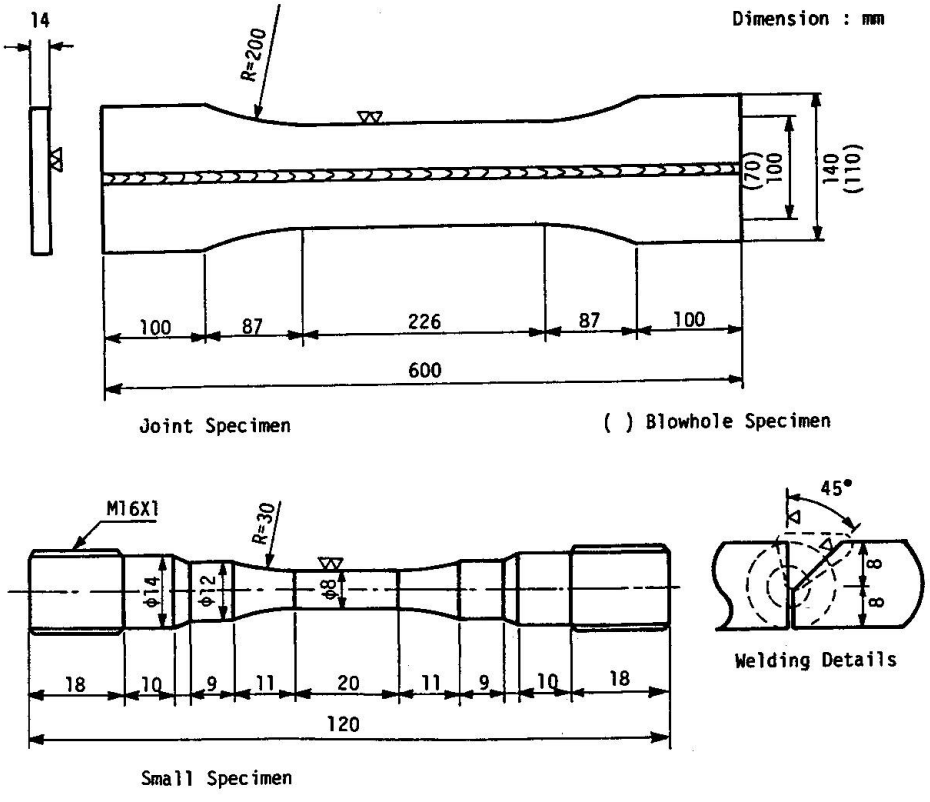

Fig. 1 Configurations and Dimensions of Specimens

completely released because this was extracted from weld zone of panel.

Fig. 2 shows the result of fatigue tests. The great difference is observed in fatigue strengths between joint specimens and small test pieces. Fatigue crack in both of joint specimen and small test pieces were initiated from root portion of weld. Considering the fact that in both type specimens the location of fatigue crack initiation are same and the cross sectional area is larger in joint specimen than that of small test piece, it is thought that the great difference of fatigue strength originated in residual stress.

2.2 Influence of Blowhole

Fig. 3 shows the results of fatigue tests of joint specimens containing blowholes in these root zone. Steel for specimen was 600 MPa class high tensile strength steel. The configuration and dimension of specimen are shown in Fig. 1. Submerged arc weld was employed for welding. Specimens were classified in accordance with the maximum width (w) of blowholes which was measured by radiographic examination. It was found that fatigue strength of no defect joint and small blowhole joint were almost same level, while fatigue strength remarkably decreased in proportion to blowhole getting larger. The occupation of blowholes in the cross sectional area was less than 0.7%, therefore area diminution by blowholes was negligible.

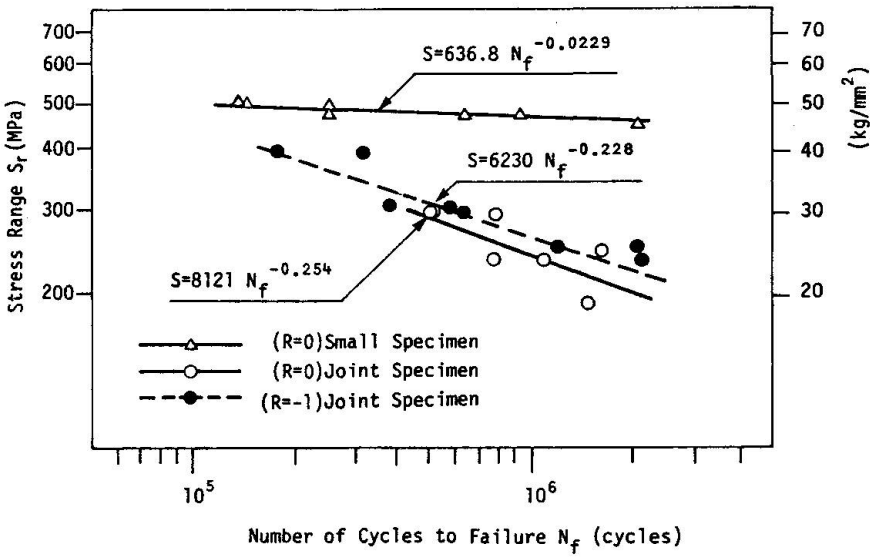

Fig. 2 Fatigue Test Results (Infruence of Residual Stress)

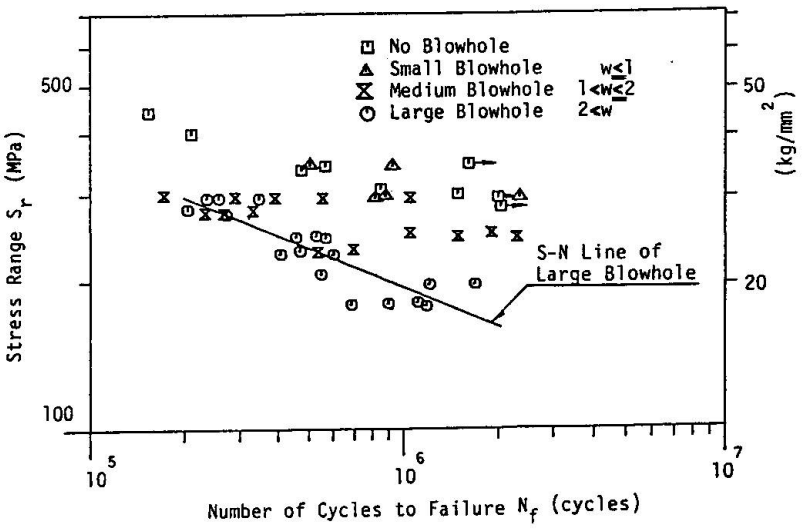

Fig. 3 Fatigue Tests Results (Influence of Blowhole)

3. INITIATION AND GROWTH OF FATIGUE CRACK

When stress condition is changed after a fatigue crack has initiated, the striae called beach mark is left on the fracture surface. In order to clarify the initiation

and growth properties of fatigue crack, beach marks were intentionally left on the fracture surface by reducing stress range to half (Beach mark test).

Fig. 4 shows the result of beach mark test on manually welded joint specimen. This specimen was failed out during the ninth halving of stress range and eight beach marks were left on the fracture surface. It is clear that the most inner beach mark was formed by the first halving of stress range. If crack initiation life (Nc) is defined as the number of cycles until formation of the most inner beach mark, Nc/Nf equals to 0.11. (Nf : failure life, Nc, Nf : not including the number of cycles in the period of stress range halving.) Therefore, most of the fatigue life was spent to the growth of fatigue crack. The initial fatigue crack was combined with the second crack which initiated shortly late, and the combined crack grew in the whole part of non weld zone while becoming circular. It was immediately before failure that this fatigue crack appeared at the surface of the specimen.

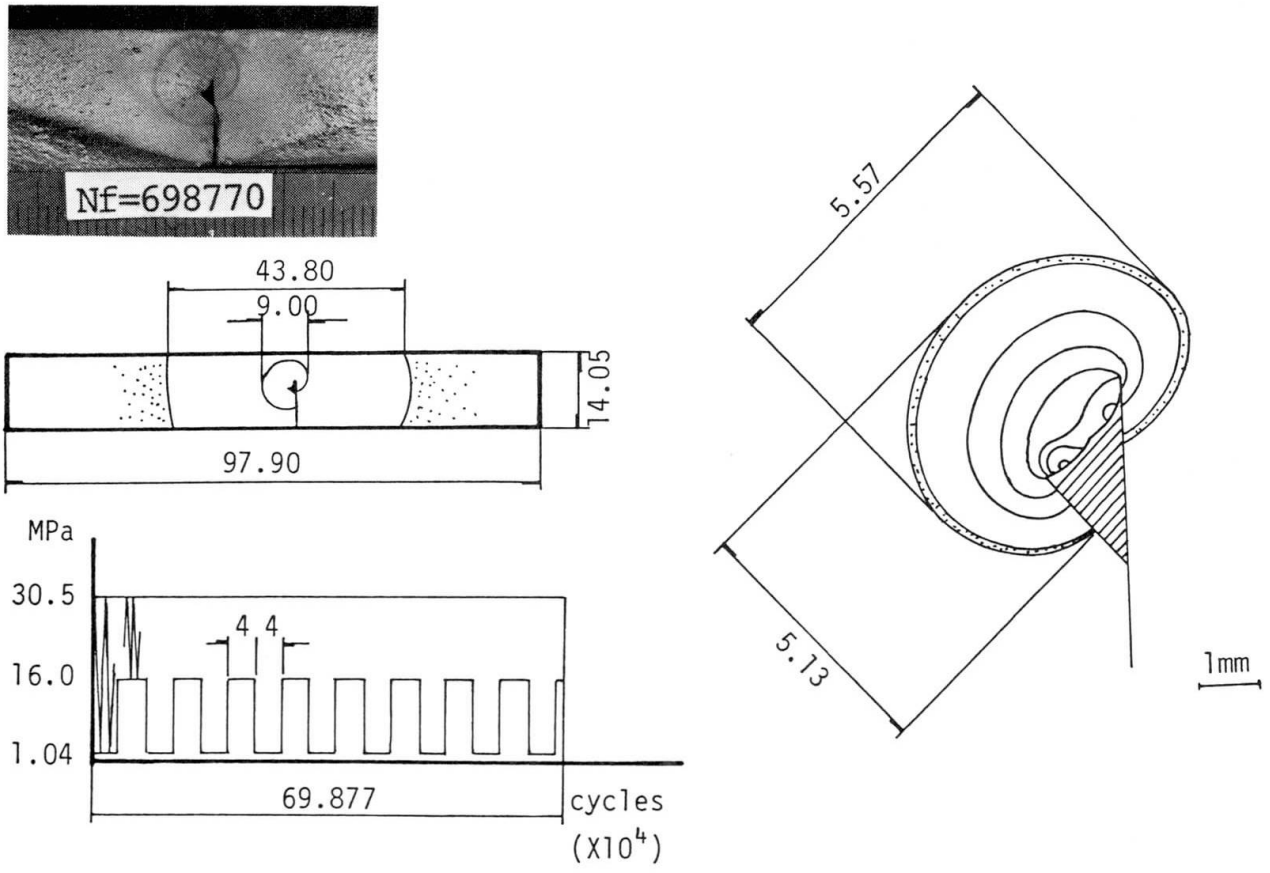

Fig. 4 Result of Beach Mark Test (Manually Welded Joint)

Fig. 5 shows the results of beach mark tests performed to submerge arc welded joint specimens. By radiographic examination given before test, specimen No. 2 was classified into no defect, No. 45 to medium blowhole, and B16 into large blowhole. In the specimen No. 2, fatigue crack was initiated from microscopic blowhole which existed in root zone, and grew into orbicular shape. In No. 45, fatigue crack was initiated from several points of the wall of tubular blowholes at the almost same time and grew into semi-circular shape. In B16, fatigue crack was initiated in the bottom face which contained semi-spindle shape blowholes and grew into semi-circular shape. The dimensions (width x depth) of beach marks at the most inner side of each specimen No. 2, No. 45 and B16 are 0.5 x 0.3 mm, 0.6 x 0.2 mm, and 1.3 x 1.6 mm respectively. Nc/Nf was 0.76, 0.44 and 0.24 respectively.

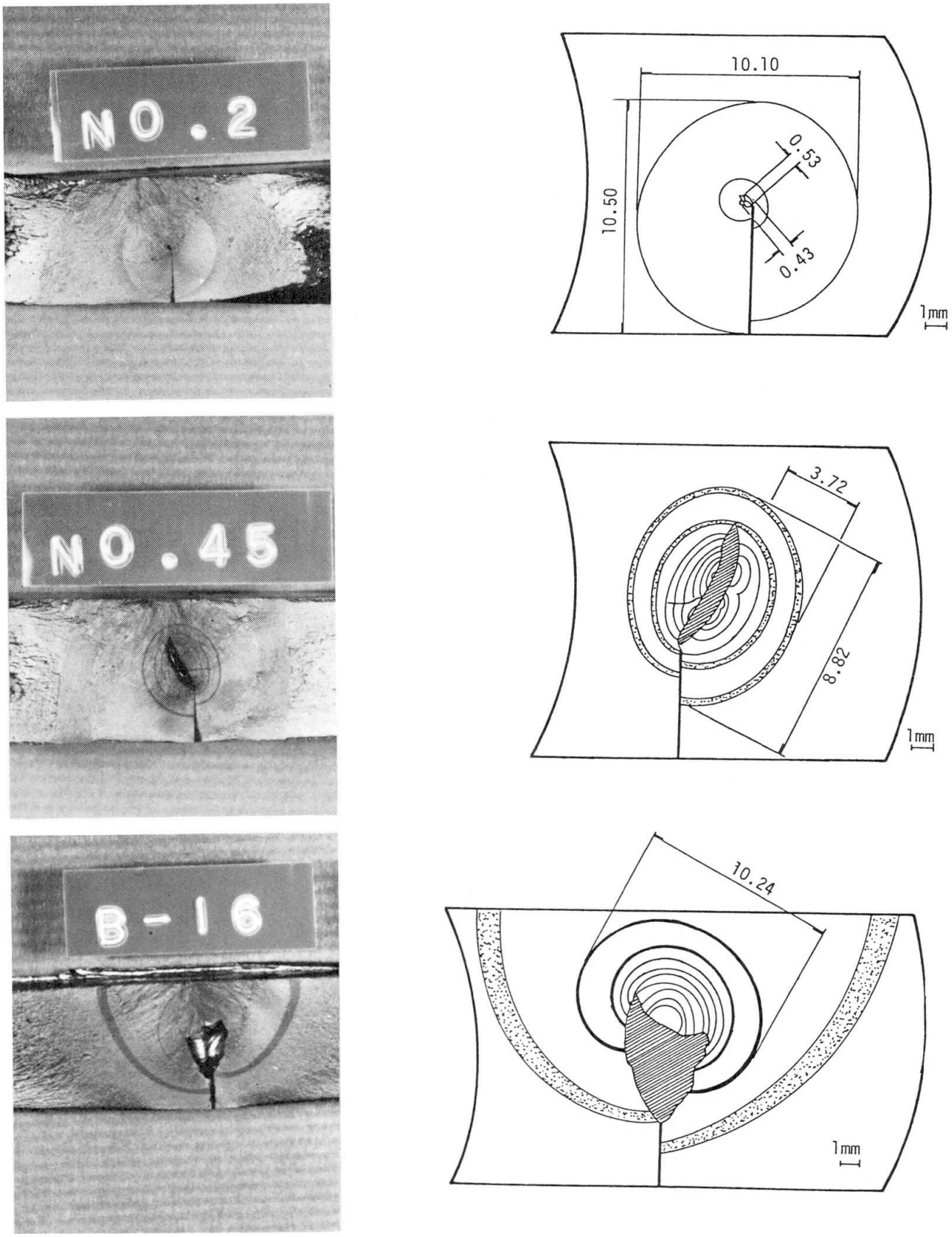

Fig. 5 Results of Beach Mark Tests (Blowhole Specimens)

4. INFLUENCE OF RESIDUAL STRESS ON FATIGUE CRACK GROWTH RATE

Fatigue crack growth tests were performed using center-crack-specimens shown in Fig. 6. Steel for testing was 800 MPa class high tensile strength steel. Weld residual stress was introduced by placing one longitudinal weld bead on the specimen. After measuring weld residual stress, it was found that 400 - 500 MPa of axial tensile residual stress existed in B-I and B-II type specimen. In A-II type specimen, 100 MPa of tensile residual stress also existed.

Fig. 7 shows the relation between fatigue crack growth rate (da/dN) and stress intensity factor range (Δk). In the region where Δk exceeds 16 MPa$\sqrt{m}$, any difference was not observed in da/dN - Δk relations in four types of specimens. However, in A-1 type specimen, fatigue crack growth rate rapidly decreases in the region where Δk is under 9.5 MPa $\sqrt{m}$ and threshold stress intensity factor range (Δk_{th}) is 9.0 Mpa $\sqrt{m}$. In other three types of specimen, Δk_{th} is 2.5 MPa $\sqrt{m}$. From this observation, it can be said that influence of residual stress is distinguished in the low Δk region.

The following equation is employed for obtaining relation among da/dN - Δk and Δk [4].

$$da/dN = c(\Delta k)^m - c(\Delta k_{th})^m \quad (1)$$

c, m maintains 5.47 x 10 and 3 respectively for quench and tempered steels by adjusting much of data. The two curves in Fig. 7 shows the result of calculation under which c, m and Δk_{th} = 9.0, 2.5 was put into the eq. (1). Both of two curves show good coincidence with the experimental values.

5. PREDICTION OF FATIGUE CRACK GROWTH LIFE

Fatigue crack growth life (Np) was predicted based on the following

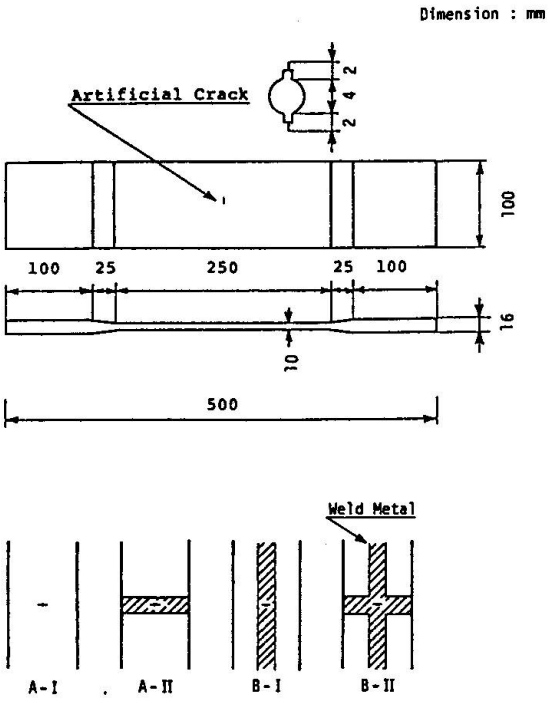

Fig. 6 Specimen for Crack Growth Tests

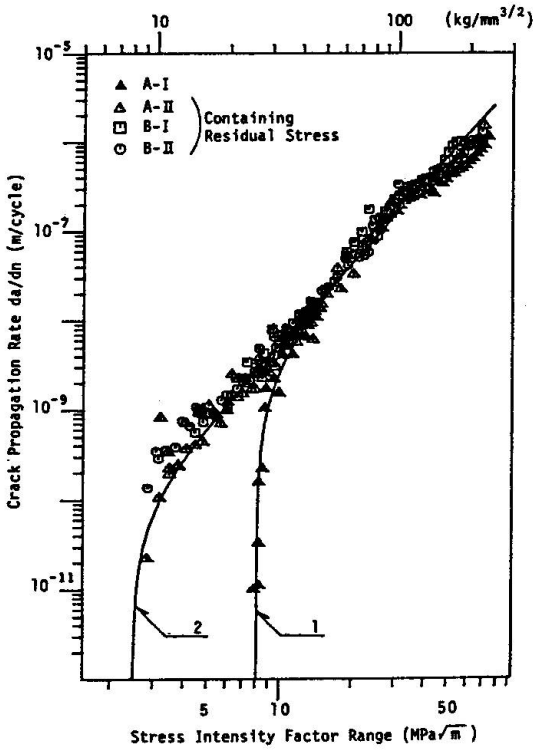

Fig. 7 Fatigue Crack Growth Rate

assumptions.

(i) The initial defect is regarded as a penny-shape crack. Fatigue crack grows keeping penny shape. Consequently stress intensity factor against this crack is calculated by the Eq. (2).

$$\Delta K = S_r\sqrt{\frac{\pi a}{Q}}\sec(\pi a/t)\ (1 - 0.025\lambda^2 + 0.06\lambda^4)$$
$$Q = \{E(h)\}^2 - 0.212\ (\sigma/\sigma_Y)^2 \qquad (2)$$

where
ΔK : Range of stress intensity factor
S_r : Stress range
a : Radius of a crack
Q : A parameter of defect form
E(h): Complete elliptic integral of the second kind, equal here to $\pi/2$
λ : 2a/t
t : Plate thickness

(ii) The final crack size (af) is supposed to be 90% of the distance from the point of crack initiation to the plate surface.

(iii) Regarding to the relation of da/dN - Δk, the curve 1 in Fig. 7 is employed for the case that fatigue crack grows in the field where weld residual stress does not exist, and the curve 2 in Fig. 7 for the growth in tensile residual stress field.

Fig. 8 shows the result of prediction of fatigue crack growth life corresponding to the results of experiment shown in Fig. 2. The initial crack size (ai) was supposed to be 0.2mm. A radius of inscribed circle to non weld metal zone which remained in the root zone was 0.3 - 0.5 mm, therefore ai was a little bit smaller than that. The predicted Sr - Np life curve in both of joint specimen and small test piece showed a good coincidence with that of experimental results. (Sr - Nf). Accordingly it is clear that the big difference of fatigue strength between joint specimen and small test piece is caused by the acceleration of fatigue crack growth rate by residual tensile stress especially in the low Δk region.

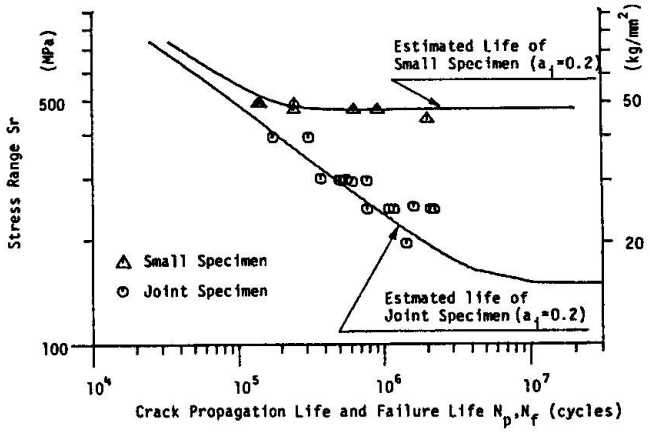

Fig. 8 Predicted S-Np Curves and Test Results (Manually Welded Joints)

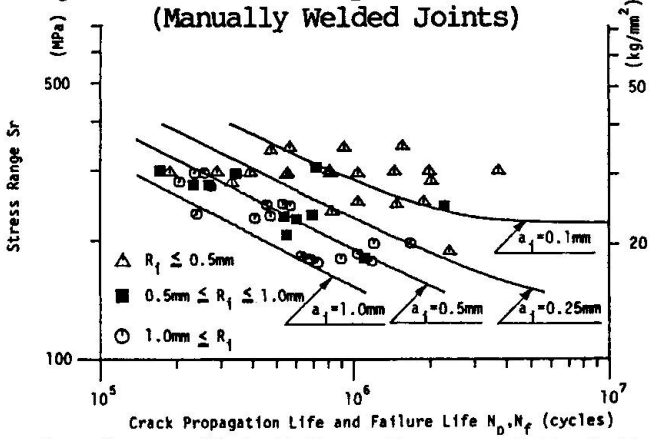

Fig. 9 Predicted S-Np Curve and Test Results (Blowhole Joints)

Fig. 9 shows predicted fatigue crack growth life

corresponding to that of experiments shown in Fig. 3. The initial crack size (ai) was supposed to be 0.1, 0.25, 0.5, 1.0 and 2.0 mm. The test value (Sr - Nf) were classified and plotted in accordance with a radius of inscribe circle of blowhole. The test results which were classified into Ri = 0.5 varies in wide range, however, predicted Sr -Np curve based on assumption of ai = 0.5 is positioned at rather long life side. This is due to the fact that a pretty lot of stress repetition was needed until the occurrence of fatigue crack. The test results which were classified into 0.5 Ri 1 were plotted between predicted Sr -Np curves of ai = 0.5 and ai = 1.0. Most of the test results which were classified into 1 Ri were plotted at the longer life side than predicted Sr - Np curve of ai = 1.0. Replacement of blowhole to the initial crack of inscribed circle dimension means prediction of life of lower bound [5], while this estimation had a good coincidence with test results, and never gave risk side predicted results.

6. CONCLUSIONS

The principal results obtained in this study are as follows.

(1) In partially penetrated longitudinal weld, the reduction in fatigue strenth due to welding residual tensile stress is very substantial. As the blowholes in weld root become larger, the fatigue strength decreases.

(2) Fatigue crack is initiated and begin to propagate at extremely early stage of stress repetitions. Fatigue crack propagate while becoming circular.

(3) The influence of residual tensile stress on fatigue crack growth rate is distinguished in the low Δk region.

(4) The predicted Sr - Np curves obtained based on the results above are very close to the experimental results in various kinds of longitudinal welds.

REFERENCES

1) JSCE : The Specifications of Steel Railway Bridges, 1974 (in Japanese)
2) JSCE : Fatigue Design for Honshu-Shikoku Bridges, 1974 (in Japanese)
3) Tajima J., A. Okukawa, M. Sugizaki and H. Takenouchi : Fatigue Tests of Panel Point Structures of Truss Made of 80kg/mm High Strengh Steel, IIW, Doc, No. XIII-831-77, July, 1977
4) Klensnil M. and P. Lukas, Effect of Stress Cycles Asymmetry on Fatigue Crack Growth, Mat. Sci. Eng., 9-4, 1972
5) Hirt M. A. and J. W. Fisher : Fatigue Crack Growth in Welded Beams. Engineering Fracture Mechanics, Vol. 5, 1973

Fatigue of Nodal Joints and Box-Section Members in a Bridge Truss

Fatigue des joints soudés, des membrures en caisson dans un pont à poutres en treillis

Ermüdungsfestigkeit von Schweissverbindungen in den Gurten eines Brücken-Fachwerkträgers

JIRO TAJIMA
Professor
Saitama University
Saitama, Japan

TATSUO ASAMA
Manager of Design
Honshu-Shikoku Bridge Authority
Tokyo, Japan

CHITASHI MIKI
Assoc. Professor
University of Tokyo
Tokyo, Japan

HIROYUKI TAKENOUCHI
Researcher
Japan Constr. Method and Machinery Res. Inst.
Shizuoka, Japan

SUMMARY
This paper describes tests to verify the fatigue strength of welded joints in quenched and tempered high strength steel. Typical welded joints from a bridge truss were tested in a 400 t maximum capacity fatigue testing machine.

RESUME
Cet article décrit des essais destinés à vérifier la résistance à la fatigue des joints soudés en acier à haute résistance trempé et revenu. Des assemblages soudés typiques d'un pont à poutres en treillis ont été essayés au moyen d'une presse pour essais de fatigue dont la capacité maximale de charge dynamique est de 400 t.

ZUSAMMENFASSUNG
Der Beitrag behandelt die Ermüdungsfestigkeit geschweisster Verbindungen aus hochwertigem Stahl. Typische Schweissverbindungen von Fachwerkträgern wurden mit einer 400 t Presse für dynamische Lasten geprüft.

1. INTRODUCTION

The Kobe-Naruto and Kojima-Sakaide routes of the Honshu-Shikoku bridges in Japan are designed to be of the highway and railway combination type. Consequentry, fatigue due to live load will pose a problem of grave imfortanse. The fatigue design criteria had been set in 1974 [1][2] based on results of past fatigue tests on various joints. However, configurations and dimensions of test specimens in past tests were fairly restricted due to limitaions in the capacities of testing machines. Considering the scale of the actual structures which will use of maximum plate thickness of 75mm, it is necessary to verify the appropriateness of this fatigue design criteria using larger specimens and structural models. Accordingly, Honshu-Shikoku Bridge Authority has had a fatigue testing machine of capacity of 400 ton made and is now carrying out fatigue tests of joints and parts of structures. This paper describes the results of fatigue tests on partially penetrated longitudinal groove welded joint and non-loadcarring cruciform fillet welded joint which are typical weld joints of truss members, and box section members and truss panel point structures as their composite structures.

2. SPECIMENS

2.1 Joint Specimens

The mechanical properties of the steels used for joint specimens are shown in Table 1. Fig. 1 shows the configurations and dimensions of the specimens. The non-loadcarrying cruciform fillet welded joint (a) simulates the stress condition at the joint of a diaphragm attached to a chord member of a truss. Welding was done manually using an electrode exclusively for fillet welds

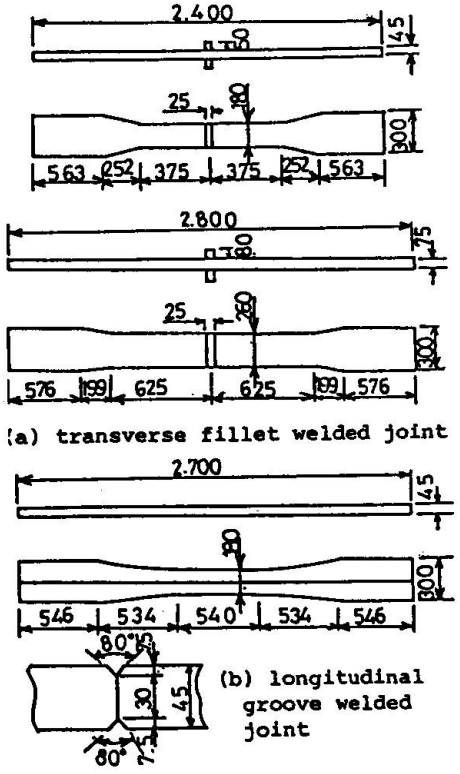

Fig. 1 Joint Specimen

Specimen	Steel	Thickness (mm)	Y.P (N/mm²)	T.S. (N/mm²)	El (%)
Joint Specimens	HT80	45	775	823	24
		75	813	862	24
Box Section BB, BA	HT80 (Flg.)	15	764	823	28
	(Web)		833	882	29
BD, BE, BF	HT80	15	794	843	26
Truss Panel Point					
A, B, C	HT80 (Flg.)	15	804	853	30
	HT80 (Web)	15	813	862	30
D, E, F	SM58	15	559	647	36
G	HT80	15	784	823	31
H	HT80	15	794	843	30

Table-1 Mechanical Properties of Steels

said to produce a regular bead shape as shown in Fig. 2. Leg length of fillet welds for 45mm thickness specimens and 75mm thickness specimens are 10mm (two paths) and 13mm (three paths) respectively. Partially penetrated longitudinal groove weld joint simulate for corner welds of truss members with box section. Welding was done using the submerged arc process.

2.2 Specimens of Box Section

The mechnical properties of the steels used for specimens of box section are shown in Table 1. Fig. 3 shows the configurations and dimensions of the specimens. Type BA has a diaphragm used SM41 steel at the center of the specimen, and other types have no diaphragm. Welding of the diaphragm was done manually using the same electrode used for joint specimens mentioned above. Corner Welding of these specimens were conducted with automatic welding. Kinds of welding are shown in Table 2. Three types, BB, BD, BF, were with partially penetrated groove welds and one type, BF, was with fillet welds.

2.3 Truss Panel Point Structures

The mechnical Properties of the steels used for truss panel point structures are shown in Table 1. Fatigue tests were performed using the loading apparatus shown in Fig. 4. The hatched portion in the figure represents a specimen. Fig. 5 gives details of the vicinities of panel points of eight varieties of test specimens. The major points of difference between the each types lie in the methods of connecting the diagonal members, the numbers of diaphragms and fillet radii of gusset plates. Corner welds of chord members were made by manual welding for the specimens A, B and C and by the submerged-arc welding for D, E, F, and G. Kinds of Corner welds are single bevel groove welds, and bevel angle is 45°, depth is 7.5mm for type A, B and C, 8mm for type D–G.

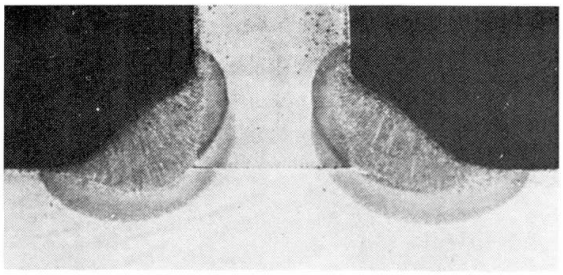

Fig. 2 Shapes of Fillet Welds

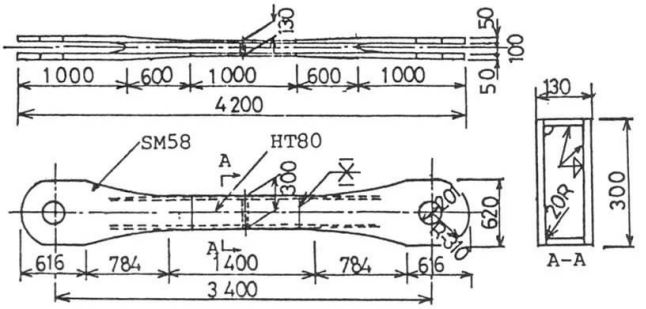

Fig. 3 Box Section Specimen

3. RESULTS OF TESTS AND DISCUSSIONS

3.1 Transverse Fillet Welds

Fig. 6 shows the results of fatigue tests on cruciform joint specimens, box-section specimens with diaphragm and panel point structures concerning about transverse fillet welds. Twelve cruciform joint specimens of t = 45mm and three cruciform joint specimens of t = 75mm

Type of T.P.	BA,BB	BD	BE	BF
Method of Weld	SAW (Single)	MIG	SAW (Double)	SAW (Single)
Kind of Joint	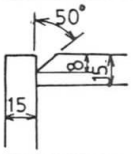	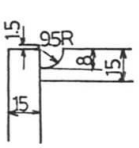	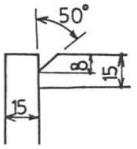	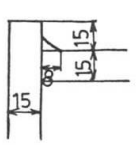
No. of Path	1	3	1	1

Table-2 Kinds of Corner Welding

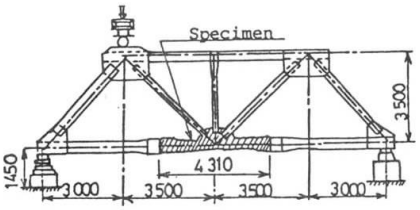

Fig. 4 Truss Type Loading Apparatus

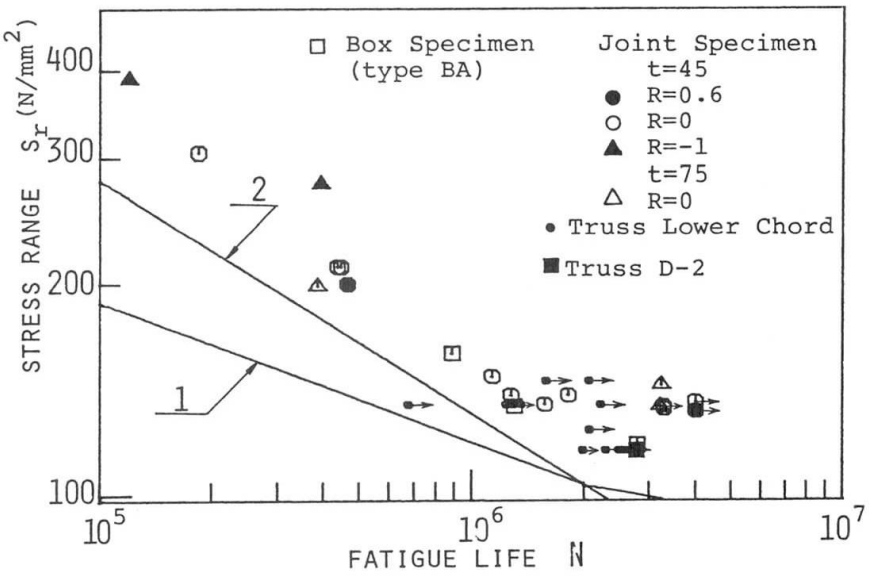

Fig. 6 Results of Fatigue Tests on Transverse Fillet Welds

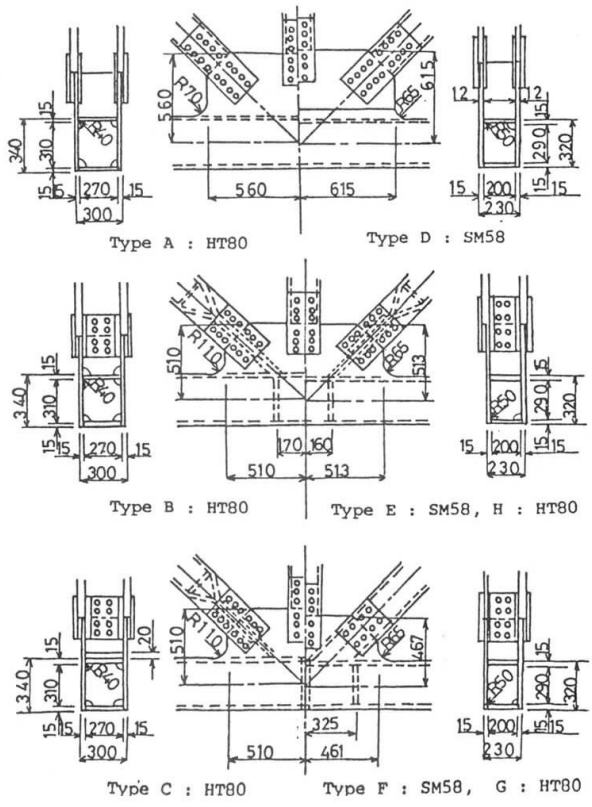

Fig. 5 Truss Panel Point Structures

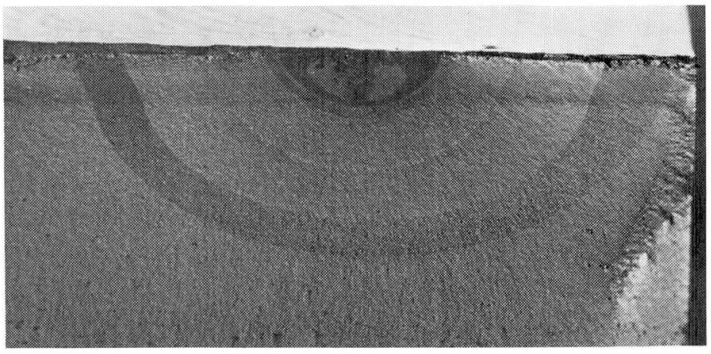

Fig. 7 Fracture Surface of Cruciform Joints

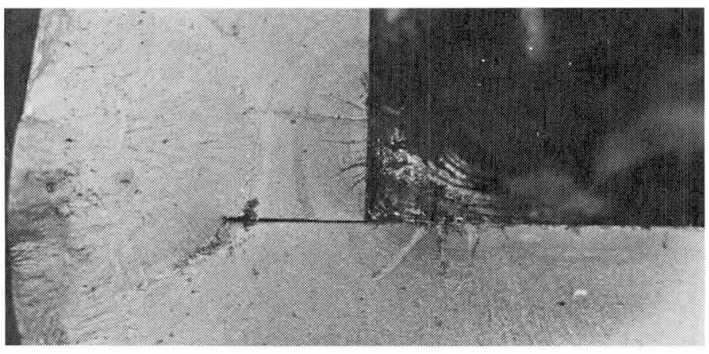

Fig. 8 Fracture Surface of Box Section Specimen

were tested. With joint specimens of t = 45mm, fatigue tests were performed with stress ratios (R) at 0.6, 0 and -1. The influences of differences of mean stress on fatigue strength are not very prominent. Differences in fatigue strengths depending on differences in plate thickness of base metals were also small. Fatigue cracks were initiated at the toe of first path fillet welds in most specimens, but in some specimens cracks were initiated at the toe of second path welds.

With one joint specimen of t = 45mm, two stage multi-stress amplitude test was performed to form the beach marks on the fracture surface (Beach mark test). Fig. 7 shows the result of beach mark test. In this figure, five beach marks can be counted, and numbers of loading block for this specimen are also five. So it was found that the fatigue crack had initiated at the first stress block (prior to 0.18 N with N_f being failure life) from the concave part at the toe of fillet weld.

Three specimens of box-section with diaphragm (Type BA) were tested. In Fig. 6 the results of these tests are plotted. Fig. 8 shows fracture surface of BA-1 specimen. With these three specimens, beach mark tests were performed. Fatigue cracks initiated at the corner of fillet welds of diaphragms at the early period in the life.

In Fig. 6, results of tests on panel point structures are also plotted. In these tests only one fatigue crack was occurred at the toe of fillet welds of diaphragms arranged in the chord members of D type specimen. Line 1 in Fig. 6 shows the former design allowable stress [3] for this type of joint under pulsating stress for the Honshu-Shikoku bridges. All of the test results satisfy the requirement of this criterion. However, the slope of line 1 is too gentle in comparison with the test results. Line 2 in Fig. 6 shows the current design allowable stress for this type of joint. This curve is revised based on the fatigue test results and the analysis of fatigue life by fracture mechanics concept.

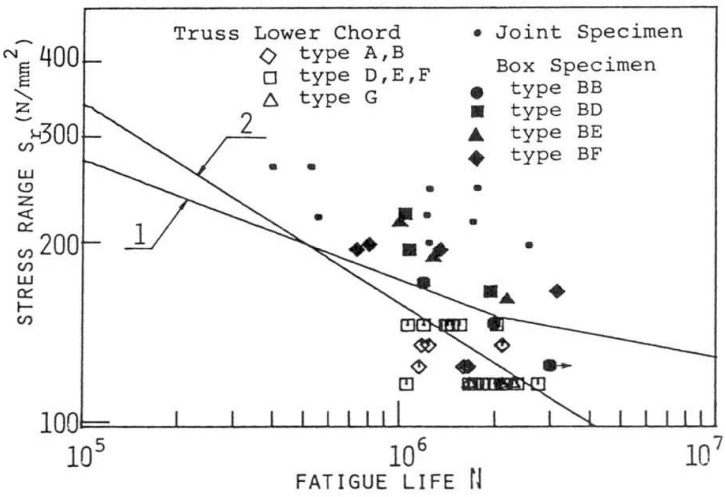

Fig. 9 Results of Fatigue Tests on Longitudinal Welds

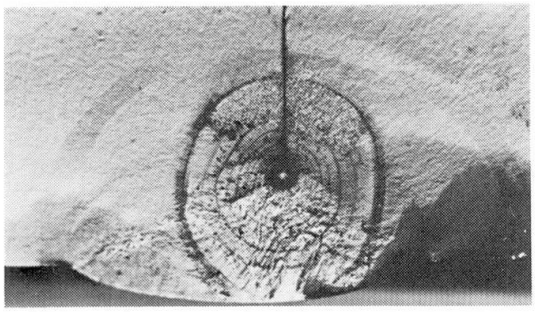

Fig. 10 Fracture Surface of Longitudinal Weld Joint

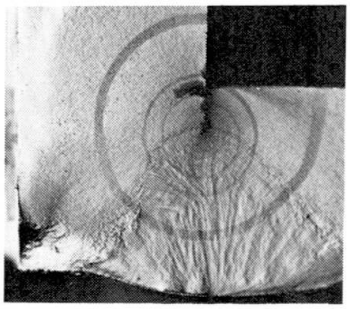

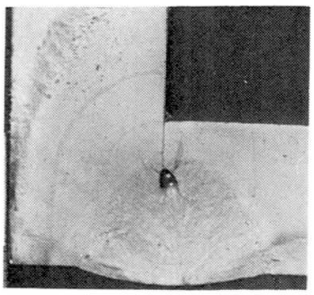

Fig. 11 Fracture Surface of BB-1 Specimen

Fig. 12 Fracture Surface of BE-2 Specimens

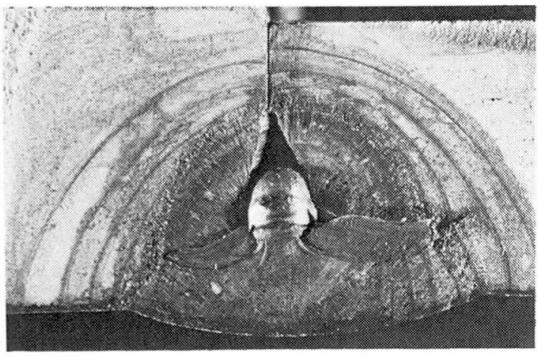

Fig. 13 Fracture Surface of Truss Lower Chord

3.2 Longitudinal Welds

Fig. 9 indicates the results of fatigue tests on longitudinal weld joints, box section specimens and panel point structures concerning about longitudinal welds. With longitudinal weld joints, initiation points of fatigue cracks in six out of the entire nine test specimens were blowholes or pores existing at roots of welds, the size being 0.6 to 1.2mm in diameter. Other initiation points were a small pit at bead surface, grinder scratch at surface of base metal and defect at part of base metal reparied by welding. Residual tensile stresses of approximately 340 N/mm^2 and 250 N/mm^2 were measured at joints of an unloaded specimen and an after fatigue test specimen, respectively.

Beach mark tests were performed with three joints specimens. Fig. 10 shows the fracture surface with beach marks. Fatigue crack had been initiated from the wall of a blowhole at the root of weld. In this fracture surface, thirty beach marks can be counted and numbers of loading block are thirty four so the fatigue crack of this specimen had started growing before 0.12 N_f cycles of loading.

With box section specimens, each three test specimens of type BB, BD and BE, and four of type BF were tested. Results of fatigue tests on these specimens are shown in Fig. 9. The locations of fatigue crack initiation in each type of specimens are as follows.

BB type : blowhole (2.5 x 1.8, 4.1 x 3.4mm) at the root of welds.
BD type : bead surface, blowhole (3.9 x 3.6mm) at the root of welds and imperfection of weld metal.
BE type : weld root (no blowhole) and blowhole (1.1 x 0.5, 1.4 x 0.7mm) at the root of welds.
BF type : slag inclusions at the end of butt joint (2 specimens) and slag inclusions at the toe of fillet weld and root.

Fig. 11 and 12 shows the fracture surface of BB-1 and BE-2 specimens.

Test specimens type BB were fabricated as the first series of test. Type BD, BE and BF were second test series, and much attention were paid in corner welding to avoid the occurance of imperfection or defect in the root of welds. In the results of fatigue tests fatigue strength of second series can be seen about 20 N/mm^2 higher than those of first series. These results are due to size of blow holes at the root of welds, and when the size of blowhole is 2mm or so, the influence of blowhole on the fatigue strength seems to be comparable to other imperfection, such as irregularily of bead surface and root line and small blowhole of butt joints near the surface of plate.

Fatigue tests on truss panel point structures were performed on two specimens each of type A - G.

All specimens except C-1 and C-2, fatigue tests were terminated by growth of fatigue cracks initiated at corner welds of bottom chord members. The relation between nominal stress range and number of cycles of stressing the fatigue crack was discovered at a bottom chord is shown in Fig. 9. In the type A and B specimens fatigue cracks at corner welds were initiated from irregularities at the roots of welds due to nonfusion or lack of penetration. The number of fatigue cracks initiated in the four specimens of type A and B was 13, with surface length from 9mm to 310mm. In the type D, E, F, and G specimens most of fatigue cracks were initiated from blowholes existing at the roots of welds. Fig. 13 shows one example of fracture surface of corner welds. In E-2 and G-1 each one crack occurred at the corner of butt joint of lower chord member, where some small pits existed near the surfaces of plates. The number of fatigue cracks initiated in the eight specimens of type D, E, F and G was 30, with

surface length 4 to 87mm.

In Fig. 9, line 1 shows the former design allowable stress and line 2 shows the current design allowable stress for this type of joints under pulsating stress. Most of experimental values of panel point structure specimens are below the former design allowable stress. Furthermore, about half of experimental values of panel point structure specimens are below the current design allowable stress. The current design allowable stress is established based on the fatigue test results of box section specimens and the analysis using fracture mechanics concept. From that analysis, weld defects as blowholes exceeding 1.5mm in diameter of inscribed circle must be avoided to remain therein.

3.3 Gusset plate

With truss panel point structure specimens, fatigue cracks were initiated in gusset plates of three specimens B-1, C-1 and C-2 in the fatigue tests. Fig. 14 shows the position of these fatigue crack occurrences at gusset plates. These fatigue cracks were all initiated from the end of fillet welds close to bottom chord member flanges of plates inserted diagonally between the gusset plates at both sides. Repeated stresses measured at outer surfaces of gusset plates of these position and number of loading cycles are shown in Table 3. Stresses at fatigue crack initiation point are expected to be higher than these values in Table 3, because at that point, there are stress concentration due to the stop of weld bead and out-plane bending. In the Table 3, N_C is loading cycles when cracks were observed at the first time, and crack length are 25mm in B-1 and 10mm in C-2. In the specimen C-1, cracks occurred at both sides of gusset plates and propagated to free edge of plates.

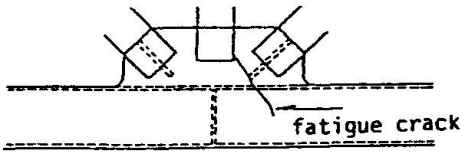

Fig. 14 Fatigue Crack in Gusset Plate

Type of T.P.	Stress Range (N/mm^2)	Nc ($\times 10^5$)	N_f ($\times 10^5$)
B-1	94	4.14	12.38
C-1	83	—	6.77
C-2	64	3.07	13.59

Table-3 Results of Fatigue Tests on Truss Panel Point Structures, type B-1, C-1 and C-2

4. CONCLUSIONS

The design allowable fatigue stress for the Honshu-Shikoku Bridge were revised based on the fatigue test results mentioned here and the analysis of fatigue life by fracture mechanics concept. All of the fatigue results of non-loadcarrying transverse fillet weld satisfied the requirement of this revised criteria. However, with the corner welds of truss chords, when weld defects of large size are contained at the root of welds, fatigue failures occurred under fairly low stresses which are below the allowable stress. Therefore, it is necessary to fabricated the members carefully to avoid the defects at the root of corner welds.

REFERENCE

(1) Japan Society of Civil Engineers : Fatigue Design for Honshu-Shikoku Bridges, 1974 (in Japanese)

(2) Tajima J., Okumura A., Tanaka Y. : Fatigue Design Criteria on Honshu-Shikoku Suspention Bridges, 10th Congress of IABSE, Sept, 1976

(3) Design Standard for Super Structures, 1981, Honshu-Shikoku Bridge Authority

Leere Seite
Blank page
Page vide

Fatigue Life Estimation Using Fracture Mechanics

Estimation de la durée de vie à l'aide de la mécanique de la rupture

Lebensdauerberechnung mit den Methoden der Bruchmechanik

K. YAMADA
Assistant Professor
Nagoya University
Nagoya, Japan

M.A. HIRT
Professor
ICOM – Construction Métallique
Lausanne, Switzerland

SUMMARY

The main portion of the fatigue life of welded details with weld defects or high stress concentrations is taken up by fatigue crack propagation. It can be conveniently analyzed using fracture mechanics. Fatigue crack propagation behaviour of tensile plates with fillet welded attachments (gusset specimens) is investigated experimentally and analytically. The results are extended to estimate the fatigue crack propagation life of beams with attachments welded to the flange tip or the web. The analytical results are generally in good agreement with test results.

RESUME

La plus grande partie de la durée de vie est absorbée par le temps nécessaire à la propagation des fissures de fatigue dans les détails constructifs soudés comportant des défauts de soudure ou des concentrations de contraintes importantes. Cette propagation des fissures peut être décrite analytiquement par les méthodes de la mécanique de la rupture. Cette analyse a été appliquée à l'étude du comportement à la fatigue d'éprouvettes avec goussets soudés et vérifiés expérimentalement. Les résultats ont ensuite été étendus aux poutres munies de goussets soudés à l'aile ou à l'âme. Les résultats de l'analyse théorique correspondent généralement bien aux résultats d'essais.

ZUSAMMENFASSUNG

Die Lebensdauer von geschweissten Konstruktionen, die Schweissfehler oder hohe Spannungskonzentrationen enthalten, wird im wesentlichen durch das Wachstum der Ermüdungsrisse bestimmt; dieses kann mit den Methoden der Bruchmechanik analytisch beschrieben werden. Das Ermüdungsverhalten von Zugproben mit aufgeschweissten Knotenblechen wird experimentell und analytisch untersucht. Die Resultate werden auf Träger übertragen, welche mit am Flansch oder am Steg angeschweissten Knotenblechen versehen sind. Die rechnerischen Werte stimmen gut mit den Versuchsresultaten überein.

1. INTRODUCTION

The fatigue life of structural details containing weld defects or high stress concentration can be analyzed using fracture mechanics methods [1] [2]. In order to use this extensively, knowledge of the fatigue crack behavior at an early stage of fatigue crack propagation is important. In fact, during this stage a large portion of the fatigue life elapses.

The fatigue crack propagation behavior in the early stages of fatigue is especially monitored by a dye-marking technique on specimens with longitudinal attachments. The test results are used to verify the analytical procedure. Based on these experiences, the fatigue crack propagation life of attachments (gussets) welded to the flange tip or to the web of beams are computed and compared with test results.

2. FATIGUE CRACK PROPAGATION ANALYSIS USING FRACTURE MECHANICS

The fracture mechanics analysis of the fatigue crack propagation consists of the two basic equations (1) and (2). The fatigue crack growth rate, da/dN in mm/cycle, can be empirically expressed as a function of the stress intensity factor range, ΔK in $N/mm^2 \cdot \sqrt{mm}$, as follows :

$$\frac{da}{dN} = C\,\Delta K^m \,, \tag{1}$$

where C and m are material dependent constants. Throughout the numerical analyses described later in this paper, fixed values of $C = 1.52 \cdot 10^{-13}$ and $m = 3$ are selected ($C = 48 \cdot 10^{-13}$ for m/cycle and $MPa \cdot \sqrt{m}$).

The stress intensity factor range is expressed as follows :

$$\Delta K = F(a)\,\Delta\sigma\,\sqrt{\pi\, a} \,, \tag{2}$$

where $\Delta\sigma$ is the nominal stress range, a is the governing crack size, and F(a) is a correction factor. For a crack emanating from a fillet weld toe, F(a) can be conveniently expressed by the product of different correction factors [3] :

$$F(a) = F_S\, F_E\, F_G\, F_W \,, \tag{3}$$

where F_S accounts for the effect of the free front surface, F_E for the elliptical crack shape, F_W for finite plate width (free back surface), and F_G for non-uniform stresses due to the stress concentration effect. Obviously, Eq. (3) contains some approximation due to interaction effects between the individual correction factors which are not considered when used in the combination. This expression is, however, very useful in practice, because it is simple and easy to use.

The fatigue crack propagation life N_p can be computed by rewriting Eq. (1) and integrating between two crack sizes :

$$N_p = \frac{1}{C} \int_{a_i}^{a_f} \frac{1}{\Delta K^m}\, da \,. \tag{4}$$

N_p is the number of cycles necessary to propagate a crack from a given (initial) crack size, a_i, to a final crack size, a_f, under constant stress range. Substituting Eq. (2) into Eq. (4), N_p can be obtained by numerical integration, for example using Simpson's rule.

It has been reported that, below a certain threshold value, ΔK_{th}, existing fatigue cracks do not propagate [2]. Substituting the ΔK_{th} values into ΔK of Eq. (2), one can estimate the fatigue limit for a given initial crack size. This gives a threshold value of the stress range below which existing initial cracks of a given size do not propagate.

3. FATIGUE TESTS OF TENSILE SPECIMENS WITH GUSSET PLATES

A tensile plate with two longitudinally welded gusset attachments, as shown in Figure 1 is often used for fatigue tests of attachments. Fatigue cracks always initiate and propagate from the fillet weld toe at the end of the attachment. In order to verify the fatigue crack propagation behavior at an early stage of fatigue, dye-penetrant was applied to the fillet weld toe of the gusset specimens during fatigue tests [4]. The dye left clear markings of the geometry of the crack on the fatigue fracture surface. These dye-marked cracks were always of semi-elliptical shape, and were present at as early as 20 percent of the total fatigue life of the specimen, N, as shown in Figure 1.

The depths of these early cracks were 0.27 to 0.42 mm. In other words, at least 80 percent of the total fatigue life consists of fatigue crack propagation. The stress intensity factor range of these semi-elliptical surface cracks, emanating from the weld toe at the gusset end, can be conveniently expressed by Eq. (3). The correction factors used are as follows :

$$F_S = 1.12 - 0.12 \frac{a}{b} , \tag{5}$$

$$F_E = \frac{1}{E_k} = \frac{1}{\int_0^{\pi/2} (1 - k^2 \sin^2 \varphi)^{1/2} \, d\varphi} . \tag{6}$$

E_k is the complete elliptical integral of the second kind, where $k^2 = 1 - a^2/b^2$, and the crack shape is expressed by its depth, a, and width, 2 b. Normally, a wide variation of the crack shape was observed at the weld toe due to the weld toe profile, weld toe irregularity, and coalescence of multiple minute cracks.

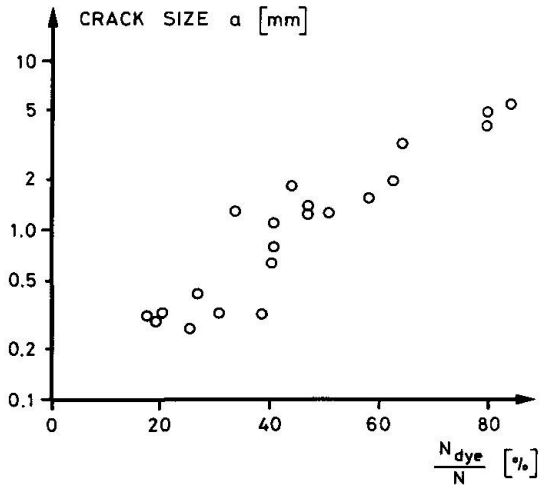

Figure 1 : Dye-marked crack depth at a given percentage of the total fatigue life.

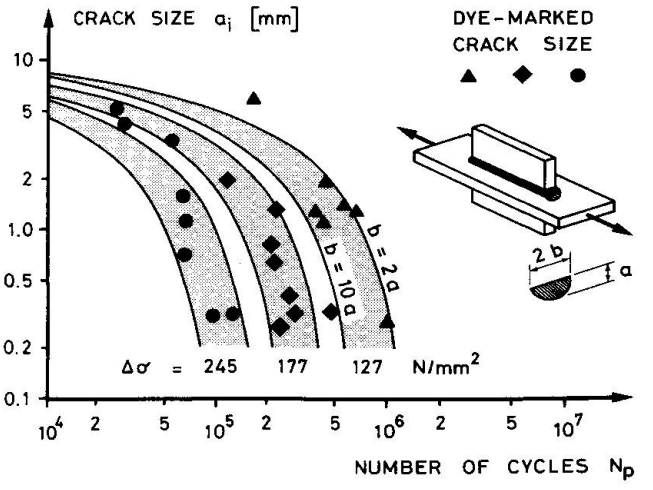

Figure 2 : Computed crack propagation life, compared with test data of gusset specimens.

The inclusion of all these factors in the analysis would yield considerable and unnecessary complexity. Therefore, only an upper and a lower bound of the crack geometry aspect ratio, a/b, are selected to represent all crack shapes [4]. The upper bound is selected as b = 2 a; the lower bound is expressed by b = 10 a, if a $\leq$ 1 mm, and b = 10 $a^{0.3}$, if a > 1 mm. This crack shape is substituted into Eq. (6). The correction factor for a finite plate width (with free back surface), is defined as follows :

$$F_W = \sqrt{\frac{2\,t}{\pi\,a} \tan\left(\frac{\pi\,a}{2\,t}\right)}, \qquad (7)$$

where t is the plate thickness.

The geometry correction factor F_G is determined from the stress distribution normal to the line where the fatigue crack is to propagate [3]. At the attachment end, the stress is raised once due to the fillet weld and again by the presence of the gusset plate. The stress concentration due to the fillet weld was computed by finite element analysis [5]. The stress concentration due to the gusset plates is estimated from stress measurements using strain gages mounted 3 mm away from the fillet weld toe. This stress concentration is about 1.5.

The computed fatigue crack propagation life N_p, of the gusset specimens, is plotted against the initial crack size a_i, as shown in Figure 2. The three stress ranges indicated correspond to the applied stress ranges used in the fatigue tests. The shape of the semi-elliptical surface crack is one of the dominating parameters affecting the computed N_p. The two bounds of the observed crack shapes result in a band of computed N_p for each stress range. The observed dye-marked crack depth and the corresponding number of cycles that are needed to propagate the crack from this size to failure are also plotted in Figure 2 for all test specimens. These results are directly comparable to the computed N_p. In spite of the fact that a simple expression of ΔK was used for the analysis, the computed results are in good agreement with the test results.

When a given initial crack size is selected, the computed N_p can then be expressed in the same way as a regular S-N diagram. The computed N_p is plotted

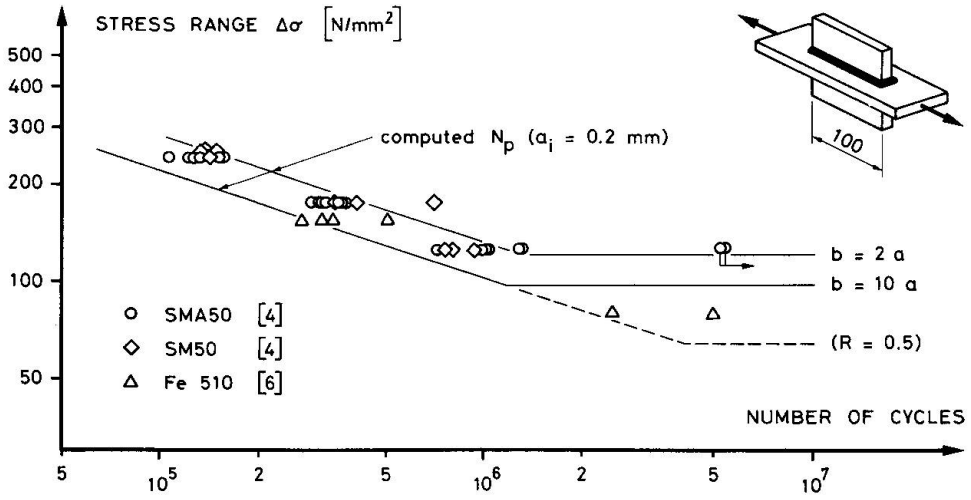

Figure 3 : Comparison between fatigue test results and the computed crack propagation life N_p for a_i = 0.2 mm.

and compared with the fatigue test data, as shown in Figure 3. Assuming the initial crack size to be a_i = 0.2 mm, almost the entire fatigue life is spent in propagating the cracks. As shown before in Figure 1, fatigue cracks of 0.27 to 0.42 mm deep already existed at the fillet weld toe at about 20 percent of the life.

The theoretical fatigue limits, computed with ΔK_{th} = 190 N/mm^2 • $\sqrt{mm}$ (R = 0.1), for the two limiting crack shapes, are also shown in Figure 3. In fact, two specimens tested at $\Delta\sigma$ = 127 N/mm^2 had not failed after 5 million stress cycles. A favorable fillet weld toe profile may reduce the initial stress condition and hence increase the fatigue limit of the specimen. Nine other specimens failed between $7 \cdot 10^5$ cycles and 2 million cycles. Note that two specimens tested at 80 N/mm^2 also showed finite lives [6].

If high tensile residual stresses exist at the fillet weld toe, a higher stress ratio exists which consequently reduces the ΔK_{th} value [2]. Considering this effect and therefore introducing ΔK_{th} = 125 N/mm^2 • $\sqrt{mm}$ (R = 0.5), the fatigue limit computed for the crack shape of b = 10 a is then below the stress range at which the two specimens were tested.

4. FATIGUE ANALYSIS OF GUSSET PLATES WELDED TO THE FLANGE TIP

4.1. Rectangular gusset plates

When an attachment is welded directly to the flange tip of a beam, a part of the stress is transferred to the attachment, which causes high stress concentration at the weld toe at the attachment end. Therefore, the crack normally initiates at the weld toe and propagates perpendicular to the principal stress. The fatigue crack propagation behavior may be modelled in three ways, depending on the exact location of the crack initiation, as shown in Figure 4.

For the edge crack, F_S = 1.12 is used. In the second model, F_S = 1.38 and F_E = 2/π are used for a quarter circular corner crack until it reaches the plate thickness of the flange. Then the crack propagates as an edge crack. The computed propagation life is the sum of these two steps. In the third model for a semi-elliptical

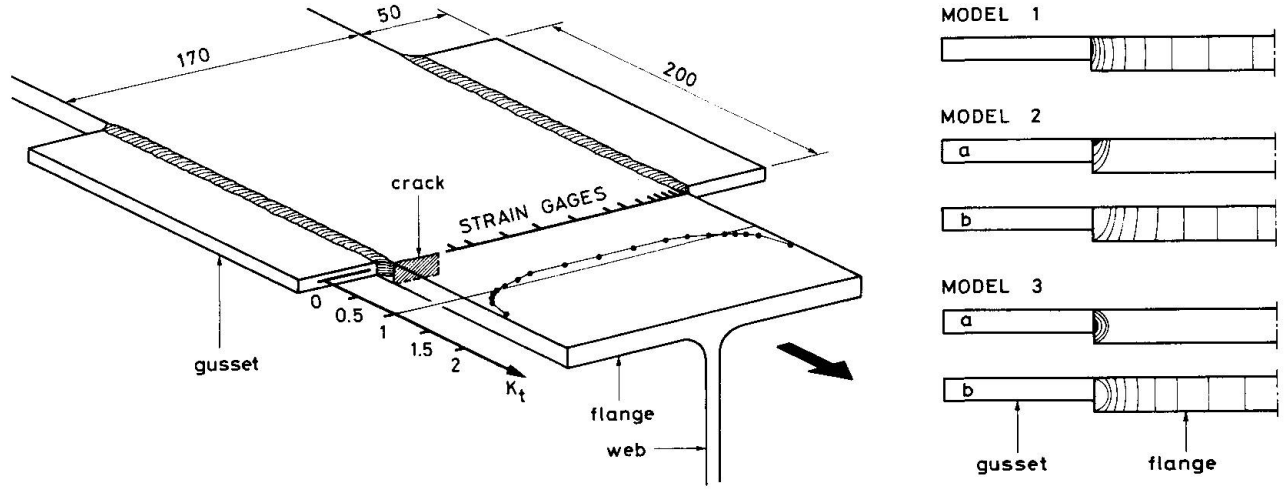

Figure 4 : Stress concentration measurement and models of fatigue cracks emanating from the weld toe at the end of gusset plates welded to the flange tip.

surface crack, $F_S = 1.12 - 0.12\ a/b$ and $F_E = 1/E_k$. Again the second stage of growth is that of an edge crack. F_W is assumed to be unity for all models since the crack size is generally small compared to the width of the flange. Thus, all correction factors are defined, except F_G.

It is proposed to divide F_G further into F_{G1} and F_{G2}. F_{G1} accounts for the local stress concentration due to the fillet weld at the end of the gusset, and F_{G2} for the global stress concentration due to the gusset. In the following analysis, the F_G value for a transverse fillet weld computed for a stiffener specimen [5] is used to define F_{G1}, provided that the fillet weld profiles are the same. The F_{G2} value is computed from the stress distribution measured by strain gages mounted across the flange plate, as shown in Figure 4. Note that a stress concentration of about 1.5 was measured, 4 mm away from the fillet weld toe. Since the stress concentration effect of the fillet weld is very localized, this value measured by the strain gages is mainly due to the gusset. The local effect due to F_{G1} is large, but decays quickly to unity after about 3 mm crack size.

The fatigue crack propagation life for a crack with inital size $a_i = 0.2$ mm, growing to a size $a_f = 50$ mm, is computed and plotted in Figure 5. Usually, a large difference in the computed N_p is expected depending on the assumed crack shape, as was previously shown in Figure 3. However, for the gusset plate attached to the flange tip, only the first stage of fatigue crack propagation is affected by the crack shape. It results in a relatively small difference of the computed N_p for the different crack shape models. The fatigue test data for 200 mm long gussets welded to the flange tip [7] are in good agreement with the test results.

4.2. Fatigue strength improvement by grinding the weld toes

One way to improve the fatigue life of a beam with gussets welded to the flange tip is to reduce the stress concentration at the end of the gusset. This can be achieved by grinding the fillet weld. A further reduction of the stress concentration can be expected when a smooth transition from the gusset to the flange is created. If the weld toe is ground completely smooth, the correction factor F_{G1} can be set equal to unity. Assuming all other factors to be the same as those previously used to compute N_p in the as-welded condition, the propagation life for the gusset with ground weld toes can then be computed; the results are plotted in Figure 6. More than a 50 percent improvement of the fatigue life can be expected by grinding completely the weld toe. The fatigue limit computed with $\Delta K_{th} = 190\ N/mm^2 \cdot \sqrt{mm}$ (R = 0.1) is almost doubled.

Fatigue test data of beams with welded gussets of various end shapes [7] indicate a significant improvement of fatigue life, compared with the as-welded gusset end. The fatigue tests were carried out for three radii of circular transition from flange to gusset : r = 10, 50 and 70 mm. Note that a large circular transition radius does not consistently improve fatigue life. This may be attributed to the imperfect grinding especially at the fillet weld toe.

The analysis shows that grinding the gusset, so as to obtain a smooth transition from gusset to flange plate, significantly improves the fatigue life of this detail. It should be noted that care must be taken when grinding the weld toe. Small portions of the weld toe missed by the grinding operation retain their local stress concentration. Moreover, grinding marks left on the ground surface, perpendicular to the stress direction, may well be the initiation point of fatigue cracks. In addition, the fatigue tests were carried out at stress ranges close to the computed fatigue limit. When this is the case, the fatigue life

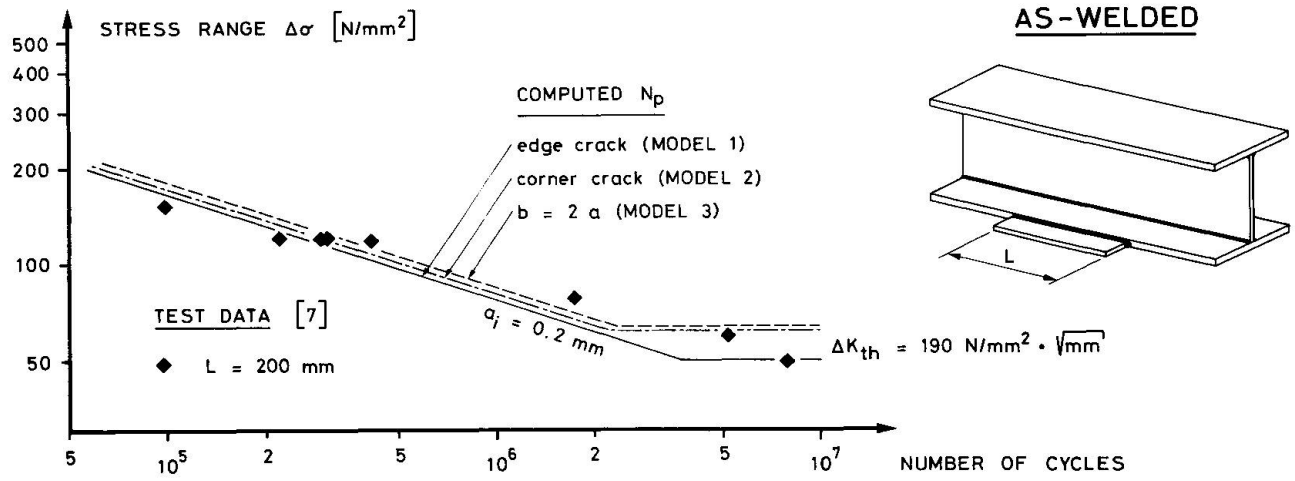

Figure 5 : Comparison between crack propagation life and observed fatigue life for rectangular gussets attached to the flange tip (as-welded).

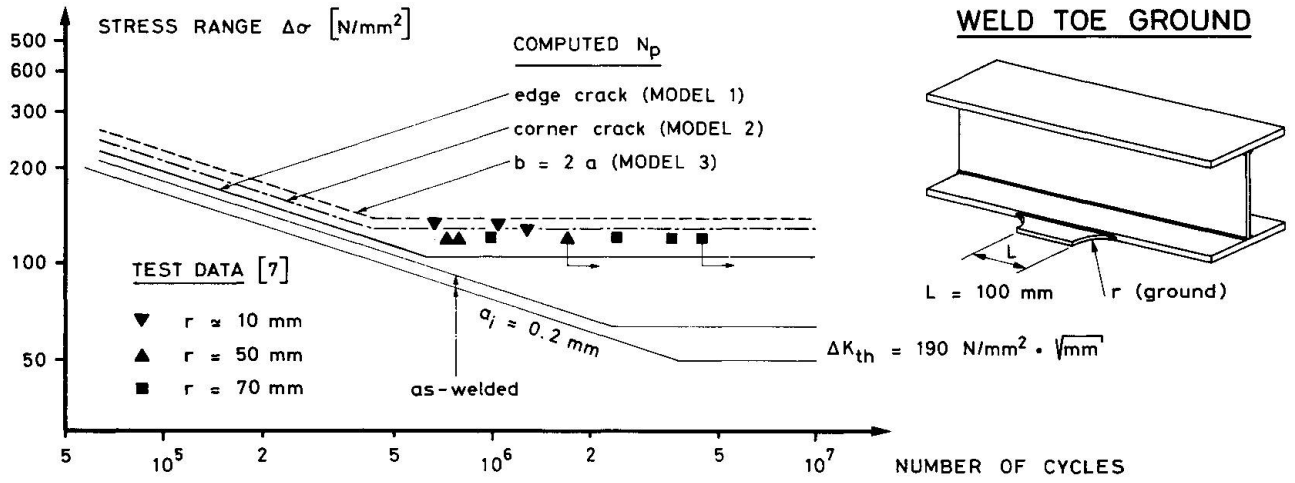

Figure 6 : Computed crack propagation life for gussets with various end radii, and comparison with test results.

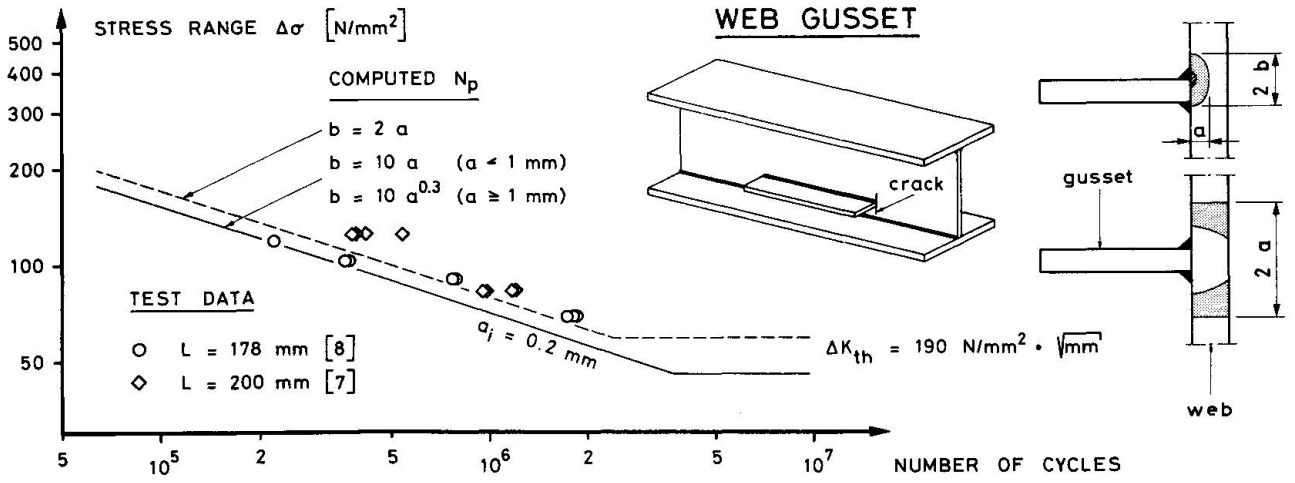

Figure 7 : Comparison of analytical prediction with test results for gussets attached to the web.

depends very much on the surface condition. In other words, a small imperfection may cause fatigue crack initiation, whilst a perfectly smooth surface gives longer life or even run-out. In fact, a large scatter of the fatigue data is observed in these types of tests.

5. FATIGUE ANALYSIS OF GUSSET PLATES WELDED TO THE WEB

When a gusset plate is horizontally attached to a beam web, fatigue cracks initiate and propagate from the toe of the fillet weld, at the end of the attachment [7] [8]. The fatigue crack propagation behavior is similar to that observed for the gussets welded to the tensile specimens previously described. Once the crack has completely penetrated the web, the crack becomes a through-thickness crack, propagating vertically upwards and downwards in the web, as schematically shown in Figure 7. The first stage of the fatigue crack propagation behavior can be modelled in the same manner as for the gusset specimens. For the geometry correction factor, however, two factors, F_{G1} and F_{G2}, are used in the same manner as for the gusset welded to the flange tip. Once the crack has completely penetrated the web plate, only F_{G2} is used to account for the global effect due to the gusset.

The computed crack propagation life for an initial crack size of 0.2 mm is plotted in Figure 7; the final crack size is again assumed as a_f = 50 mm. Fatigue test data of the attachments welded to the web are also plotted for comparison [7] [8]. Although a more accurate stress analysis might be needed for this welded detail, the computed crack propagation lives N_p are in relatively good agreement and show the trend of the fatigue test data. What must be done in future fatigue tests of this detail is to check whether the fatigue crack initiates at an early stage. Also, a more precise stress analysis or stress measurements must be carried out.

6. SUMMARY

The fatigue crack propagation behavior of gusset plates welded to tensile specimens is used to demonstrate how fatigue cracks propagate and how fracture mechanics analysis can be used to predict the crack propagation behavior. The results are then applied to similar structural details, such as attachments welded to the flange or web of beams. The computed fatigue propagation life of these structural details is generally in good agreement with test data. It is speculated that the majority of the fatigue life of these details is spent in propagation of cracks from minute sizes, for example a_i = 0.2 mm, and that the crack initiation period is very short or even non-existant.

REFERENCES

[1] *MADDOX, S. J. Assessing the Significance of Flaws in Welds Subjected to Fatigue. Welding Research Supplement, 1974.*

[2] *ROLFE, S. T. and BARSOM, J. M. Fracture and Fatigue Control in Structures, Application of Fracture Mechanics. Englewood Cliffs, Prentice-Hall, 1977.*

[3] *ALBRECHT, P. and YAMADA, K. Rapid Calculation of Stress Intensity Factors. Proc. of ASCE, New-York, Vol. 103, No. ST2, 1977.*

[4] *YAMADA, K. et al. Fatigue Analysis based on Crack Growth from Toe of Gusset End Welds. Proc. of JSCE, Tokyo, No. 303, 1980.*

[5] *YAMADA, K., MAKINO, T. and KIKUCHI, Y. Fracture Mechanics Analysis of Fatigue Cracks Emanating from Toe of Fillet Weld. Proc. of JSCE, Tokyo, No. 292, 1979.*

[6] *HIRT, M. A. und KUMMER, E. Einfluss der Spannungskonzentration auf die Ermüdungsfestigkeit geschweisster Konstruktionen. VDI-Berichte Nr. 313, 1978.*

[7] *HAUSAMMANN, H., HIRT, M. A. et CRISINEL, M. La résistance à la fatigue des poutres en âme pleine composées-soudées : Effet des détails constructifs et comparaisons avec la norme SIA 161. Lausanne, EPFL, ICOM (en préparation).*

[8] *BARDELL, G. R. and KULAK, G. L. Fatigue Behavior of Steel Beams with Welded Details. Edmonton, University of Alberta, Dept. of Civil Engineering, Report No. 72, 1978.*

Residual Stresses in Welded Members Subjected to Cyclic Loading

Contraintes résiduelles dans les éléments soudés soumis à des charges cycliques

Restspannungen bei geschweissten Bauteilen unter Schwingbelastung

K. HORIKAWA
Associate Prof.
Osaka University
Suita, Japan

S. FUKUDA
Associate Prof.
Osaka University
Suita, Japan

S. WATARI
Eng.
N.S.C.
Kita-kyushu, Japan

Y. KISHIMOTO
Eng.
M.E.S.
Tamano, Japan

SUMMARY
The effect of residual stress on fatigue crack growth was studied experimentally on base plate and welded specimens of 800 N/mm^2 tensile strength steel. The results indicated that crack growth rate in welded members can be estimated as that of base metal specimens with a stress ratio of 0.5. In addition, the use of stress relief heat treatment has little effect on crack growth rate unless it completely removes the residual stress.

RESUME
L'effet des contraintes résiduelles sur la propagation des fissures dues à la fatigue a été étudié expérimentalement sur des échantillons de plaque de base et soudés en acier dont la résistance à la traction était de 800 N/mm^2. Les résultats indiquent que le taux d'accroissement des fissures dans les éléments soudés peut être estimé égal à celui des échantillons de plaque de base avec un rapport de contrainte de 0,5. L'utilisation d'un traitement thermique a peu d'effet sur le taux d'accroissement des fissures à moins qu'il ne supprime complètement les contraintes résiduelles.

ZUSAMMENFASSUNG
Die Auswirkungen der Restspannung auf die Wachstumsrate von Ermüdungsrissen wurden an Mustern von Grundplatten und geschweissten Teilen aus Stahl mit 800 N/mm^2 Zugfestigkeit experimentell untersucht. Die Experimente zeigten, dass sich die Wachstumsrate von Ermüdungsrissen bei geschweissten Bauteilen mit der Wachstumsrate von Ermüdungsrissen der Grundplattenmuster mit einem Spannungsverhältnis von 0.5 abschätzen lässt. Spannungsfrei Glühen hat keinen Einfluss auf die Wachstumsrate von Ermüdungsrissen, wenn dadurch die Restspannung nicht vollständig abgebaut wird.

1. INTRODUCTION

It is very important to know the fatigue crack growth rate in the plate with residual stress to estimate the fatigue life, when we disign a welded steel structure under cycle loading, since the most of fatigue cracks initiate from welding beads or their vicinity, and propagate in the welding residual stress field. But, there seems few, if any, systematic studies on the effect of welding residual stress on fatigue crack growth rate . In the past studies, it is reported that fatigue life of welded members was shorter than that of non-welded members. For instance, in reference [1], the fatigue life of half-scale model of box chord members with high tensile strength steel, was much shorter than that of small specimen. This shortness in fatigue life is considered as caused by the effect of welding residulal stress, or welding residual stress makes fatigue life short.

If the fatigue crack growth rate of welded members is faster than that of base metal by the existence of welding residual stress, it might be said that welding residual stress should be decreased.

From these standpoint, the effect of welding residual stress on fatigue crack growth rate was studied on 80kg/mm^2 tensile strength steel.

The experiment was carried out by using three types of specimen; base metal, as-welded and stress relieved. Fatigue crack growth rate and welding residual stress were measured. Crack opening and closure was also observed.

2. EXPERIMENT

2.1 Material and specimen

The material used was 80kg/mm^2 tensile strength steel plate of 6.4mm in thickness. Its' chemical composition and mechanical properties are shown in Table 1. The center-notched specimens, shown in Fig. 1, were used. Fig. 1 also shows the detail of notch. Three types of specimen were used ; base metal specimen, as-welded specimen and stress relieved specimen.

The welded specimen was prepared by submarged-arc-welding as beads-on-plate welds on an edge preparation of 5.5mm width and 2mm depth to obtain a uniform distribution of welding residual stress through the plate thickness. Welding consumables (wire and flux) for 50kg/mm^2 tensile strength steel were used, but it was considered to be no trouble for this study's purpose, since the welding was made only to give residual stress. From the observation of the hardness distribution in the vicinity of the beads of welded specimen, the value of hardness drops to that of base metal at the point of 7mm away from the center of the beads. Therefore the initial center notch length was chosen as 10mm and the

Table 1 Chemical composition and mechanical properties the plate

Steel	Chemical composition (%)									
	C	Si	Mn	P	S	Cu	Cr	Mo	V	B
HT80	0.12	0.26	0.88	0.017	0.005	0.23	0.89	0.31	0.04	0.0007

Y.S. (kg/mm^2)	T.S. (kg/mm^2)	El. (%)
80	85	22

Y.S.:Yield stress
T.S.:Tensile strength
El. :Elongation

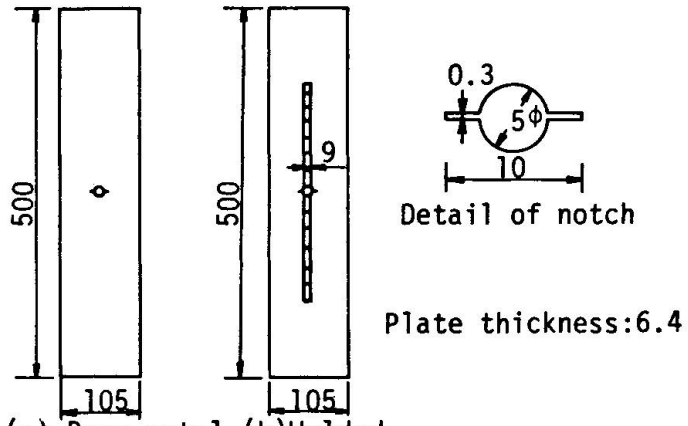

Fig.1 Geometry and size of specimen

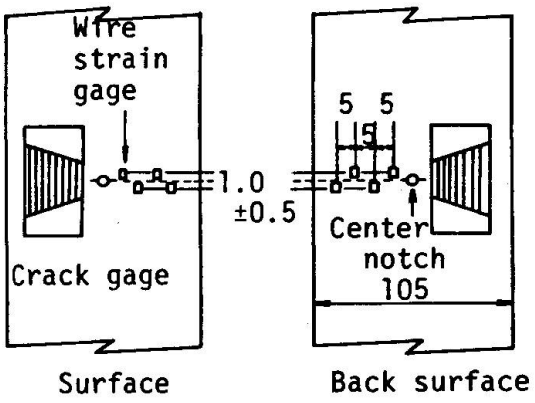

Fig.2 Gage location

fatigue crack growth rate was estimated from at the point of 2mm away from the tip of initial notch.

2.2 Testing procedure

This investigation was devided into two series of tests. First series were conducted under variable stress ratio and constant residual stress, another series were under constant stress ratio and variable residual stress.

All tests were conducted by using an electrohydraulic closed loop servo fatigue testing machine. The testing freguency was 10Hz.It was dropped, however , to 0.1Hz or 1.0Hz when observing a crack opening and closure. Crack length was measured by using a crack gage and the observation of crack opening and closure was made by attaching small wire strain gages at the points quite close to the expected fatigue crack extension line. (Fig. 2)

In this investigation, the crack opening or closure was determined from a deflection point in a hysteresis curve between a load cell output (Y-axis) and an output of a wire strain gage near the crack tip (X-axis), as is illustrated in Fig. 3. Stress relief heat treatment was carried out by using electric furnace, and temperature was controlled by C-A thermo couple.

Welding residual stress was measured by eleven small wire strain gages attached along the center line of longitudinal of the specimen.

K-value is caluculated by using Forman's formula.

$$K = \sigma_0\sqrt{\pi a \cdot \sec(\pi a/W)}$$

where a:Half crack length W:Specimen width σ_0:Uniform tensile stress

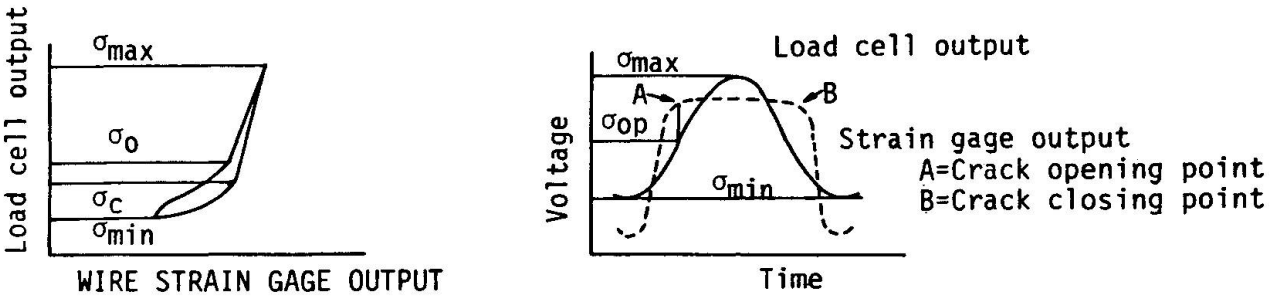

Fig.3 Observation of crack opening and closure

3. TEST RESULTS AND DISCUSSION

3.1 Variable stress ratio test series

Fig.4 shows the distributions of welding residual stress for base metal specimen and as-welded specimen.

Stress ratio was changed from R=0.5 (HB1) to R=-1.0 (HB5) for base metal specimen and from R=0.5 (HW1) to R=-∞ (HW8) for as-welded specimen. Fig.5 shows the relationship between fatigue crack growth rate da/dN-ΔK .Secant formula was used in evaluating ΔK. It can be seen that da/dN decrease with the decrease of stress ratio R, for base metal specimen. While,the data of welded specimens in small ΔK region or more precisely in small crack length region fall within a narrow band no matter what value the stress ratio may be, which is quite different from the case of base metal specimens.

The data of HW8, which was obtained under repeated compression loading (R=-∞),show that da/dN quite rapidly after exceeding approximately $\Delta K = 60 Kg/mm^{3/2}$. Unlike other cases, the right hand side data and the left hand side data of HW8 are quite different so each result is shown in the figure as HW8-A and HW8-B.But in either case of A or B, a crack is found to propagate even under repeated compression loading, where a crack is considered never to propagate if the welding residual stress is not present and the remarkable effect of welding residual stress can be observed. The da/dN of as-welded results of Fig.5, usingΔKeff which is evaluated by Eq,(2) based on experimentally obtained U value. [2]

$$\Delta Keff = U \times \Delta K \qquad (2)$$

Where $U = \frac{\sigma_{max} - \sigma_{close}}{\sigma_{max} - \sigma_{min}}$

It is generally observed by comparing Fig.5 with Fig.6 that experimental results which scatter quite widely on da/dN- K plots fall within a narrow band if they are replotted using Keff.

Thus, it is easily understood that the behavior of crack opening and closure plays quite an important role in evaluating the effect of stress ratio R in base metal specimens and in evaluating the effect of welding residual stress in welded specimens. In as-welded specimen except HW8 (R=-∞) and base plate specimen with stress ratio R=0.5 (HB1), crack did not close or U=1.The fatigue crack growth rate of as-welded specimens can be estimated as that of base metal specimen with the stress ratio of 0.5.

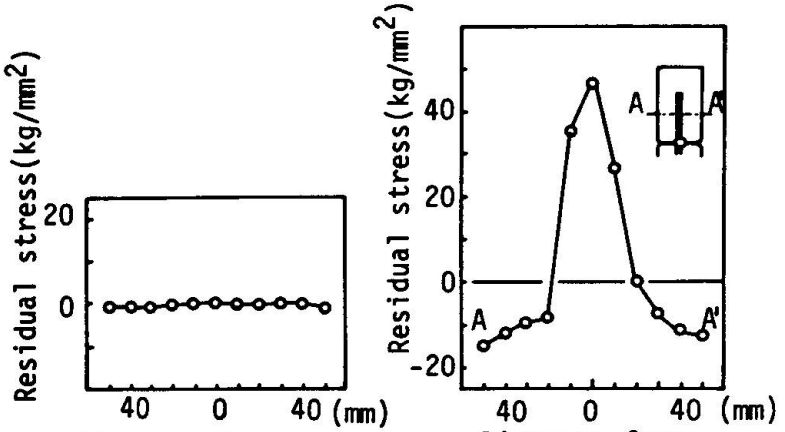

Fig.4 Residual stress distributions

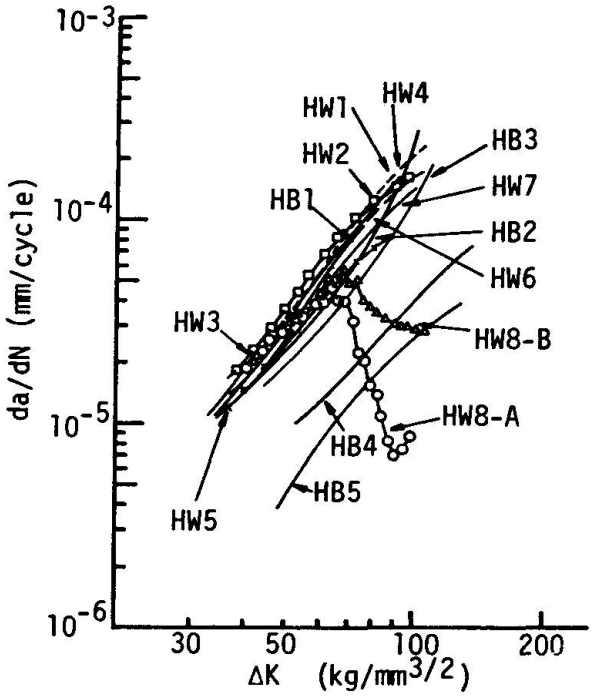

Fig.5 da/dN-ΔK relations

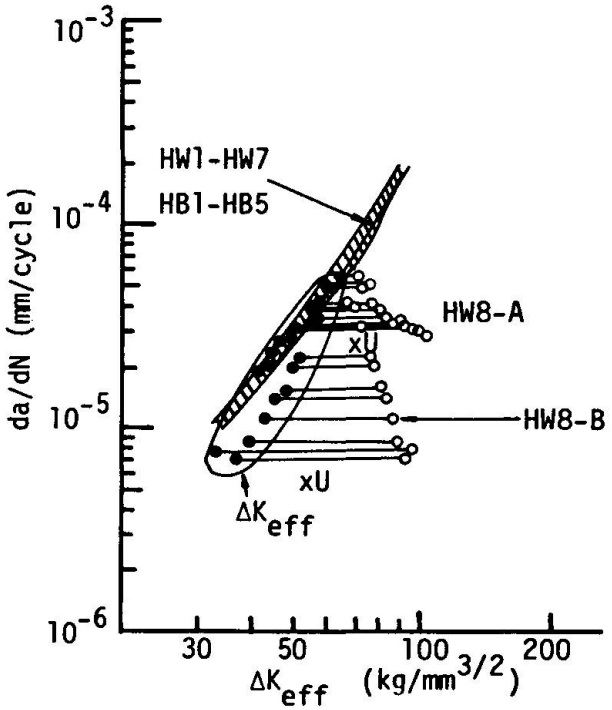

Fig.6 da/dN-ΔK_{eff} relations

3.2 Variable residual stress test series

Fig.7 shows the residual stress distributions of stress relieved specimens.HS-2, HS-4,and HS-6 are the specimens stress relieved at 580° C for 1 hour, 3 hours, and 12hours, respectively. These results show the increase of holding time length doesn't affect the decrease of residual stress. The other hand, HS-8,HS-2,HS-10 and HS-12 are the specimens stress relieved for 1 hour at 500°C, 580°C,630°C and 650°C respectively. These results show the more increase of holding temperature, the more decrease of welding residual stress. The hardness of the specimen stress-relieved at 650°C is a little lower than the others. The different 6 types of the stress relieved conditions yield 4 types of residual stress distributions, in short, maximum tensile stress is nearly equal to 20kg/mm^2, 10kg/mm^2 ,5kg/mm^2 and 2kg/mm^2. Fig.8 shows the results of the fatigue crack growth rate in these specimens. The data of stress relieved specimens in small ΔK region fall within a narrow band no matter what value the initial tensile residual stress may be. Especially, three lines, which except the date of initial tensile residual stress is 2kg/mm^2,are almost same , up to the range of ΔK=70kg/mm$^{3/2}$. This figure also shows that the da/dN in stress relieved specimen,except the specimen of initial tensile residual stress is 2kg/mm^2,are just as same as the da/dN in as-welded specimen up to the region of ΔK=70kg/mm^2

It is very important that the da/dN in stress relieved specimen, whose initial tensile residual stress is 5kg/mm^2,is as same as that in as-welded specimen, whose initial tensile residual stress is 40kg/mm^2. In spite of the initial tensile residual stress is decreased to 1/8,the fatigue crack growth rate in those two specimens are same. This result is seemed that stress relief heat treatment may be of little effect on fatigue crack growth rate, if it is not cancel the residual stress perfectly. The stress relieved specimens change their growth rate, as the residual stress is released according to their fatigue crack growth. In prototype members, the release of residual stress may

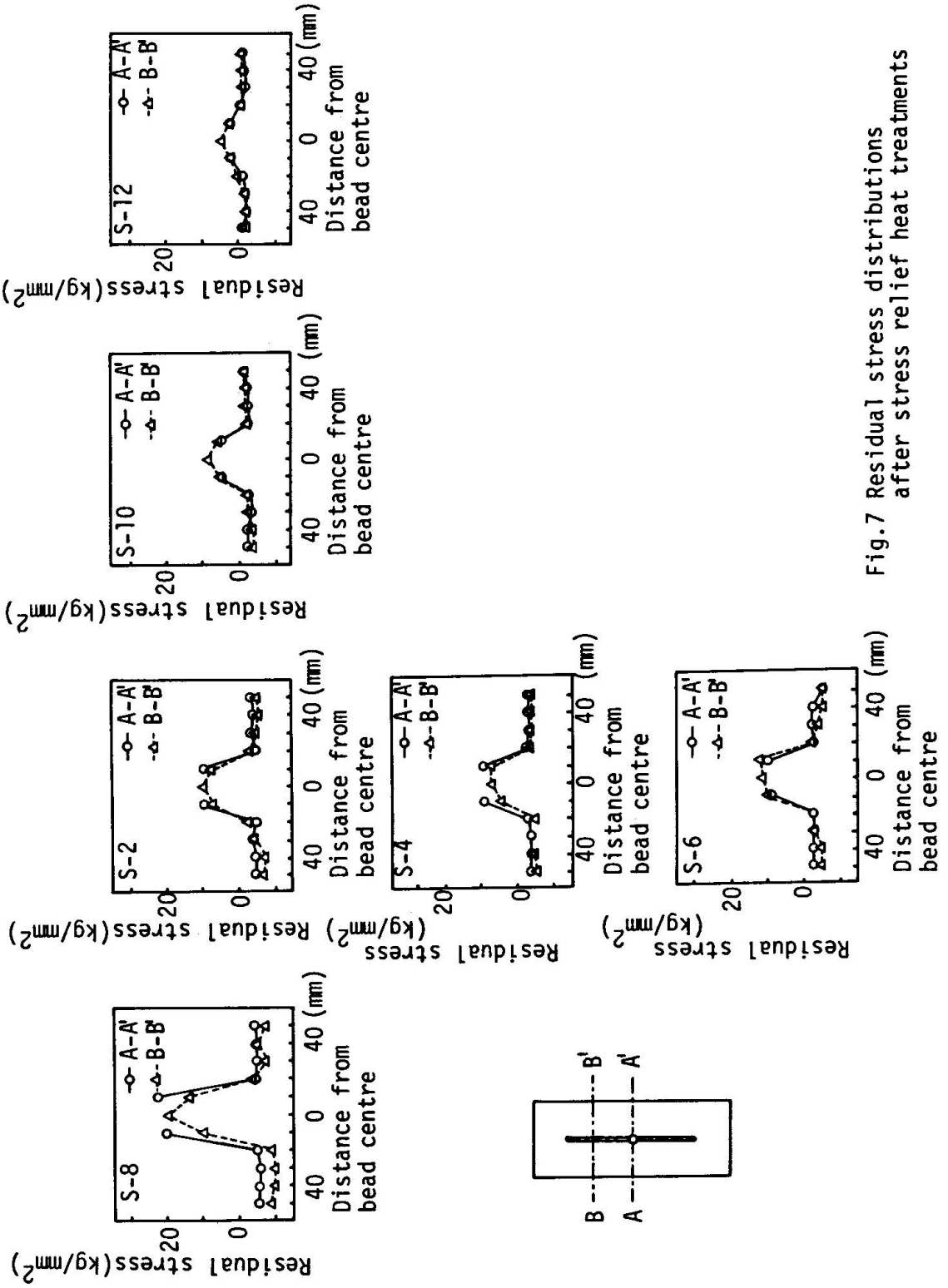

Fig.7 Residual stress distributions after stress relief heat treatments

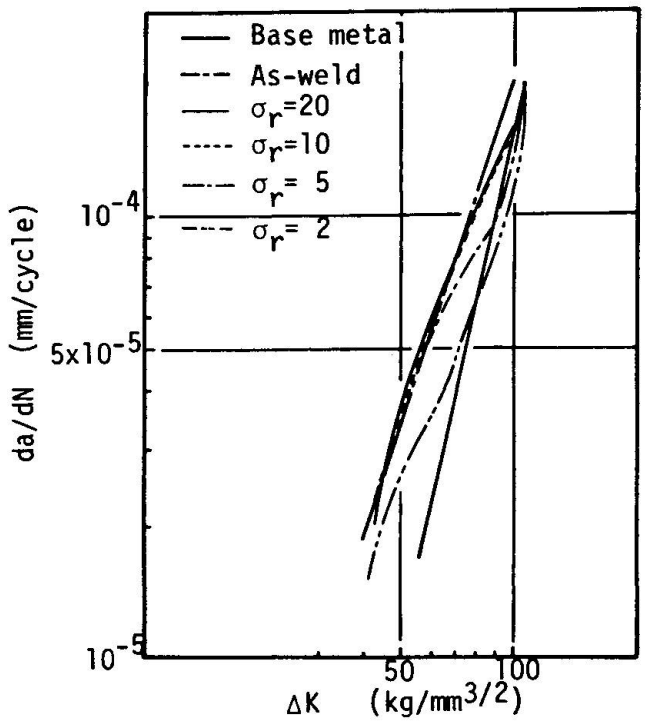

Fig.8 da/dN-ΔK relations after stress relief heat treatment

be less than this type of splecimens, since the length of fatigue crack is very short, as compared with the ligament length. So, the fatigue crack growth rate in stress relieved members may be same to that in as welded members up to finial unstable fracture in prototype members. From these considerations stress relief heat treatment on prototype members may be of little effect from viewpoint of fatigue crack growth rate.

4. CONCLUSIONS

The major conclusions obtained are as follows;

(1) Although the lines of da/dN-ΔK differ for different stress ratios in the case of base metal specimens, the data of da/dN-ΔK for small crack length fall within a narrow band in the case of welded specimens, even though their stress ratios are different. In this study, da/dN of as-welded specimens is as same as that of base metal specimen with the stress ratio of 0.5.

(2) In the presence of welding residual stress, fatigue cracks are found to propagate even under fully repeated compression loading.

(3) All data of welded specimens and base metal specimens which scatter quite extensively on da/dN- ΔK plots fall within a narrow band if they are replotted by ΔKeff.

(4) In the specimens stress relieved at 580°C, the lengthen of holding time is not much effective on release of residual stress. The other hand, in the specimens, stress relieved at 500°C to 650°C, the more increase of heat treatment temperature yields the more decreare of residual stress.

(5) The fatigue crack growth rate in stres relieved specimen , whose residual stress is 5Kg/mm^2 , is same to that in as-welded specimen, whose initial tensile residual stress 40Kg/mm^2, up to the region of ΔK= 70Kg/mm$^{3/2}$. Stress relief heat treatment is of little effect on fatigue crack growth rate.

(6) If residual stress can't be canceled perfectly, it seems that stress relief heat treatment on prototype members is of little effect on fatigue crack growth rate.

REFERENCE

1. Jiro Tajima, et al.:Fatigue Strength of Large Size Weldments of High Tensile Strength Steels, Proceedings of International Conference on Welding Research in the 1980's
2. Elber,W.: Significance of Fatigue Crack Propagation, ASTM STP 486

Improving the Fatigue Lives of Fillet Welds by Shot Peening

Augmentation de la durée de vie des cordons de soudure par grenaillage

Erhöhung der Lebensdauer von Schweissnähten durch Kugelstrahlverfahren

S.J. MADDOX
Head of Fatigue Laboratory
The Welding Institute
Abington, Cambridge, England

SUMMARY
Circumstances under which shot peening would improve the fatigue strength of attachment fillet welds in steel were investigated. The treatment was found to be more effective for transverse welds than welds around the ends of longitudinal attachments and the benefit increased with steel strength. However, it decreased with increases in stress ratio. Preliminary tests indicated that shot peening was still beneficial under variable amplitude loading. The benefit of shot peening varied with peening conditions and even for nominally identical conditions. In practice, the treatment is particularly effective in the high-cycle regime.

RESUME
Le grenaillage contrôlé peut améliorer la résistance à la fatigue de cordons de soudure en acier. Le traitement est plus efficace pour les soudures transversales que pour les soudures aux extrémités d'attaches longitudinales; l'effet bénéfique augmente avec la résistance de l'acier. Par contre, il diminue aver l'accroissement du rapport des contraintes. Des essais préliminaires montrent que le grenaillage est également bénéfique dans le cas de sollicitations d'amplitude variable. L'effet bénéfique varie avec les conditions de grenaillage voire même sous des conditions en principe identiques. En pratique, le traitement est particulièrement efficace dans le cas d'un nombre de cycles élevé.

ZUSAMMENFASSUNG
Die Verhältnisse, unter welchen das Kugelstrahlverfahren eine Verbesserung der Ermüdungsfestigkeit von Kehlnähten bringen kann, wurden untersucht. Das Verfahren erwies sich als vorteilhafter für Quernähte als für Schweissungen an den Enden von Längsrippen, wobei sich die Wirksamkeit mit steigender Stahlqualität verbessert, mit grösserem Spannungsverhältnis jedoch abnimmt. Versuche zeigten, dass das Kugelstrahlverfahren auch wirksam bei Belastungen mit variabler Amplitude ist. Die Wirksamkeit variierte in Abhängigkeit der Bearbeitung, auch unter praktisch gleichen Bedingungen. In der Praxis ist das Kugelstrahlverfahren speziell im Bereich der Langzeitermüdung vorteilhaft.

1. INTRODUCTION

One of the most effective techniques for improving the fatigue strength of welded joints which fail from the toe is the introduction of compressive residual stresses by peening [1]. For example, the fatigue strength of mild steel transverse fillet welds at 2 x 10^6 cycles can be raised by 91% by hammer peening along the weld toe [2]. Another method which is widely used to improve the fatigue strength of unwelded, and usually machined, components is controlled shot peening. Although the value of this technique has been widely demonstrated for such components (eg. [3]) surprisingly little work has been done in relation to welds, particularly steel fillet welds. However, some investigations have confirmed that shot peening of welds can effect an improvement, sometimes as high as that obtained by hammer peening [4,5], but usually less [5,6]. Even so, in practice shot peening may prove to be more convenient and cheaper than hammer peening, especially in the case of small components which could be treated in batches. Also, it may offer a particular advantage over other imrpovement techniques in terms of control of the process to ensure that the expected imrpovement in fatigue strength is actually realised.

The beneficial effect of shot peening is likely to depend on many factors and these must be appreciated before design recommendations can be made. Clearly, the peening conditions are important and some may not introduce any significant improvement in fatigue strength [5]. Equally, a method of checking that the required shot peening conditions have been achieved is required. At present, it seems to be assumed that the curvature introduced into an Almen strip by shot peening provides a satisfactory indication of the residual stresses produced, but reservations have been expressed about this [6]. The service loading conditions are also expected to be significant. Applied stresses are superimposed onto the compressive residual stress and clearly the effective (tensile) stress will increase with increase in peak applied stress. Thus, applied stress ratio R will be significant, such that the beneficial effect of shot peening will decrease with increase in positive R value but should increase for negative values, as has been found for hammer peened welds [7]. In addition, there is evidence [8,9] that the application of strains above yield, which could occur in the region of stress concentration at the weld toe under nominally elastic conditions, can relax the compressive residual stress due to shot peening. For this reason, there is concern that any improvement technique which relies on compressive residual stresses may be unreliable under random loading [1]. One factor which might enhance the benefit of shot peening is an increase in the tensile strength of the steel, due to a proportionate increase in the level of residual stress introduced. Certainly this has been confirmed for plain steel [3] and hammer peened welds [2].

The above factors were investigated in the present work. Other factors which might prove significant, including working environment and original weld condition, are currently being investigated. The aim of the project is to establish design S-N curves for shot peened fillet welds in steel.

2. TESTING PROGRAMME

2.1. Test Specimens

Two types of fillet welded joint which normally fail from the weld toe were tested, plates with longitudinal attachments fillet welded to the surface with welds which continued around the ends of the attachments (Fig.1a) and plates with transverse fillet welded attachments (Fig.1b). The virtue of the former is that test data usually exhibit little scatter. However, the transverse weld

probably typifies more fillet welded joints which arise in practice. The specimens were waisted to reduce the risk of failure in the grips. Both types of specimen were fabricated from structural steels to BS 4360, Grades 43A and 50B. In addition, the specimens with longitudinal attachments were fabricated using two high strength low alloy quenched and tempered structural steels, QT445A and RQT700. The chemical and tensile properties are given in Table 1. The specimens were welded by the manual metal arc process in the flat position using conditions appropriate to the parent steel. The welds to be shot peened were standardised by using batches which had similar fatigue strengths in the as-welded condition, as confirmed by testing.

Table 1. Material properties

Steel	Element, wt% C	S	P	Si	Mn	Ni	Cr	Mo	Nb	Al
BS 4360 Grade 43A	0.22	0.037	<0.005	0.04	0.86	0.01	<0.01	<0.01	<0.005	<0.005
BS 4360 Grade 50B	0.18	0.017	0.017	0.04	1.40	0.02	0.01	<0.01	0.036	<0.037
QT 445A	0.18	0.017	0.023	0.46	1.00	0.03	0.82	0.30	<0.005	0.072
RQT 700	0.19	0.014	0.010	0.42	1.28	0.02	0.14	0.16	0.036	0.105

Steel	Yield stress, N/mm^2	UTS N/mm^2	Elongation, %	Reduction in area, %
BS 4360 Grade 43A	262	472	38	60
BS 4360 Grade 50B	392	564	36	67
QT 445A	727	834	23	65
RQT 700	824	881	23	66

2.2. Shot peening conditions

The shot peening was carried out commerically under controlled conditions which complied with U.S. Defence Department Specification 'Shot peening of metal parts' MIL-S-131 65B, 1979. Most specimens were treated in the same way (condition A) but in three batches (A1,A2 and A3) and by two different companies (A1 and A2 by the first, A3 by the second. Two other conditions, B and C, were also used by the first company. Condition A used 0.6mm diameter shot to produce a peening intensity of 0.012 - 0.016 inches arc height in a type 2 Almen strip. Condition B gave the same intensity with 0.8mm diameter shot while condition C gave a higher intensity, 0.016 - 0.020 A2, with 0.8mm diameter shot. 55 - 65 Rockwell C hardness cast steel shot was used in every case and the operation was carried out in two passes (200% coverage) in order to achieve full coverage in the region of the weld toe.

Table 2. Test conditions

Joint type	Steel	R	Loading	Weld treatment: As-welded	Shot peened: A1	A2	A2 + stress relief	A3	B	C
Transverse non-load carrying fillet welded attachment	43A	0	constant amplitude	✓	✓					
	50B	0	"	✓	✓	✓	✓	✓	✓	✓
	50B	0	Random	✓				✓		
	50B	-1	constant amplitude	✓		✓				
	50B	0.5	"	✓		✓				
Longitudinal non-load carrying fillet welded attachment	43A	0	"	✓	✓					
	50B	0	"	✓	✓					
	QT445A	0	"	✓	✓					
	RQT700	0	"	✓	✓					

2.3. Test conditions

All specimens were tested axially under the conditions summarised in Table 2. Failure was taken to be complete fracture of the specimen.

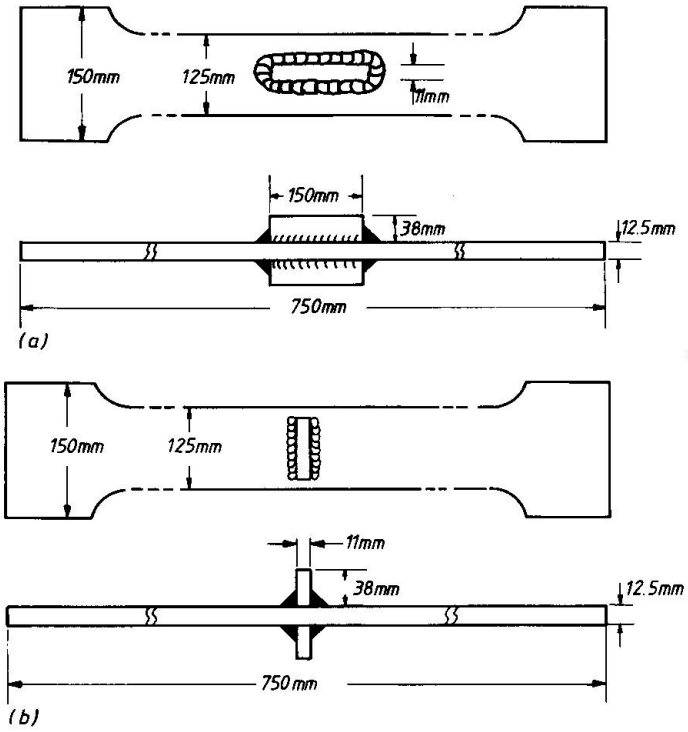

Fig. 1. Test specimens:
a) plate with longitudinal fillet welded attachment
b) plate with transverse fillet welded attachment.

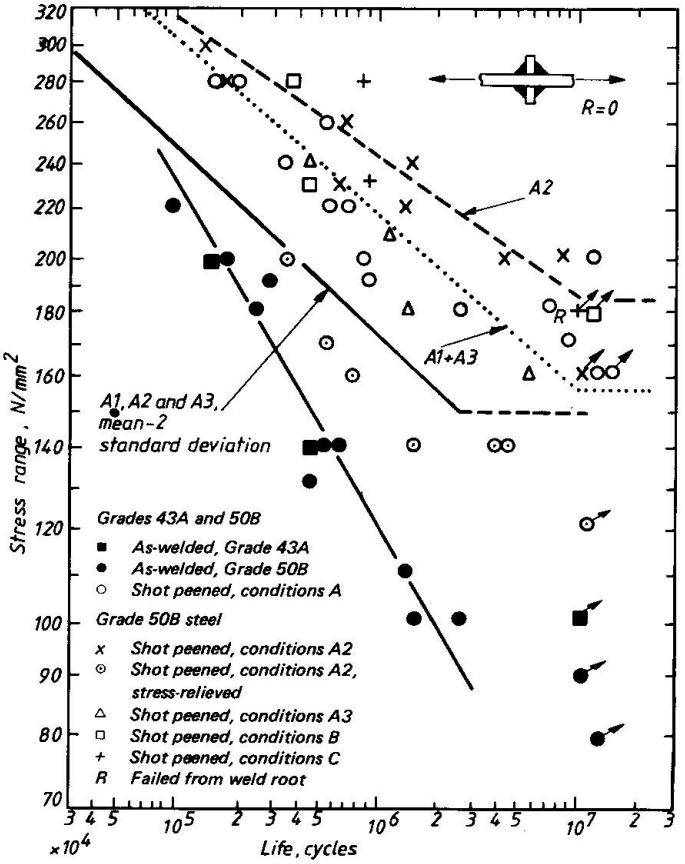

Fig. 2. Fatigue test results for shot peened specimens with transverse fillet welded attachments.

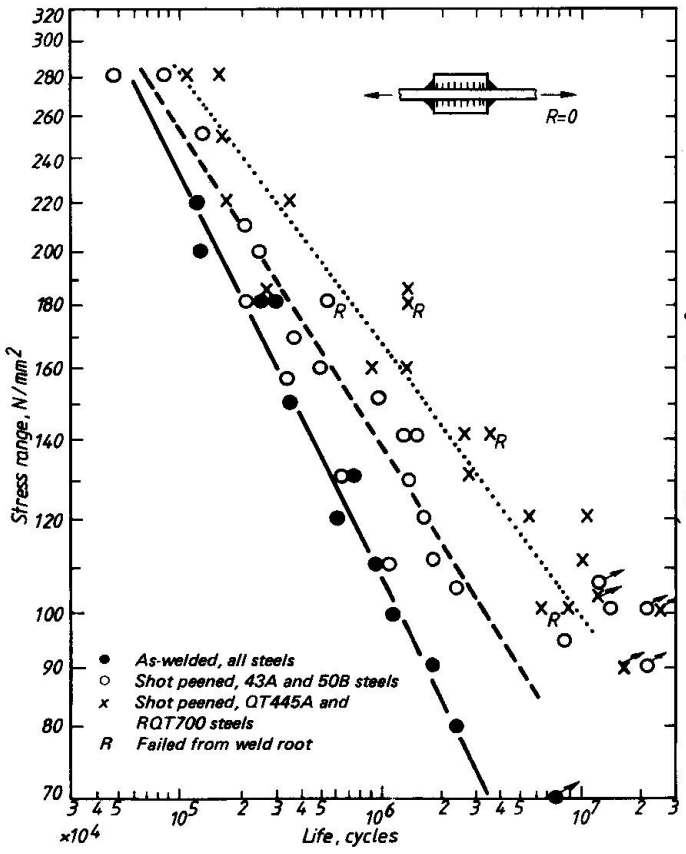

Fig. 3. Fatigue test results for shot peened specimens with longitudinal fillet welded attachments.

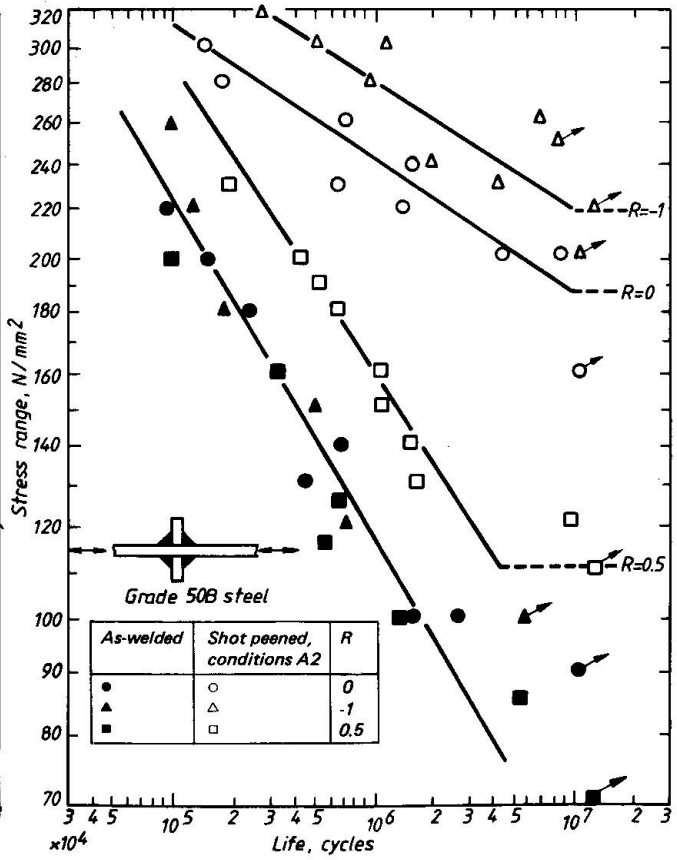

Fig. 4. Effect of stress ratio on fatigue strength of shot peened specimens with transverse fillet welded attachments.

3. PRESENTATION AND DISCUSSION OF RESULTS

3.1. Effect of shot peening

The level and extent of compressive residual stress introduced by shot peening was checked on transverse weld specimens in 50B steel peened using A2 conditions by X-ray diffraction and by a relaxation technique [10]. Both methods indicated that compressive residual stresses close to tensile yield in magnitude were present near the surface. The relaxation technique further showed that they fell to zero 0.75mm below the surface.

The fatigue test results are presented in Figures 2 to 4 together with mean S-N curves fitted to the results from specimens which failed. Fatigue failure occurred from the weld toe unless otherwise indicated. It will be seen that shot peening usually introduced an improvement in fatigue strength, although the results for shot peened joints were more scattered than those for the as-welded joints and there was some overlap of results. As expected, the improvement increased with decrease in applied stress, so that the S-N curve was rotated. The fatigue limit was not clearly established in any of the test series but the indications are that it was increased considerably by shot peening.

Factors affecting the degree of improvement due to shot peening are discussed in the following sections. A number of variables were considered and in this respect it should be noted that the need for clarity in the figures and the shortage of space in the present paper have meant that in some cases results obtained under different conditions have been combined. However, these measures were taken only if analysis of the separate results showed that any differences between them were not statistically significant at the 99% level.

3.2. Influence of weld type

The results obtained for the two weld types in the same steels, 43A and 50B, are given in Figures 2 and 3. As can be seen, the improvement was considerably greater in the transverse than in the longitudinal weld detail, particularly near the fatigue limit. Tests on grit blasted specimens led to the same conclusion [11]. Based on the mean S-N curves at 2×10^6 cycles, the improvement in fatigue strength for the longitudinal detail was 35% while that for transverse welds was 93%. There was still a 33% improvement at 10^5 cycles in the case of the transverse welds but virtually none in the longitudinal weld. A possible explanation for this difference is that the tensile residual stresses due to welding, which would have been higher in the specimens with longitudinal welds than in those with transverse welds [1], inhibited the introduction of compressive residual stresses by shot peening or reduced their beneficial effect. Alternatively, the weld geometry at the end of a longitudinal attachment is less amenable to shot peening treatment.

3.3. Influence of steel strength

The influence of the steel strength can be examined by reference to the results obtained from specimens with longitudinal attachments, in Figure 3. There was no significant difference between results obtained from the two carbon structural steels or for the two QT steels, perhaps because in each case the difference between the strengths of the two steels was not large. As anticipated the improvement obtained from specimens made from high strength QT steels appeared to be considerably higher than that obtained from carbon steels. At 2×10^6 cycles, the improvement was 70% compared with 33% for the lower strength steels, and at 10^5 cycles there was still a 25% increase. However, because of the

scatter in the results, the difference between the S-N curves for the QT and carbon steels was not statistically significant above the 80% level.

3.4. Influence of shot peening conditions

Limited tests were carried out to investigate the effect of changes in the shot peening conditions but what proved to be of more interest was the opportunity to compare the results from welded joints shot peened under nominally identical conditions at different times and by different companies. All the results are given in Figure 2 where it will be seen that the selected variations in peening conditions had no consistent effect on the degree of improvement but there is a difference, which is statistically significant at the 90% level, between the results obtained from the batch of specimens shot peened using conditions A2 and the other two (A1 and A3). It is interesting to see that this difference did not arise as a result of a change from one shot peening company to another, A1 and A2 referring to the same company. From the practical viewpoint these results are important because they demonstrate that shot peening conditions which produce the same Almen intensity do not necessarily give the same fatigue strengths.

Examination of the shot peened welds indicated that conditions A2 had introduced a distinct improvement in the weld toe geometry whereas conditions A1 and A3 had not and this could explain the superior fatigue strengths for A2 specimens. The beneficial effect of the improved weld toe geometry in A2 specimens was demonstrated by testing specimens which had been stress relieved at 580 - 620°C for one hour, as seen in Figure 2.

Although there is scope for exploring other shot peening conditions, it would appear that of those used in the present investigation conditions A were the most suitable. Certainly the large number of failures originating at the weld root in QT steels (Figure 3) suggests that no further improvement in those joints is possible.

3.5. Influence of loading conditions

The results in Figure 4 shows that, as expected, there was an increase in the fatigue strength of shot peened specimens for R = -1 and a decrease for R = 0.5, compared with results for R = 0. Theoretically, assuming elastic conditions, the effective tensile stress resulting from the superposition of an applied stress range S and a residual stress S_{res} is $S_{max} + S_{res}$, where S_{max} is the peak tensile applied stress. But $S = (1-R)\ S_{max}$ and therefore the applied stress ranges which result in the same effective stress, and hence fatigue life, for the three R values should be in the ratio 1: 2: 4 for R = 0.5, 0 and -1 respectively. Clearly, these estimates based on elastic conditions will be most reliable at the fatigue limit. Referring to Figure 4, the actual values for R = 0 and 0.5 differ by a factor of approximately 1.7, but for R = 0.5 and -1 the factor is 1.95, about half that predicted. A possible explanation for this is that the application of a compressive stress during cycling under R=-1 relaxes the original compressive residual stress, an effect observed by Kodama [9]. To check this, residual stresses were measured in an unbroken specimen tested at ±100 N/mm^2 for 10^7 cycles. They were found to be between -50 and -100 N/mm^2, which represents a reduction of around 75% compared with the levels measured in untested specimens.

Thus, the present results indicate that the fatigue strength improvement due to shot peening depends on the magnitude and type of loading, both from the point of view of the dependence of the effective stress on the peak applied stress and

the possible reduction in residual stress. In practice, this could be particularly important if shot peened joints operate under a spectrum of loads, especially if it contains high tensile stresses and compressive stresses.

An investigation of the fatigue behaviour of shot peened transverse fillet welded joints under random loading is in progress and preliminary results are presented below. Initially use was made of a spectrum based on the highway bridge axle load spectrum in BS 5400 which, from tests on as-welded joints, was known to produce fatigue lives up to double those estimated using Miner's rule, an indication that some crack growth retardation occurred as a result of high tensile stresses in the spectrum. It was:

Applied stress/ Max. applied stress	1.0	0.94	0.88	0.78	0.72	0.66	0.61	0.56	0.50	0.44	0.39	0.34	0.22	0.17
No. of occurrences in $\sim 5 \times 10^5$ cycle repeat block, kilocycles	44.0	58.7	11.0	11.0	33.0	11.0	30.4	53.5	27.3	22.0	58.7	69.7	11.0	66.1

The results obtained with R = 0 from 50B steel specimens were as follows:-

Condition	maximum stress range in spectrum, N/mm^2	Life cycles	actual life / predicted life
as-welded	211	690,000	1.4
shot peened (A1)	211	5,467,422	1.1
as-welded	188	2,063,085	2.8
shot peened (A3)	188	14,425,000 unbroken	> 1.4

As will be seen, shot peening still improved the fatigue lives of joints tested under random loading. The 8-fold increase in life obtained under the higher stress was approximately that expected from the constant amplitude results at 0-211 N/mm^2 (see Fig.2), suggesting that the highest stress in the spectrum might determine the degree of improvement due to shot peening. The actual lives all exceeded those predicted using Miner's rule in conjunction with the appropriate mean constant amplitude S-N curves, although it would appear that the margin is less with shot peened joints than as-welded.

4. CONCLUDING REMARKS

This work has confirmed that under some conditions the fatigue strength of steel fillet welds can be improved by shot peening. However, it has also shown that the degree of improvement can vary significantly depending on the loading conditions and shot peening conditions. An increase in positive R value, with the corresponding increase in peak tensile stress and hence increase in effective stress, reduces the benefits seen under R = 0. The application of partly compressive loading leads to an increased benefit but not as great as expected, probably because the compressive residual stresses are partly relaxed. It was feared that some relaxation would also occur under random loading but it was encouraging to find from preliminary tests that this will not necessarily happen. It is possible that such a problem will only arise if compressive stresses occur. Although high tensile stresses might relax the compressive residual stresses due to shot peening, they should then leave a new compressive residual stress field which will still reduce subsequent fatigue damage (the crack growth retardation phenomenon). The effect of the known variation in shot peening conditions was not so significant and a more striking variation was that seen between different

groups of specimens shot peened under nominally, the same conditions. This finding, together with the fact that overall the scatter obtained in the results for shot peened specimens was large, suggests that the current method of assessing the effect of shot peening, the Almen strip, is not sufficiently sensitive, or that the anticipated reproducibility of a given set of peening conditions cannot be realised. In practice, it may prove to be unrealistic to expect greater consistency, in which case due account will need to be taken of the wide scatter in test results when design S-N curves are derived. As an illustration of the consequences of such an approach, the mean -2 standard deviations S-N curve from regression analysis of all the results from specimens peened using condition A for R = 0 is shown in Figure 2. Clearly, the full potential of shot peening would not be achieved using such a curve. Even so the improvement over the as-welded joint is still considerable, particularly in the high-cycle regime. More work is required before firm proposals can be made, particularly to ensure that qualifications (eg. relating to loading conditions, weld type and condition, environment) to be placed on the applicability of such proposals are fully appreciated.

The increased benefit observed in high strength steels suggests that further work using transverse fillet welds, which derive greater benefit than the longitudinal weld details used so far, would be worthwhile.

ACKNOWLEDGEMENTS

The author is glad to acknowledge the work of the Fatigue Laboratory staff under Mr. R. A. Males and his colleagues J. G. Summers, B. J. Fitzpatrick and G. Slater. The project was financed jointly by Research Members of The Welding Institute and the Engineering Materials Requirements Board.

REFERENCES

1. GURNEY, T.R.: Fatigue of Welded Structures, Cambridge University Press, 1979.
2. KNIGHT, J.W.: Improving the fatigue strength of fillet welded joints by grinding and peening, Welding Research Int., Vol.9, No.3, 1979.
3. FUCHS, H.O.: Forecasting fatigue life of peened parts, Metal Progress, May 1963.
4. BRINE, F.E., WEBBER, D. and BARON, H.G.: Effect of shot peening on the fatigue properties of maraging steel and Al-Zn-Mg alloy, British Welding Journal, November 1968, p.541-546.
5. DESCLOUX, J.C.: Influence du genaillage controle sur le comportement en fatigue d'assemblages soudes en acier, Soudage et Techniques Connexes, Vol. 29, No.9-10, Sept.-Oct. 1975, p.341-352.
6. FAULKNER, M.S. and BELLOWS, D.S.: Improving the fatigue strength of butt welded steel joints by peening, Welding Research Int., Vol.5, No.3, 1975, p.63-72.
7. BOOTH, G.S.: The effect of mean stress on the fatigue lives of ground or peened fillet welded steel joints, Welding Institute Members Report, 34/1977/E, March 1977. (To be published).
8. POTTER, J.M. and MILLARD, R.A.: The effect of temperature and load cycling on the relaxation of residual stresses, Proc. Conf. Advances in X-ray Analysis, Syracuse University, 1977.
9. KODAMA, S.: On the decrease of residual stress due to cyclic stress, Tokyo Metropolitan University, V-441/B, 1972-73.
10. LEGGATT, R.H. and KAMATH, M.S.: Residual stresses in 25mm thick weld metal COD specimens in the as-welded and locally compressed states, Welding Institute Members Report, 145/1981.
11. GURNEY, T.R.: Exploratory fatigue tests on plastic coated specimens, Brit. Welding Journal, October 1963, p.530-533.

Improvement of Fatigue Life of Welded Beams by TIG-Dressing

Augmentation de la durée de vie des poutres soudées traitées selon le procédé TIG

Erhöhung der Ermüdungsfestigkeit geschweisster grosser Träger durch WIG-Verfahren

H.H. MINNER
Dr. -Ing.
Ingenieurbüro Minner
Hamburg, BRD

T. SEEGER
Prof. Dr. -Ing.
Technische Hochschule Darmstadt
Darmstadt, BRD

SUMMARY
The fatigue strength of large welded beams has been investigated. The beams were fabricated from StE 460 or StE 690 high strength steel and had either staggered splice details or stiffeners. Some were tested as-welded and others with the weld TIG-dressed. The test results are discussed and compared with results in the literature for smaller beams. The improvement factor of 1.4 to 1.5 obtained by TIG-dressing is lower than that found for smaller beams. In addition, the larger have 20% to 35% less fatigue strength because of welding faults.

RESUME
La résistance à la fatigue des grandes poutres soudées a été examinée. Les poutres étaient en acier à haute résistance StE 460 et StE 690 et avaient soit des joints échelonnés, soit des raidisseurs. Quelques unes avaient des soudures brutes, d'autres avaient des soudures traitées selon le procédé TIG. Les résultats des essais sont discutés et comparés avec ceux donnés dans la littérature pour des petites poutres. Le facteur d'augmentation de 1,4 à 1,5 obtenu avec le procédé TIG est plus bas que celui trouvé pour des petites poutres. De plus, les grandes poutres ont une résistance à la fatigue 20 à 35 % plus faible à cause des défauts dans les soudures.

ZUSAMMENFASSUNG
Die Schwingfestigkeiten von geschweissten und WIG-nachbehandelten grossen Trägern mit Stumpfstoss und Aussteifungen wurden untersucht. Die Träger waren aus hochfesten Feinkornbaustählen StE 460 und StE 690 hergestellt. Die Versuchsergebnisse werden vergleichend mit denen der ebenfalls untersuchten kleinen Träger und Proben diskutiert. Sie zeigen, dass die Erhöhungsfaktoren WIG-nachbehandelter grosser Träger 1.4 bis 1.5 betragen, was etwas geringer ist als für kleine Träger und Proben. Schweissnahtinnenfehler führen hingegen bei grossen geschweissten und WIG-nachbehandelten Trägern zu einem Schwingfestigkeitsabfall von 20% bis 35%.

1. INTRODUCTION

During the last years innumerable investigations of the fatigue behaviour of welded specimens made of different steel grades were carried out. The results showed that there is no or only a little difference between the fatigue strength of low and high strength steels (see literature of reference |1|). Especially concerning high strength steels these findings led to the efforts to find economic and effective methods of increasing the fatigue strength. Besides mechanical treatments of the welds thermic methods seemed to offer more important advantages in terms of efficiency and economy. These methods known as TIG- or Plasma-dressing brought a considerable improvement of fatigue strength up to 170% (see literature of reference |2|).

Nearly all of these investigations were performed on small specimens and only a few were concerned with the fatigue strength of component parts. Beyond that the range of most of the tests was limited and the published results left some questions unanswered. Therefore in 1975 the authors started an extensive research program which dealt with fatigue strength investigations of welded high strength steels in as-welded and TIG-dressed conditions. One of the aims of this research program was to answer the question for transferability of test results from small specimens to larger component parts which is more important for the determination of allowable stresses in design rules and standards.

Essential parts of the whole research program which contains fatigue tests with small specimens, small and larger beams have already been reported |2, 3|. In the following the actual situation of our investigations is presented with special regard to the results of welded larger beams. These results will be compared with those of the smaller beams which are published before |2|.

2. TEST MATERIAL, TYPES OF BEAMS AND PERFORMANCE OF FATIGUE TESTS

The investigations were carried out on weldable high strength steels StE 460 and StE 690. The mechanical properties and chemical composition of the used material is shown in Tab. 1. All values are in accordance with the German standard DASt-Richtlinie 011 which regulates the use of weldable high strength steels in static and fatigue loaded structures.

The constant amplitude fatigue tests were performed under four-point bending on two types of welded larger beams, beams with staggered splices and beams with stiffeners, both in as-welded and TIG-dressed conditions. In addition to this rolled beams of steel StE 460 with a butt weld in the top flange and with stiffeners were also tested in aswelded and TIG-dressed conditions. Weld details and dimensions of investigated beams are shown in Fig. 1 to Fig. 4.

3. RESULTS AND DISCUSSION OF FATIGUE TESTS

3.1 BEAMS WITH STAGGERED SPLICES

The results of larger beams with splices in as-welded and TIG-dressed conditions are shown in Fig. 1 and Fig. 2. They are compared with those of the small beams which are plotted in the unified scatter-band of the S-N-curves for welded |4| and TIG-dressed |2| joints. It can be seen that for the small beams both steel grades have nearly the same fatigue strength. The increasing factor due to the TIG-dressing of the butt welds is about 1,7 which is conform to the improvement of fatigue strength of small specimens with TIG-dressed butt welds |2|.

In case of larger beams the endurable fatigue life is partially much lower than

that of the smaller beams. The evaluation of all test results showed that there is a 20% decrease of fatigue strength for both beams in as-welded condition (Fig. 1) and a 35% decrease in TIG-dressed condition (Fig. 2). The main reasons for this lower fatigue life are fatigue crack initiations from TIG-weld porosities or undercuts (Fig. 2) and from the inside of flange butt welds and longitudial fillet welds caused by slag inclusions and hydrogen induced cold cracks (Fig. 1 and Fig. 2). The cold cracks occured only at the longitudial fillet welds of StE 690 beams and were sometimes distributed over the whole weld length.

Only welded beams of StE 460 in as-welded condition which have a normal fatigue crack initiation from the weld toe of the flange butt welds show a tendency to the same fatigue strength as the smaller beams. Not so rolled beams of StE 460 in as-welded condition which have also a normal fatigue crack initiation. Here are the number of cycles comparable with those beams which failed from weld defects (Fig. 1). A possible reason for this fact might be seen in the MAG-welding by hand of the butt welds of rolled beams which produced sometimes a very low weld reinforcement in connection with small base metal undercuts.

Larger beams in TIG-dressed condition show only a small improvement of fatigue life due to the very high number of failures inside the welds (Fig. 2). As mentioned in former publications |2, 3| a successful utilization of the TIG-dressing is ony given if the dressed welds have neither systematic inner notches nor larger inner faults and porosities or undercuts of the TIG-weld. Otherwise the fatigue crack starts at these faults and the TIG-dressing process produces no or only a little effect. Therefore the increasing factor in the present case is lower than for the smaller beams and reaches only a value of about 1,4.

3.2 BEAMS WITH STIFFENERS

Fig. 3 shows the results of beams with stiffeners in as-welded condition. In contrast to the larger beams the results of smaller beams plotted in the unified scatter band of the S-N-curve for welded joints |4| have no uniform fatigue strength for both steel grades. The difference in the endurable fatigue limit stresses between smaller beams of StE 460 and StE 690 is about 50%. Reasons for this discrepancy are unknown. Influences of residual stresses which could not be removed by post-weld heat treatment are possible.

The fatigue strength of larger welded beams, however, is nearly the same for both grades of steel and within the scatter of the small beams. Only the slope of the S-N-curve seems to be a little bit steeper and therefore not in accordance with the given slope $k_{50\%} = 3{,}75$ of the statistical evaluation. Here again larger rolled beams have a lower fatigue life than larger welded beams although all investigated beams had a normal fatigue crack initiation from the weld toe of the stiffener welds.

The results of stiffened beams in TIG-dressed condition are presented in Fig. 4. In contrast to the fatigue behaviour of small beams in as-welded condition (Fig. 3) we can see a similar fatigue strength of TIG-dressed small beams for both grades of steel. Only the limit number of cycles N_A which for TIG-dressed joints is normally given at 10^6 cycles could be shifted to a value of $2 \cdot 10^6$ cycles. This decrease of fatigue limit stresses seems to be caused by small undercuts of the TIG-weld run. The increasing factors are about 1,5 for StE 690 and 2,4 for StE 460 if the limit number of cycles $N_A = 10^6$ for TIG-dressed beams is compared with $N_A = 2 \cdot 10^6$ for as-welded beams. The latter increasing factor of 2,4 results from the very low fatigue limit stress of small StE 460 beams in as-welded conditions (Fig. 3).

The evaluation of all test results of larger beams in TIG-dressed condition show a decrease of the endurable fatigue strength of about 30%. For the larger

welded beams of StE 460 also undercuts lead to a lower endurable fatigue life. Here the TIG-welds have undercuts with a greater depth than for the smaller beams. Rolled beams of StE 460 with normal fatigue crack initiations from the transition between the base metal and the TIG-weld run have a better fatigue life behaviour which is near to the lower limit of the scatter-band of the small TIG-dressed beams. In case of larger welded StE 690-beams again the fatigue cracks initiate at the inside of the longitudial fillet welds but they are still in the range of StE 460-beams.

3.3 COMPARISON WITH SMALL SPECIMENS

As mentioned before one of the aims of the investigations was to answer the question of transferability of fatigue data from small specimens to larger component parts. In Fig. 5 and Fig. 6 the test results of small and larger beams are compared with those of the specimens both in as-welded and TIG-dressed condition. The endurable stress amplitudes σ_A of all investigated test series and stress ratios are plotted in the Haigh-diagram verse the mean stress σ_m. For the comparison the fatigue limit stresses σ_A of as-welded joints are related to $N_A = 2 \cdot 10^6$ number of cycles and for TIG-dressed joints to $N_A = 10^6$ cycles.

Joints with butt welds (Fig. 5) show a very good conformity of small specimens and small beams. Influences of the Steel grade or the type of specimen are hardly evident. The TIG-dressing process produces a considerable improvement of fatigue strength with no difference between small specimens and small beams. The increasing factors are nearly independent of the stress ratio and have a mean value of about 1,6 which is comparable with other international investigations (see references of literature in |2|). As-welded and TIG-dressed joints have similar mean stress dependences. Larger beams, however, which were only investigated at a stress ratio R = 0,1 do not confirm these statements. In as-welded condition they have a 20%-decrease of fatigue strength in comparison with the small beams and in TIG-dressed condition the decrease is about 35%. The reasons for this fact are weld defects inside the longitudial fillet welds and the flange butt welds which bring especially in case of dressed larger beams a very low fatigue strength. Due to this the increasing factor of dressed larger beams is only 1.4 (see chapter 3.1).

In contrast to the joints with butt welds joints with stiffeners have no uniform fatigue strength behaviour (Fig. 6). As-welded small specimens of both steel grades differ in the range of R = -3 up to R = 0,4. Possible reasons for this fact might be seen in residual stress influences as well as in the specimen geometry |2|. Small beams with stiffeners show similar fatigue limit stresses for the stress ratio R = 0,1 as the small specimens. In case of TIG-dressed small specimens only the steel StE 690 was investigated. Here a change of the crack initiation from the transition between the base-metal and TIG-weld run to the weld root under the stiffener shifted the limit number of cycles $N_A = 10^6$ to a value of about $N_A = 2 \cdot 10^6$ coincident with lower endurable fatigue stresses |2|. Therefore the increasing factors of TIG-dressed small specimens with stiffeners made of StE 690 reach only a mean value of about 1,4 which is nearly the same for small StE 690-beams with stiffeners. TIG-dressed small beams of StE 460, however, have an increasing factor of about 2,2 which is caused by the very low fatigue limit stresses of beams in as-welded condition.

Larger beams with stiffeners in as-welded condition show the same fatigue strength as the small StE 460-beams. In both cases the fatigue crack started at the weld of the stiffener welds. In TIG-dressed condition the endurable fatigue stresses of larger beams are much lower than those of comparable smaller beams. Responsible for this decrease which is about 30% are again failures inside the longitudial welds of StE 690 beams (cold cracks) and TIG-weld undercuts of StE 460 beams. Therefore the increasing factor is only 1,50 (see chapter 3.2).

4. CONCLUSION

The present investigations were performed on larger welded beams of high strength steels StE 460 and StE 690 and on a small number of larger rolled beams of StE 460 both with staggered splices and with stiffeners in as-welded and TIG-dressed conditions. The results of the fatigue tests made clear that problems arised not only by the welding but also by the TIG-dressing of high strength steels in larger dimensions under normal service conditions.

The main welding problem, hydrogen induced cold cracks, occured although the choice of the welding parameters |3| was done with attention to the particular specifications of the steel StE 690. These cracks lead to a decrease of the endurable fatigue life which was pointed out by the present fatigue tests. On the other hand TIG-dressing with undercuts produces only a little increasing effect as shown by the test results of StE 460 beams. Due to these reasons the endurable fatigue limit stresses of larger beams in as-welded and TIG-dressed conditions decrease for the investigated stress ratio R = 0,1 between 20% and 35% in comparison with the smaller beams. The increasing factors of TIG-dressed larger beams reached only values of 1,4 and 1,5 which is lower than those of the small beams and comparable small specimens |2|. The above mentioned reasons, cold cracks and TIG-weld undercuts, can be avoided by changing of the welding parameters and a better manual technique of TIG-dressing.

To sum up it can be said that in general the fatigue strength is evidently increased by the TIG-dressind process. As the test results showed this is not only valid for small specimens but also for larger component parts. Therefore the possibility of higher design stresses of TIG-dressed joints is given.

REFERENCES

|1| OLIVIER, R, and RITTER, W.: Catalogue of S-N-curves of welded joints in structural steels. Part 1: Butt joints, Part 2: Transverse stiffener, Part 3: Cruciform joint. DVS-Report No. 56. Deutscher Verlag für Schweißtechnik (DVS) GmbH, Düsseldorf 1979/1980/1981.

|2| MINNER, H.H., and SEEGER, T.: Investigations on the fatigue strength of weldable high strength steels StE 460 and StE 690 in as-welded and TIG-dressed conditions. IIW-Document XIII-912-79 (1979).

|3| MINNER, H.H., and SEEGER, T.: Fatigue strength of welded beams of high strength steels. IIW-Document XIII-951-80 (1980).

|4| HAIBACH, E.: Die Schwingfestigkeit von Schweißverbindungen aus der Sicht einer örtlichen Beanspruchungsmessung. Laboratorium für Betriebsfestigkeit, Darmstadt. Report No. FB-77 (1968).

Steel grade	C %	Si %	Mn %	P %	S %	N %	Al %	Cr %	Cu %	Ni %	Mo %	V %	Zr %	σ_y N/mm^2	σ_{UTS} N/mm^2	δ_5 %
StE 460	0,17	0,35	1,52	0,017	0,007	0,015	0,025	0,01	0,01	0,58	0,02	0,13	-	480	630	30
StE 690	0,15	0,58	0,93	0,014	0,011	0,009	0,048	0,78	0,11	0,09	0,26	0,02	0,10	770	830	21

Tab. 1 Chemical composition and mechanical properties of investigated steels

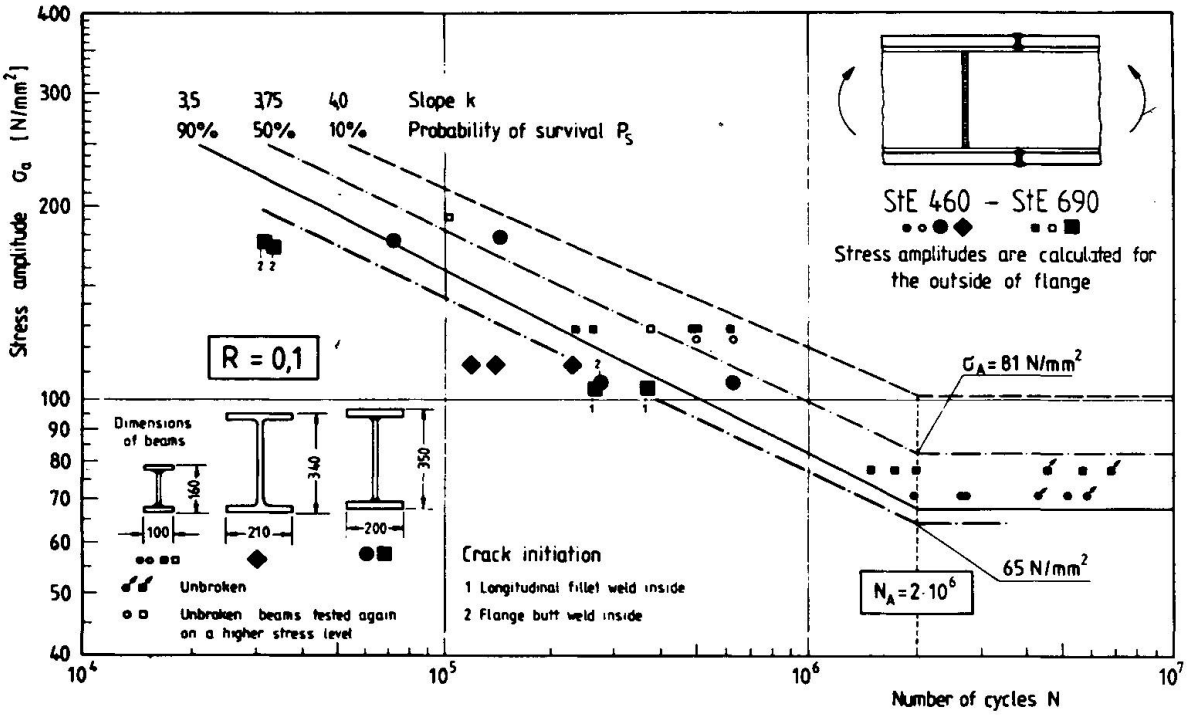

Fig. 1 S-N-curve for welded high strength steels - Beams with staggered splices

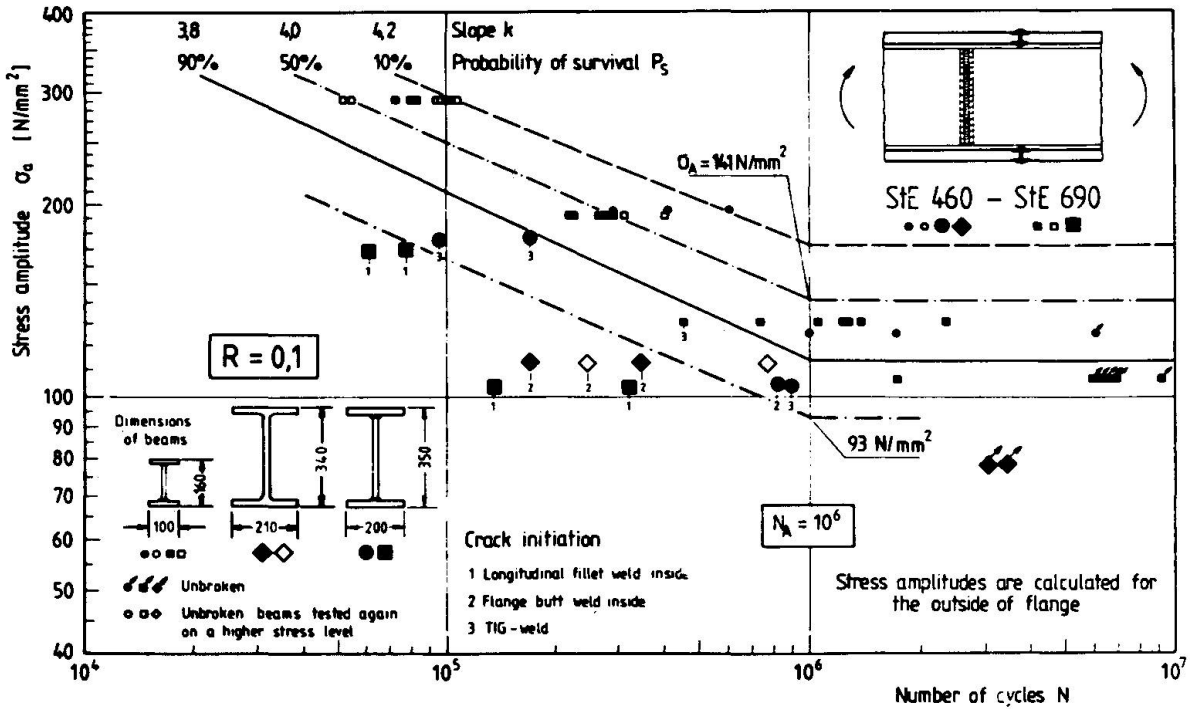

Fig. 2 S-N-curve for TIG-dressed high strength steels - Beams with staggered splices

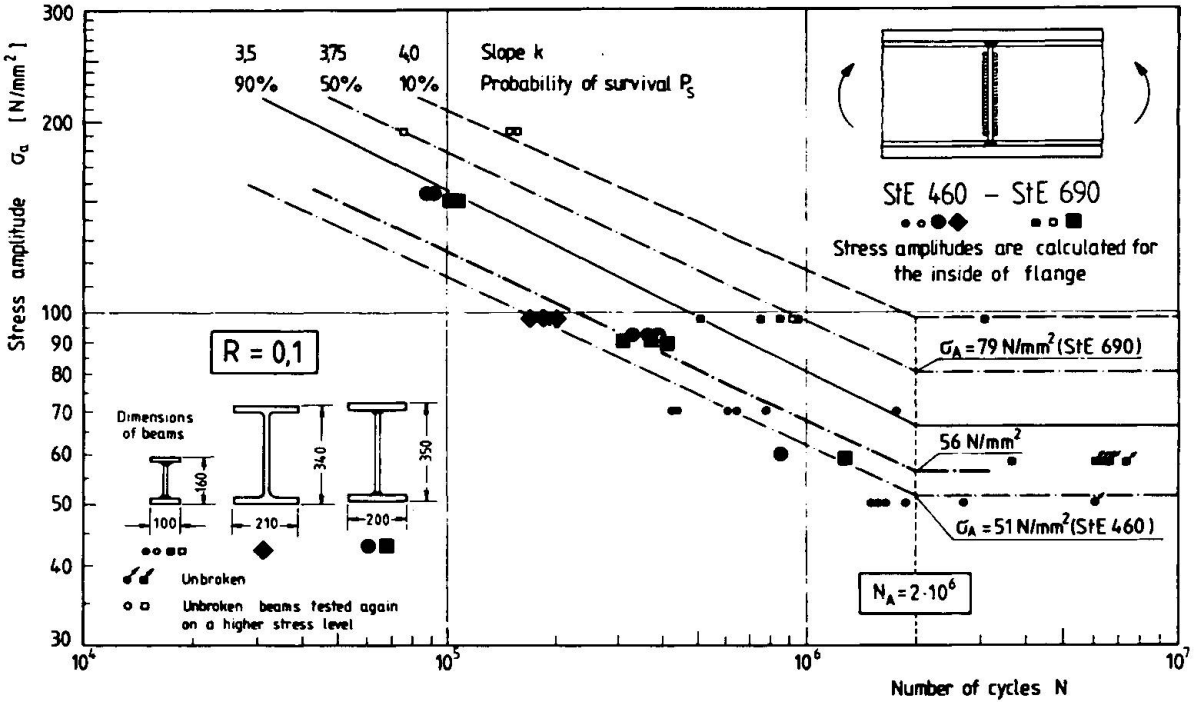

Fig. 3 S-N-curve for welded high strength steels-Beams with stiffeners

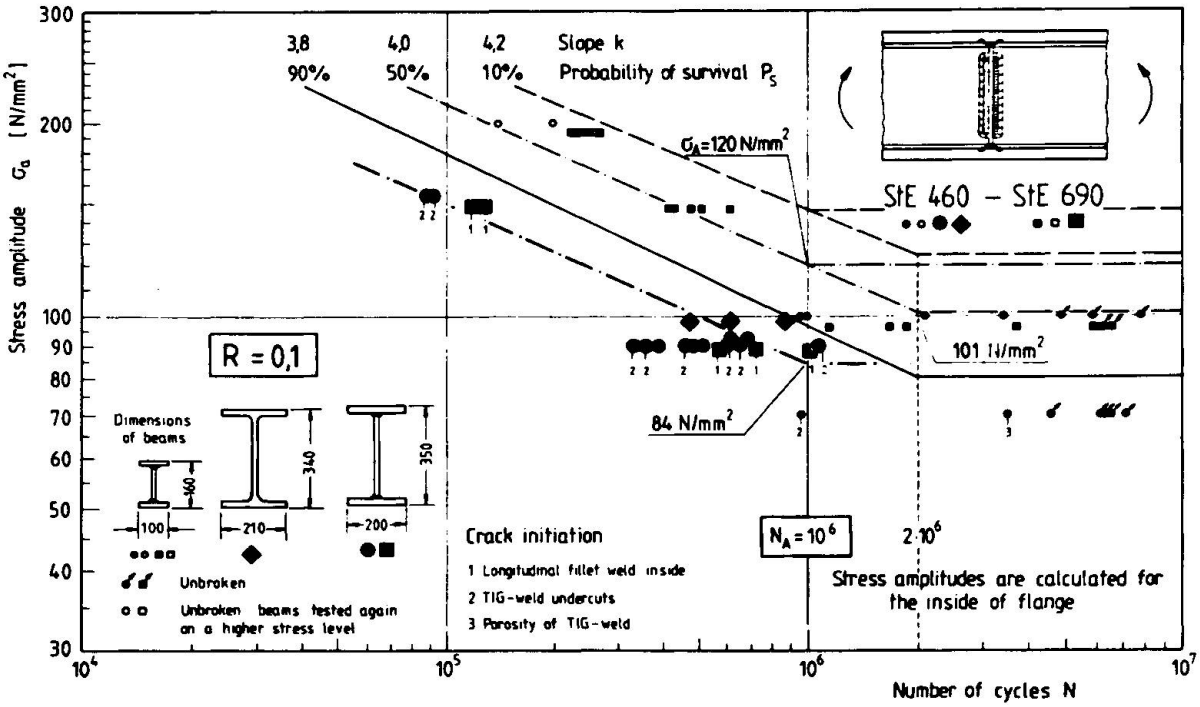

Fig. 4 S-N-curve for TIG-dressed high strength steels-Beams with stiffeners

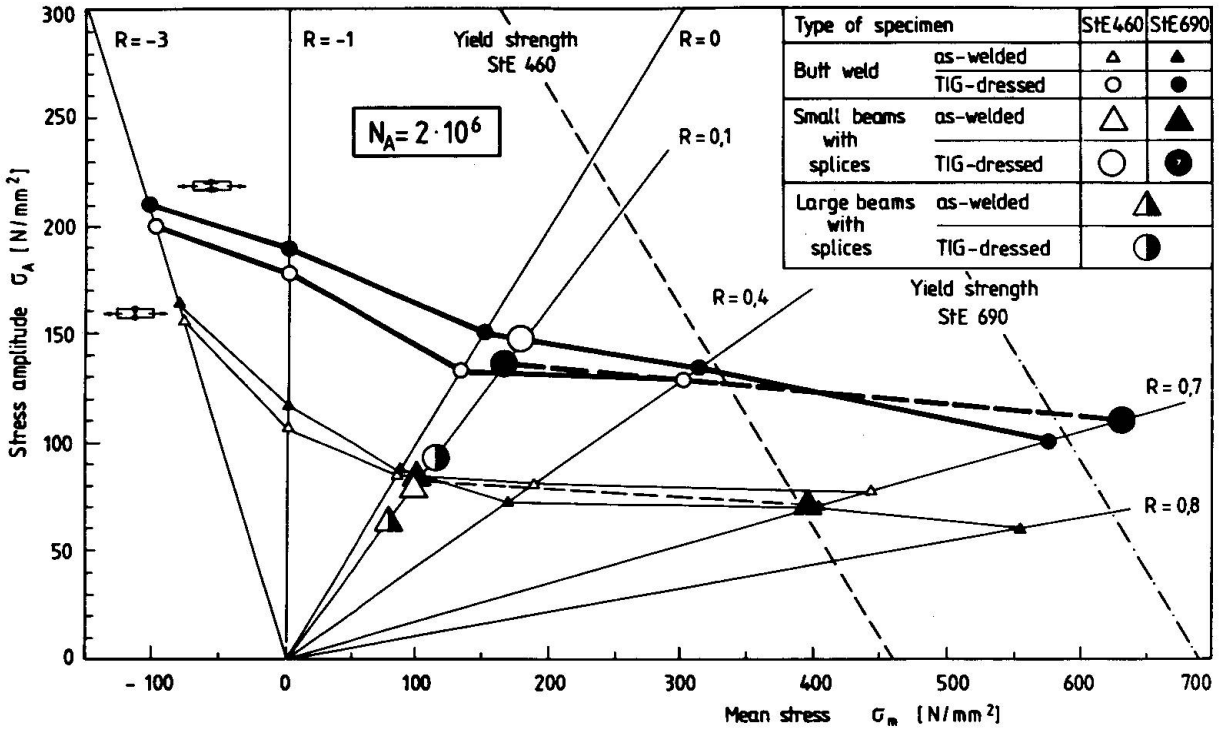

Fig. 5 Comparison of as-welded and TIG-dressed specimens - Joints with butt welds

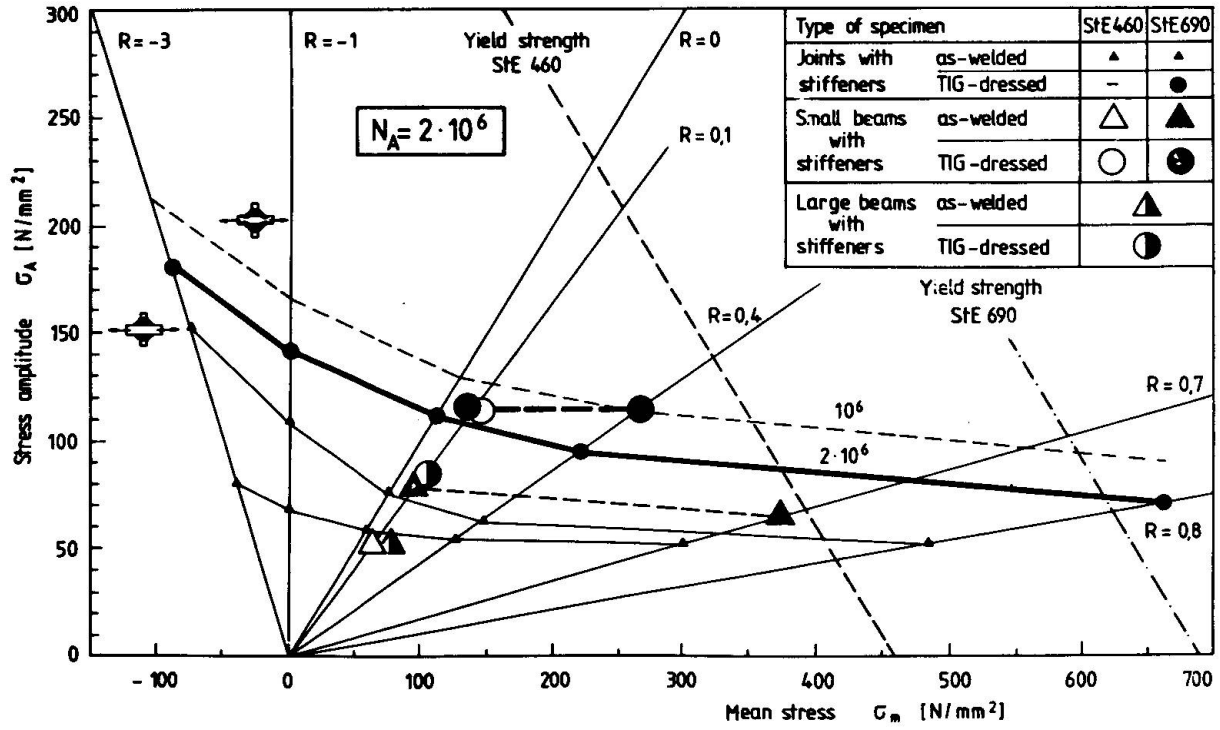

Fig. 6 Comparison of as-welded and TIG-dressed specimens - Joints with stiffeners

Fatigue Performance of Adhesive Bonded Joints for Bridge Deck Construction

Résistance à la fatigue d'assemblages collés pour la construction du tablier des ponts

Ermüdungsfestigkeit geklebter Verbindungen für den Bau von Brückenfahrbahnplatten

G.C. MAYS
Lecturer
University of Dundee
Dundee, U.K.

W.J. HARVEY
Lecturer
University of Dundee
Dundee, U.K.

SUMMARY
This paper describes numerous laboratory tests in fatigue which have been carried out on adhesive bonded open sandwich beams and slabs and on adhesive bonded steel/steel lap joints both before and after being subjected to various potentially adverse treatments. A good joint has been shown to possess excellent fatigue properties, superior to many details in welded steel. Research is now in hand to investigate the potential benefit of adhesive bonded web stiffeners in place of the conventional, fatigue prone, welded or bolted connections.

RESUME
Cet article décrit de nombreux essais de fatigue effectués en laboratoire sur des poutres et dalles mixtes, béton-tôle d'acier, dont la connection est réalisée par collage, ainsi que sur des assemblages collés acier-acier avec plaque de recouvrement. Les essais ont été soumis avant et après collage à des traitements potentiellement défavorables. Un bon assemblage a été remarqué possédant d'excellentes qualités d'endurance, supérieures à bien des détails en acier soudés. La recherche est maintenant à même d'étudier les avantages potentiels des raidisseurs collés au lieu des assemblages conventionnels, soudés ou boulonnés, de faible endurance.

ZUSAMMENFASSUNG
Der Bericht beschreibt zahlreiche Laborversuche an geklebten Bauteilen unter Ermüdungsbeanspruchung. Balken und Platten in geklebter Verbundbauweise sowie zweischnittige geklebte Stahlverbindungen sind untersucht worden. Die Prüfkörper wurden vor den Versuchen verschiedenen ungünstigen Umgebungseinflüssen ausgesetzt. Es wurde festgestellt, dass gut ausgeführte Verbindungen ausgezeichnete Ermüdungsfestigkeiten aufweisen, die diejenigen vieler geschweisster Details übertreffen. Die Forschungsarbeiten sind soweit gediehen, dass jetzt die möglichen Vorteile geklebter Stegsteifen gegenüber den geschraubten oder geschweissten untersucht werden können.

1. INTRODUCTION

The use of a conventional reinforced concrete slab is a common method of forming the roadway deck of medium span bridges. In longer spans the self weight forms a greater proportion of the total load, and a welded steel orthotropic deck becomes more economic. The "open sandwich" and "inverted catenary" decks described by SMITH & CUSENS [1] are both lighter than conventional reinforced concrete and cheaper than a welded steel deck. The open sandwich slab has a uniform thickness of concrete bonded to a flat mild steel plate. In the inverted catenary type the plate is curved to form a shallow arch. In both types the connection between steel and concrete is made with epoxy resin adhesive. The slabs are being developed for factory precasting.

Structural developments applied to bridges must remain sound when exposed to cyclic loading and to extremes of temperature for many years. The extensive programme of research carried out in the Wolfson Bridge Research Unit into adhesive bonded joints and their application to these decks has been summarised by MAYS & SMITH [2]. The present paper describes the fatigue testing of joints which forms part of the overall programme. Much of the fatigue testing for slabs has been carried out on small scale open sandwich beams but some half scale and full scale slabs have been tested. The fatigue performance of epoxy resins in shear has also been investigated using large numbers of double shear steel to steel lap joints. The results of these tests have led to work on adhesive bonded stiffeners for steel plates.

2. OPEN SANDWICH BEAMS

2.1 Specimen Manufacture

Beam specimens were 26 mm wide by 344 mm long with 17.2 mm of concrete on a 0.6mm steel plate. This represents, to a scale of approximately 1:6, a transverse strip from an open sandwich slab in a composite bridge. Steel plate, cut to size, was degreased by washing with detergent, rinsed with tap water and dried in warm air. Mill scale was removed with a mechanical sander and the surface was hand roughened with emery. Approximately 1 mm of adhesive was applied to the steel. Ordinary portland cement concrete with 5 mm maximum size aggregate was placed on the fresh adhesive and compacted on a vibrating table. The beams were demoulded after 24 hours and cured for 27 days at 20°C and 95% relative humidity.

The adhesives used were:
- (1) XD800; a thixotropic paste mixed with 10% of its own weight of liquid hardener understood to be an aliphatic polyamine;
- (2) AV100 + HV100; a high viscosity liquid resin mixed with its own weight of polyamide hardener;
- (3) AY105 + HY953F; a liquid resin mixed with its own weight of polyamide hardener;
- (4) XD548 + HY941; a pigmented paste mixed with half its own weight of medium viscosity liquid hardener understood to be an aromatic polyamine.

All are two part cold cure epoxy resins supplied by Ciba-Geigy Ltd.

2.2 Fatigue Testing

After curing, three beams made with each of adhesives 1,2 and 4 were subjected to control fatigue tests in four point bending on a span of 310 mm (Fig. 1). The loads were applied symmetrically 52 mm apart. Constant amplitude sinusoidal load cycles were applied at a frequency of 15 Hz. The minimum load in each cycle was 10% of the maximum. Beams which survived 1.5 million cycles were later tested in static flexure.

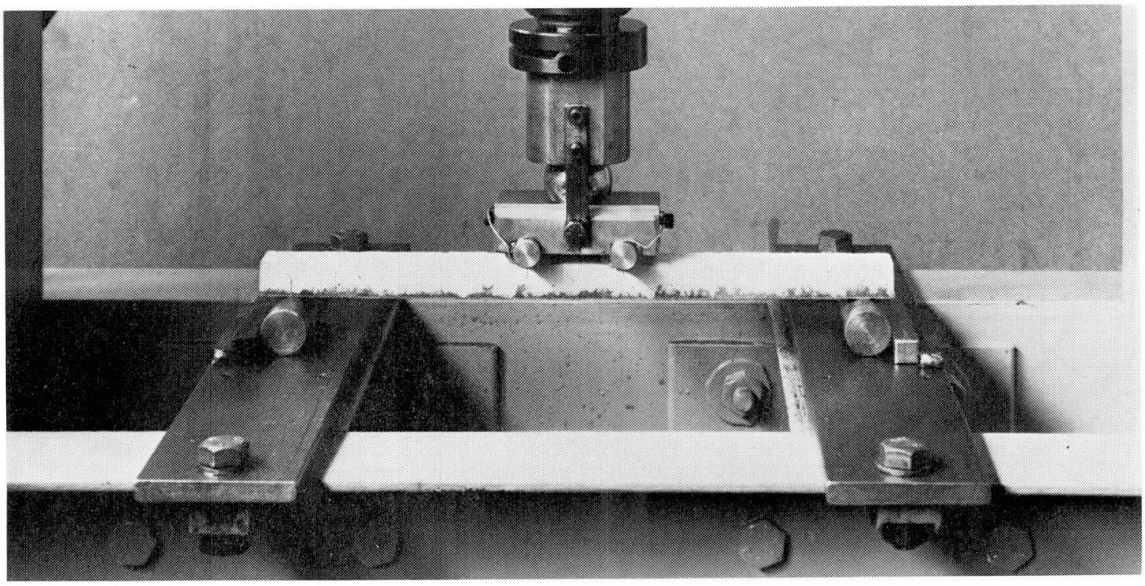

Figure 1 Open sandwich beam under test

A further nine beams for each adhesive were waterproofed with a coating of paraffin wax on all but their top surface and subjected to one of the following treatments:
- (1) continuous immersion in tap water for 8 weeks;
- (2) wetting in tap water for 6 hours twice weekly for 26 weeks;
- (3) as 2 but in 3% w/w salt solution.

These treatments were more adverse than that used on similar specimens reported by CUSENS & SMITH [3]. At the end of the treatment period, these beams, together with others which had been stored in the laboratory for the same period, were fatigue loaded in a similar manner to that described for the controls. Further beams have been stored for later treatment.

Reliable specimens could not be made with adhesive (3) and tests were abandoned after completing the study of treatment (1).

2.3 Results and Discussion

The results of the fatigue tests are presented in Figure 2. They are superimposed on the mean stress range versus endurance curves for grade 50 steel from BS5400 part 10 [4] plotted on log log scales with the stress range expressed as a fraction of the static (yield) strength.

Control beams with adhesive (1), (2) or (4) performed better than a class B welded detail. No significant deterioration took place during 32 weeks storage in the laboratory. Beams made with adhesive (1) deteriorated to class D after treatment (1) and had little strength after treatments (2) or (3). Those made with adhesives (2) or (3) showed poor resistance to fatigue after any of the treatments. These two adhesives had similar hardeners. In all these specimens rust was found on the steel plate after testing. The appearance of the rust suggested that aggregate particles had penetrated the adhesive layer, probably during compaction. In beams made with adhesive (4) aggregate penetration of the adhesive was also apparent, but corrosion was not significant at the time of testing. These beams still had high fatigue strength after treatments (1), (2) or (3).

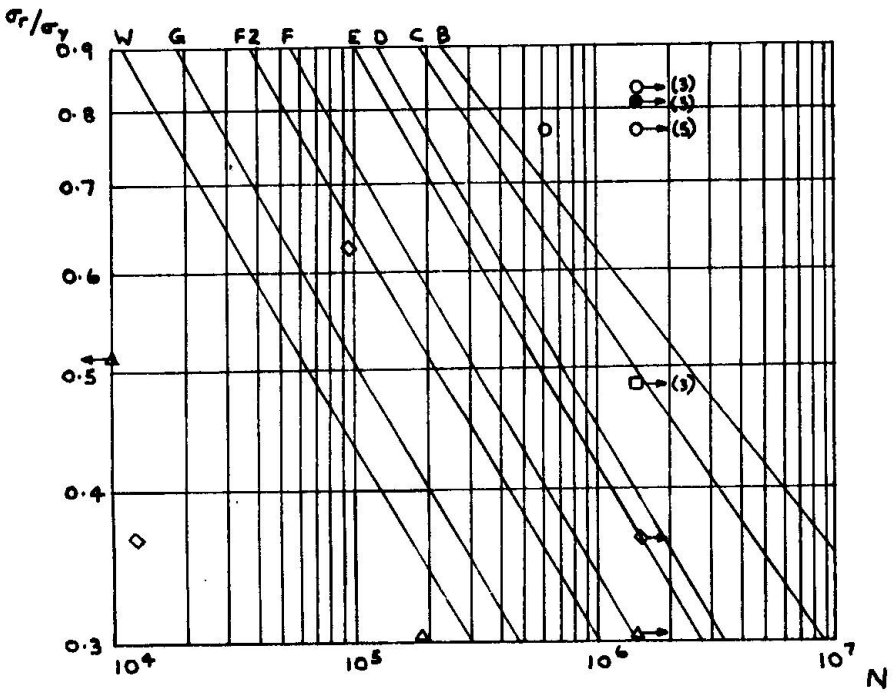

Adhesive (1)

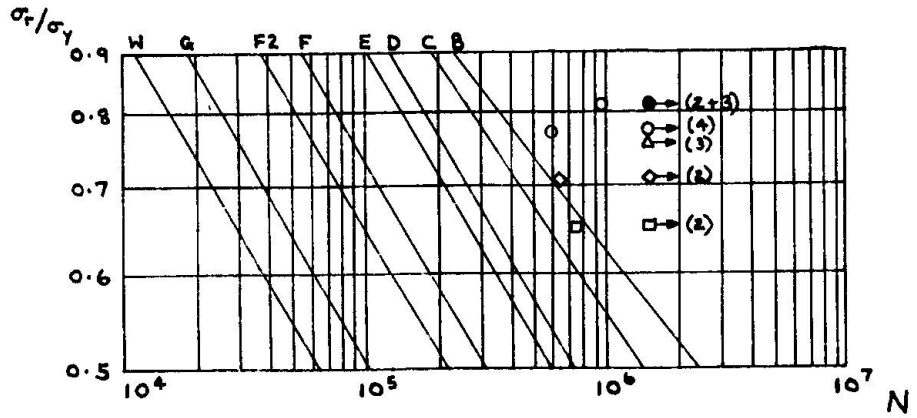

Adhesive (4)

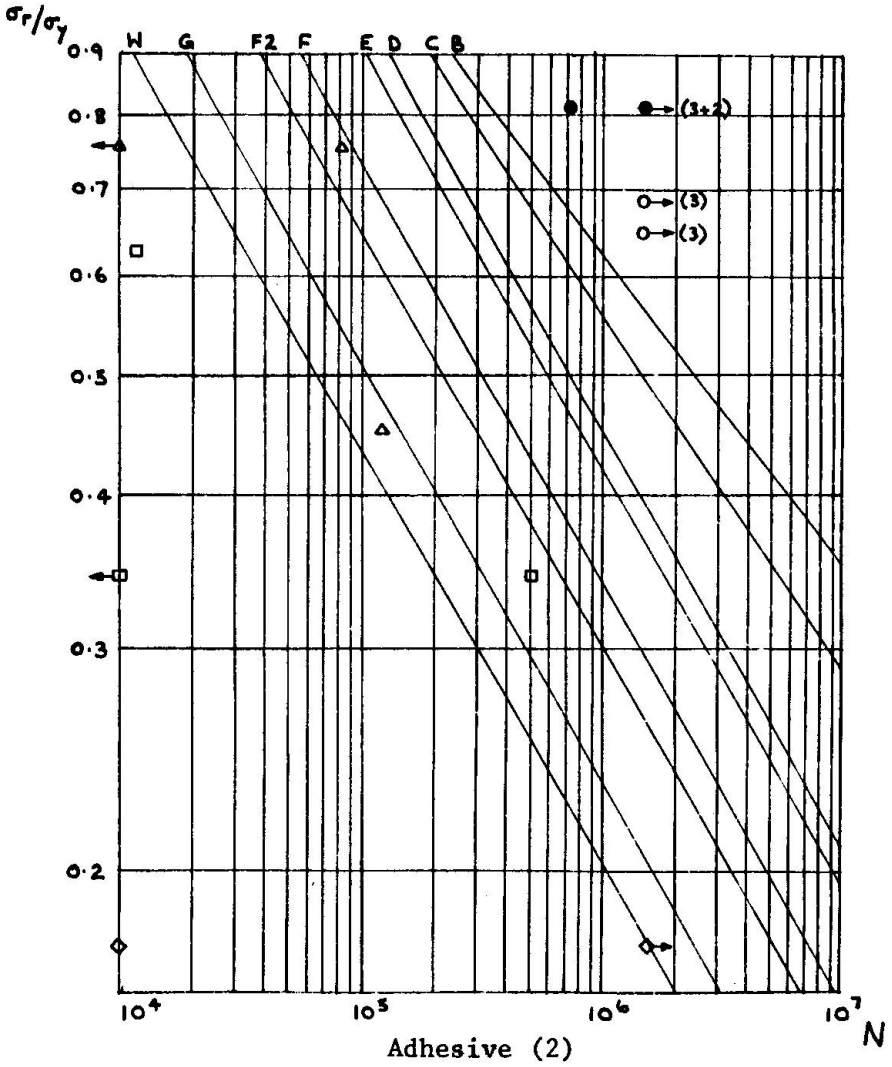

Adhesive (2)

o control ● 32 weeks' ageing

□ treatment (1) △ treatment (2)

◇ treatment (3) → did not fail

Figures in brackets denote numbers of specimens

Figure 2 Fatigue test results for open sandwich beams

Work is now in progress using beams with two layers of adhesive (4), the first of which is allowed to harden prior to casting. Fatigue results to date for control beams and after treatment (2) are all superior to a class B detail. There is little, if any, evidence of rusting and no tendency for separation between the layers.

3. OPEN SANDWICH SLABS

The performance of open sandwich slabs under traffic is being monitored over a period of years. A 2 m square slab has recently been installed in a test pit in Dundee's outer peripheral trunk road. Two half scale models have been tested in fatigue in the laboratory by applying patch loads at various positions on each slab. Each slab survived 7.5 million cycles of 28 kN load, and only failed after at least a further 1.7 million cycles at loads of up to 2.5 times this value. The shear failure mode was similar to that observed in static test.

4. STEEL TO STEEL LAP JOINTS

CUSENS & SMITH [3] reported fatigue test results for steel to steel double lap shear joints with adhesives 1, 2 and 4 after curing at room temperature, 40°C and 80°C. Further fatigue tests have been carried out on similar joints with different steel surface preparations.

4.1 Specimen Manufacture and Testing

Bright steel bar 25.4 mm x 5 mm was butt jointed with two 80 mm long cover plates of the same section. Bonding surfaces were cleaned of rust, degreased with acetone and blasted with metal grit to a finish resembling Swedish Standard ASa 2½ [5]. Three variations of steel surface condition were used to ascertain the effect of imperfect preparation on fatigue performance. The surfaces were:

- (1) standard clean rough surface as described;
- (2) as (1) but blasted with grade 50 sand to give a clean smooth surface resembling ASa 3 [5]:
- (3) as (1) but with cover plates allowed to rust over 15% of their area.
- (4) as (1) but cover plates dipped in 5% w/w salt solution to produce rust over 20% of their area after 20 hours.

The joints were assembled in a jig to give a glue line thickness of 0.65 mm. The ends of the main bars were debonded to eliminate direct stress transfer. Some specimens were heated at 15°C per hour then cured at elevated temperatures for 24 hours before being allowed to cool slowly. The specimens were then gripped in mechanical wedge grips (Fig. 3) and cycled under load control with a sine wave form at a frequency of 15 Hz. The minimum load in each cycle was 10% of the maximum. Specimens which survived 1.5 million cycles were tested at progressively higher loads until failure.

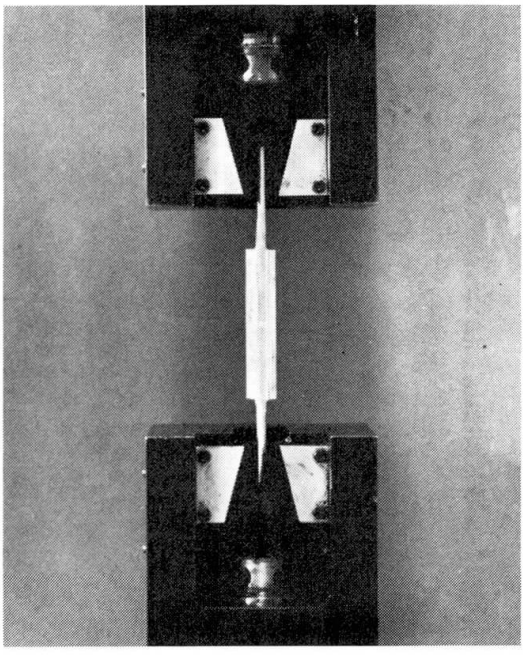

Figure 3 Lap joint under test

4.2 Results and Discussion

Results of fatigue tests on lap joints with the standard surface (1) are summarised in Table 1.

Adhesive	Curing Temp.	Mean shear stress range		Endurance (cycles)
		N/mm^2	as % static strength	
(1)	Room temp.	5.8	4.5 - 45	321,357
	80°C	6.4	4 - 40	307,653
(2)	Room temp.	5.2	4 - 40	388,075
	80°C	7.3	4 - 40	835,487
(4)	Room temp.	5.5	5 - 50	Survived 1,500,000
		7.7	7 - 70	29,700
	80°C	5.6	5 - 50	Survived 1,500,000
		7.8	7 - 70	18,357

Table 1 Endurances for lap joints

Static strength was reduced with surface conditions (2), (3) and (4) by up to 20% for adhesive (1) and 12% for adhesive (2). Adhesive (4) attained 83% of its control strength on surfaces (3) and (4) but only 53% on the smoother surface (2). All specimens were tested in fatigue at the proportion of their static strength indicated in Table 1. No reduction in endurance was noted for any group. All results are the mean for three tests.

Testing at controlled temperatures between -25°C and + 55°C is now in progress at endurances of up to 100 million cycles. Control results for adhesive 1 show no loss of fatigue strength at temperatures between -25°C and 45°C. A dramatic loss of fatigue strength was found at + 55°C. Specimens with all four adhesives are ageing in a variety of environments before testing and further results will be published shortly [6].

5. FATIGUE SUSCEPTIBLE DETAILS IN WELDED STRUCTURAL STEELWORK

The good fatigue resistance of the steel to steel lap joints described above suggested the use of adhesives in steel fabrications where stresses were low but fatigue damage was a serious problem. The most promising application is in the attachment of stiffeners to girder webs. The stress in these connections is usually low but welding seriously reduces the fatigue strength of the main material. The alternative bolted connection exhibits better fatigue resistance but reduces the area of metal available to carry direct stress. A preliminary study using the adhesives described above in specimens as shown in Figure 4 indicated that, although a saving was available, a different adhesive formulation would be required, possibly combined with a redesigned joint.

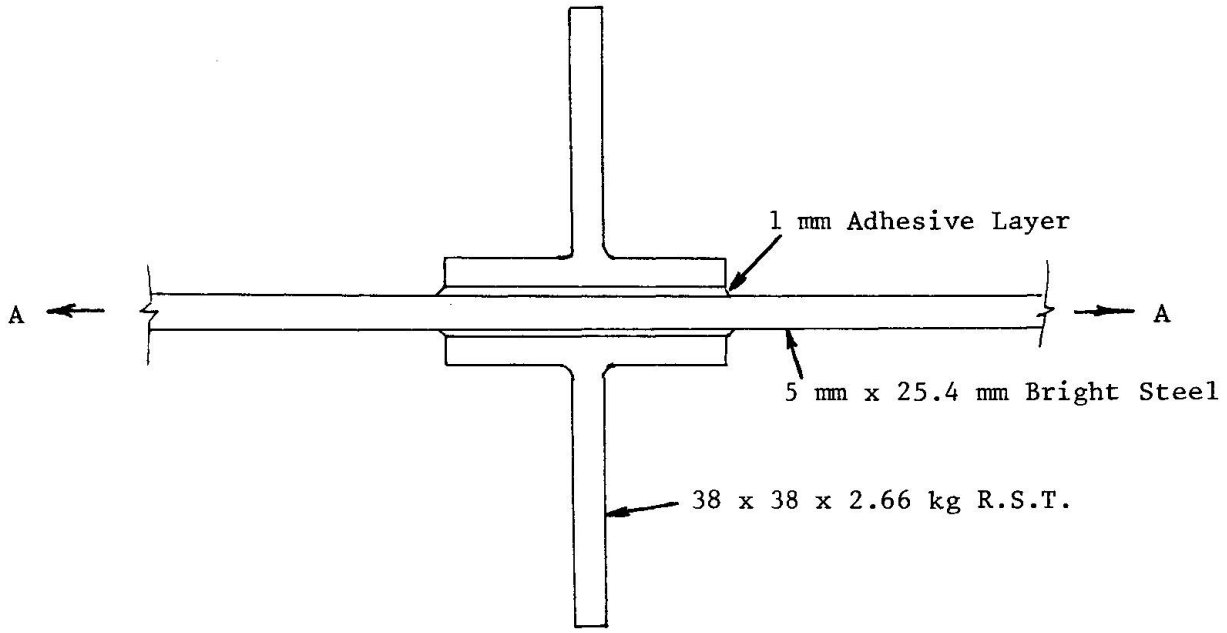

Fig 4. Test Specimen, Adhesive Bonded Unstressed T

5.1 Choice of Adhesive

The different elastic properties of steel and adhesive ensure that even small notionally unstressed attachments bonded to stressed steel result in long joint effects in the adhesive. Of the materials so far considered Permabond ESP105 exhibits the best static strength and fracture toughness. It also seems less susceptible to imperfect surface preparation than some others. Its high fracture toughness makes it resistant both to the long joint shear stresses mentioned above and to the cleavage or peel stresses likely to be induced by accidental damage to the attachment. A disadvantage of this adhesive is the need to cure at elevated temperatures, though 100 to 150°C should be readily achievable in fabrication shops where preheating for welding is common.

5.2 Test Methods

Specimens as shown in Figure 4 were first subjected to cyclic loading in tension in direction A. The attachments were then pulled off, by gripping the outstand of the Ts, to indicate residual strength and to allow inspection of any cracks induced by fatigue.

5.3 Results

The preliminary tests indicate that with stress ranges up to 100 N/mm^2 in tension in the main material, glue lines up to 40 mm long remain undamaged after 3.5 million cycles. At a stress range of 130 N/mm^2 fatigue damage is significant after 1 million cycles.

A substantial test programme is now in hand. This will include flexural loading of girders with adhesive bonded stiffeners. The search for suitable adhesives continues.

6. ACKNOWLEDGEMENTS

The work described here was carried out in the Wolfson Bridge Research Unit, director Professor A.E. Vardy, with financial assistance from the Science & Engineering Research Council and the Transport & Road Research Laboratory. The majority of the experimental and theoretical work was undertaken by the following students: G. Ching, L.M. Goh, K.C.G. Ong.

7. REFERENCES

1. SMITH, D.W. & CUSENS, A.R. Composite bridges of reduced weight. Final report of IABSE Symposium, Main trends in the development of steel structures pp 47 - 53, Moscow 1978.

2. MAYS, G.C. & SMITH, D.W. Slab of the future? Concrete, V14 No. 6, pp 13 - 16, June 1980.

3. CUSENS, A.R. & SMITH, D.W. A study in epoxy resin adhesive joints in shear. The Structural Engineer, V58A No.1, pp 13 - 18, January 1980.

4. BS5400: Part 10:1980. Steel, concrete and composite bridges. British Standards Institution.

5. SVENSK STANDARD SIS 05 59000 - 1967. Pictorial surface preparation standards for painting steel surfaces. Swedish Standards Institute.

6. MAYS, G.C. & TILLY, G.P. Fatigue performance of bonded structural joints at long endurances. Adhesion & Adhesives (to be published 1982).

Application of Photon Tomography to Weld Inspection

Application de la tomographie par photons au contrôle des soudures

Anwendung der Photon-Tomographie zur Kontrolle von Schweissnähten

KARL H. FRANK
Associate Professor
University of Texas at Austin
Austin, TX, USA

TERRY L. KOHUTEK
Graduate Research Assistant
University of Texas at Austin
Austin, TX, USA

SUMMARY
The results of a study of the application of photon tomography to weld inspection are presented. The evaluation of two weld cores containing defects is presented and compared with standard radiography. The results indicate that tomography may be an extremely useful method of weld inspection.

RESUME
Les premiers résultats d'une étude de l'application de la tomographie par photons au contrôle des soudures sont présentés. L'examen de deux échantillons soudés contenant des défauts a été effectué par ce procédé et comparé à celui effectué par la radiographie habituelle. Les résultats indiquent que la tomographie peut être une méthode extrêmement utile pour le contrôle des soudures.

ZUSAMMENFASSUNG
Die Resultate einer Untersuchung von Schweissstellen mit der Methode der Photon-Tomographie werden vorgestellt. Zwei defekte Schweissungen werden mit Hilfe der neuen Methode beurteilt und die Resultate mit denjenigen der Röntgen-Methode verglichen. Der Vergleich lässt darauf schliessen, dass die Photon-Tomographie eine äusserst nützliche Methode zur Kontrolle von Schweissnähten ist.

1. INTRODUCTION

The purpose of inspecting weldments nondestructively is to ensure that weldments do not contain defects which will cause the welds to perform unsatisfactorily. The fatigue performance of a full penetration butt weld with its reinforcement round off is governed by the size of the internal defects in the weld and the stress range it will be subjected to in service. Most inspection specifications contain a statement requiring that welds which contain sharp crack-like planar defects, such as lack of fusion, inadequate penetration, and cracks, be rejected. This requirement is based on the reasoning that these sharp planar defects will produce welds with short fatigue lives compared to welds containing small amounts of porosity and slab inclusion. However, it must be understood that for each type of inspection technique there is an associated detection level and resolution level. For example, ultrasonic inspection techniques can easily detect very small defects of the order 1 to 2 mm, but cannot easily resolve, determine the size and shape, defects this size.

This paper presents the preliminary results of a research project sponsored by the Federal Highway Administration, Office of Research, to determine the feasibility of using photon tomography for the inspection of weldments. A laboratory scanner is used to determine the detectability and resolution of tomography. The results will be compared with ultrasonics (U.T.) and radiography (R.T.) testing to determine the value of tomography relative to these existing inspection methods.

2. TOMOGRAPHY TECHNIQUE

The tomography technique consists of taking a series of radial views around an object to construct a two-dimensional image of the object perpendicular to the viewing plane. Normally a collimated system is used which restricts the area to be imaged to a narrow slice through the object. The resulting two-dimensional image or tomogram is a graphical representation of the object's opacity to the interrogating source.

A comparison of the information obtained from computerized tomography (CT) and RT inspection of a butt weld is shown in Fig. 1. The defect geometry in the slice plane is obtained in the tomogram while the radiograph yields only the length of the defect. The image of the defect in the tomogram allows the significance of the defect to be rationally assessed.

The tomography scanner used in this study is described in detail in Ref. 1. Briefly, it consisted of a gamma ray isotope source, a rotating table for the object to be examined, and a photon counting detector array. The gamma ray source is placed opposite the detector array, with the object in the center, as shown in Fig. 2. The object is rotated to produce major positions and the detector array moved a smaller amount for minor subpositions. The detector array consists of 31 fast plastic scintillators coupled to photomultiplier tubes. The digital output of the photomultipliers is stored and subsequently analyzed in a PDP 11/35 computer. The tomogram is produced by employing the filtered back-projector analytical method.

The tomograms shown in this paper were produced with a ^{60}Co source. A 2 mm aperature is used at both the source and detector, yielding an effective slice plane thickness of 2 mm.

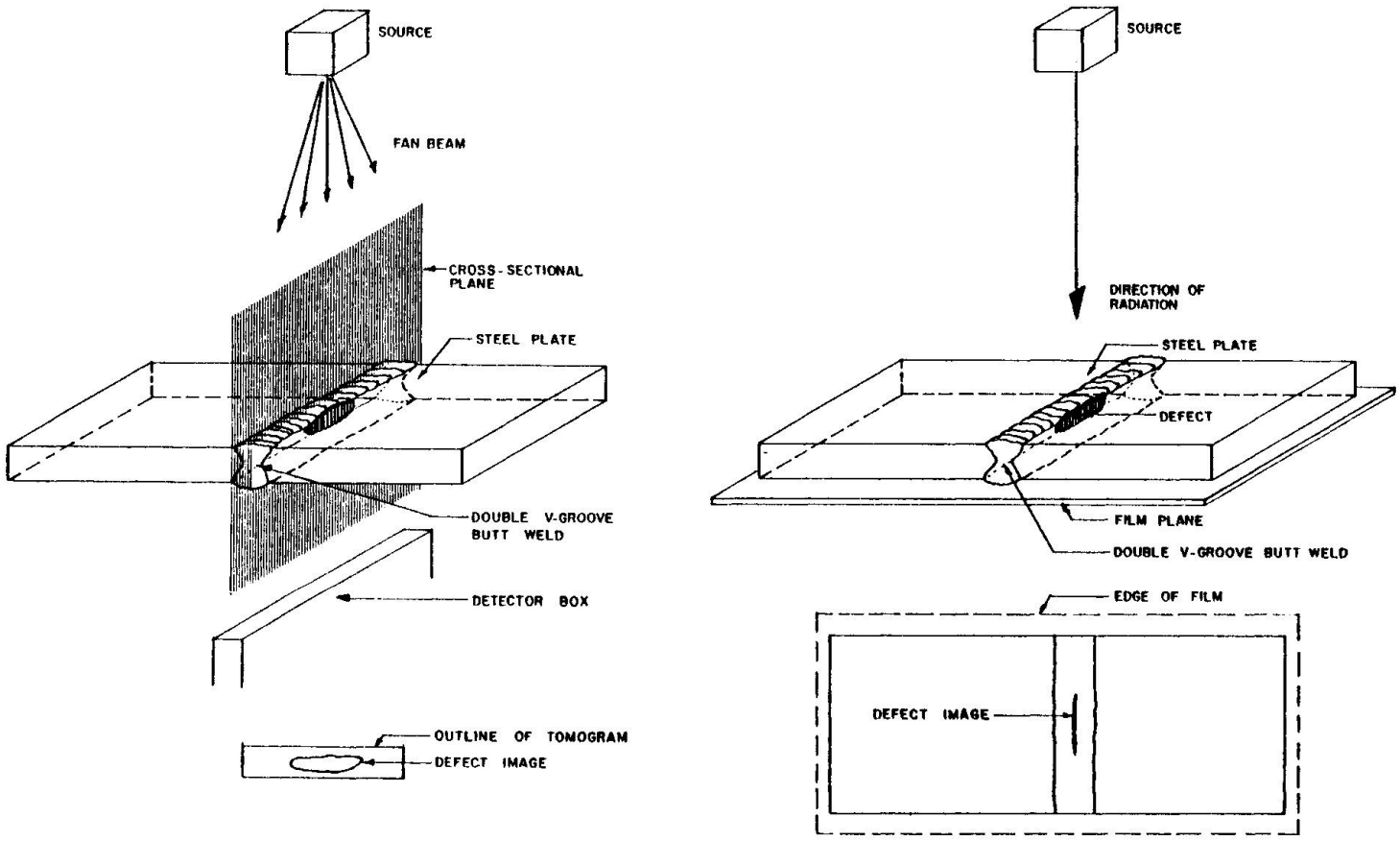

Fig. 1 Defect Imaging with CT and RT

3. EXPERIMENTAL VARIABLES

The applicability of CT to weld inspection is being determined by inspecting cores removed from in-service bridges, laboratory fabricated welds made with a variety of purposely introduced defects, and control specimens called phantoms containing carefully machined adjustable voids. The influence and interaction of beam height (slice plane thickness), defect dimensions both in and out of the slice plane, partial view data caused by lack of transmission in rectangular objects, and scanning increments upon the sensitivity of the method. The results of the study on weld cores containing sharp cracks from an in-service bridge are given in the next section.

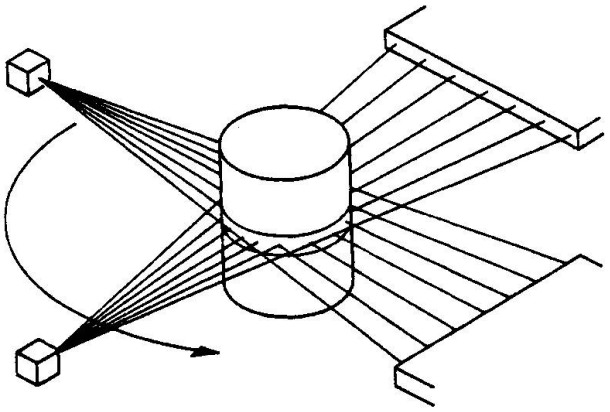

Fig. 2 CT Scanning Process (Courtesy of Scientific Measurement Systems)

4. EVALUATION OF TOMOGRAPHY USING WELD CORES

Weld cores from the Silver Memorial Bridge located at Point Pleasant, West Virginia, U.S.A., were scanned as part of a study to determine the significance of the cracks found in a field inspection of the bridge. The details of the study are given in Ref. 2. The results of two weld cores are detailed below.

Many of the cores from the bridge had visible cracks at the edge of the weld. These welds were butt welds used to join the plates comprising the flanges of the "H" shapes used for the members of the truss. A typical example is shown in Fig. 3. The edge of the weld, at the flange tip, contains two large defects. Standard radiography of the cores, at 1% sensitivity, did not image these large cracks. A tomogram was taken of the core perpendicular to the face shown in Fig. 3. The results are shown in Fig. 4. Both defects are imaged. The curved shape and depth of the upper defect was confirmed by destructive examination.

In another core, a defect was found by radiography. An internal defect was interpreted as porosity by the radiographer. A tomogram across the weld at the defect produced the results shown in Fig. 5. Figure 6 shows a cross section of the weld at the location of the tomogram slice plane. The defect imaged in the tomogram agrees with the results of the destructive examination. The defect is not porosity but a fusion line defect.

5. CONCLUSIONS

The results of these two cores indicate that the sensitivity of tomography exceeds radiography and provides a much easier to interpret image. Further work is underway to evaluate tomography with other weld defects and phantoms. The results to date indicate tomographic inspection of weldments is a potentially very useful and powerful technique.

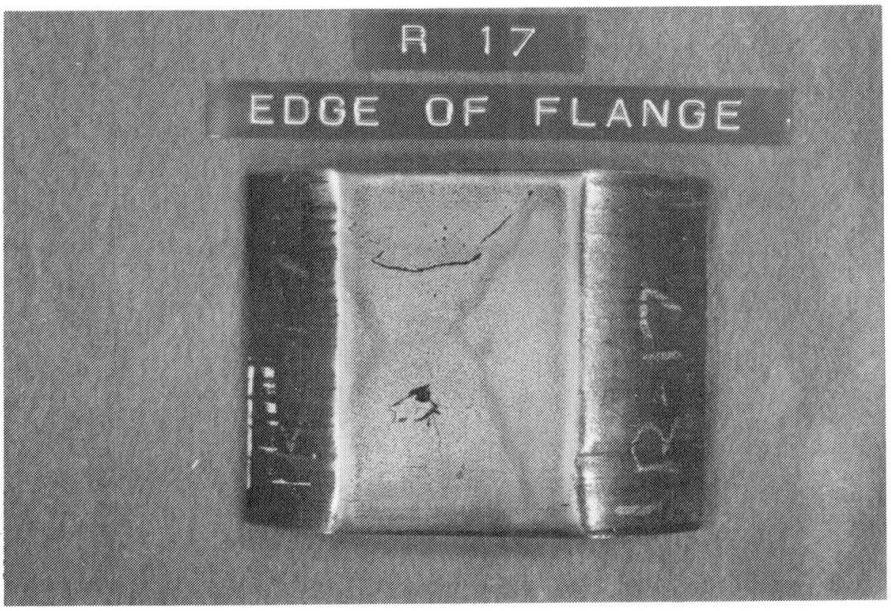

Fig. 3 Edge of Core Showing Two Defects

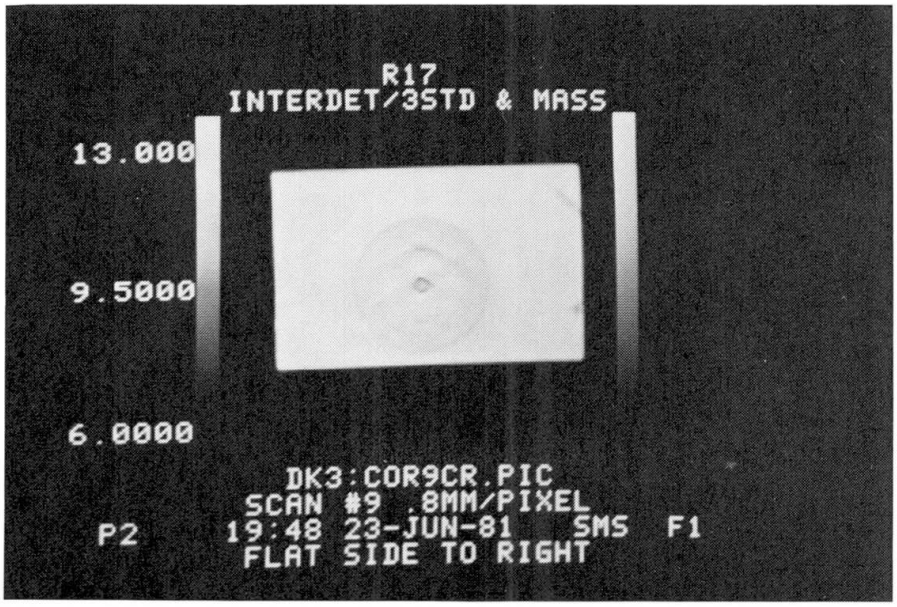

Fig. 4 Tomogram Through Edge Defects

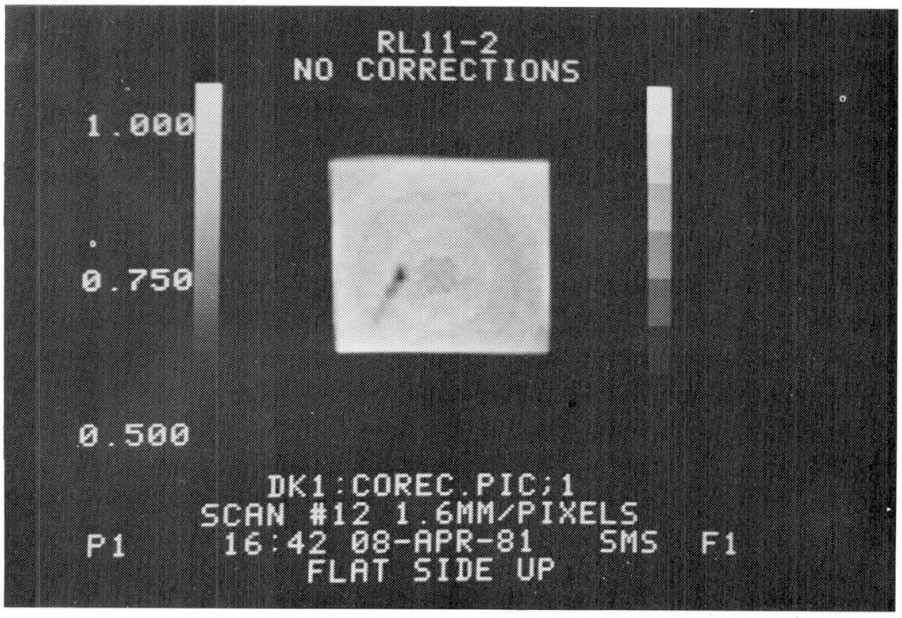

Fig. 5 Tomogram of Embedded Defect

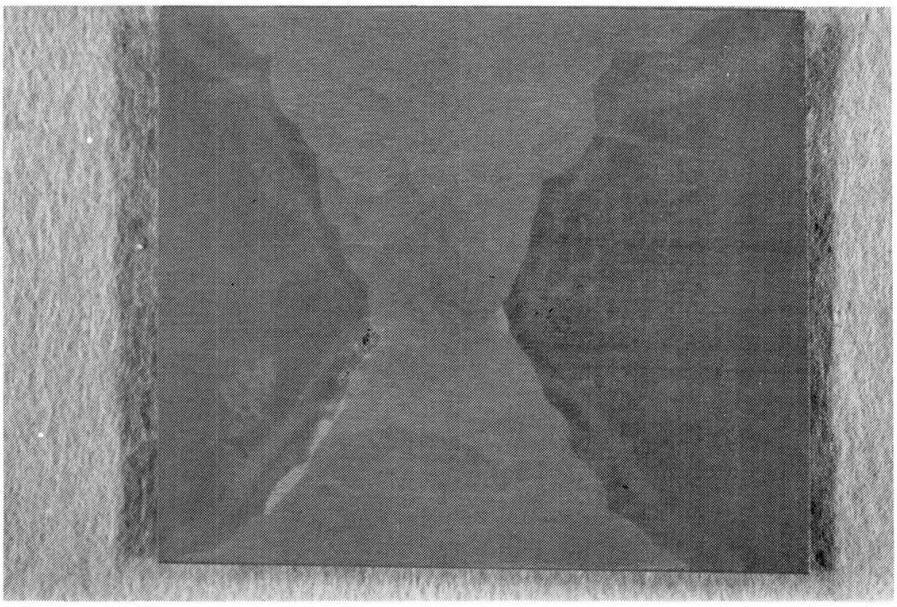

Fig. 6 Cross Section of Weld at Embedded Defect

REFERENCES

1 ELLINGER, H., et al, "Tomographic Analysis of Structural Materials," Proceedings of the Society of Photo-Optical Instrumentation Engineers, Vol. 182 - Imaging Applications for Automated Industrial Inspection and

2 FRANK, K. H., and COLWELL, A. B., "Evaluation of Silver Memorial Bridge - Phase III - Weld Metal Core Evaluation," PMFSEL, U. of Texas at Austin, July 1981, PMFSEL-WV-2.